CHARACTERIZATION OF A NOVEL HETEROZYGOUS NFKB2 VARIANT IN A MULTIPLEX FAMILY WITH COMMON VARIABLE IMMUNE DEFICIENCY

A THESIS SUBMITTED TO
THE GRADUATE SCHOOL OF ENGINEERING AND SCIENCE
OF BILKENT UNIVERSITY
IN PARTIAL FULFILLMENT OF THE REQUIREMENTS FOR
THE DEGREE OF
MASTER OF SCIENCE
IN
MOLECULAR BIOLOGY AND GENETICS

By
Alperen Baran
August 2024

To my mom,
for always loving and supporting me

CHARACTERIZATION OF A NOVEL HETEROZYGOUS NFKB2 VARIANT IN A MULTIPLEX FAMILY WITH COMMON VARIABLE IMMUNE DEFICIENCY

By Alperen Baran

August 2024

We certify that we have read this thesis and that in our opinion it is fully adequate, in scope and in quality, as a thesis for the degree of Master of Science.

Serkan Belkaya (Advisor)

Pınar Önal

Emel Timuçin

Approved for the Graduate School of Engineering and Science:

Orhan Arıkan

Director of the Graduate School

ABSTRACT

CHARACTERIZATION OF A NOVEL HETEROZYGOUS NFKB2 VARIANT IN A MULTIPLEX FAMILY WITH COMMON VARIABLE IMMUNE DEFICIENCY

Alperen Baran

M.Sc. in Molecular Biology and Genetics

Advisor: Serkan Belkaya

August 2024

Common variable immune deficiency (CVID) is a complex primary immunodeficiency characterized by low levels of serum immunoglobulins (IgG, and IgA and/or IgM) and higher vulnerability to recurrent infections, autoimmunity, and malignancies. Despite extensive clinical characterization, the underlying genetic causes of CVID remain elusive in many cases, complicating both diagnosis and treatment. In our study, we conducted a detailed genetic investigation of a multiplex family, in which both father and his two sons were affected by CVID. To identify inborn monogenic defects underlying CVID in this family, we performed whole exome sequencing (WES) on two affected members. We discovered a novel missense heterozygous variant (NM_001322934.2:c.2602T>A:p.Y868N) in *NFKB2*, encoding NF-κB2 protein, present in all patients but absent in the healthy mother, consistent with an autosomal dominant mode of inheritance with complete penetrance. To characterize the impact of this variant on the expression and function NF-κB2, we conducted various biochemical and functional studies using overexpression systems and patients' cells. We showed that the p.Y868N variant impairs the generation of active p52 from p100, thereby culminating in p100 accumulation. This accumulation

leads to a gain-of-function (GOF) in inhibitory activity of IκBδ and a loss-of-function (LOF) in transcriptional activity of p52. These results suggested a causative link between the *NFKB2* mutation and CVID in the patients. Our findings further expand the genetic spectrum of CVID and emphasize the importance of incorporating next generation sequencing technologies, such as WES, in the diagnostic evaluation of patients with CVID. Genetic dissection of CVID not only enhances our current understanding of its pathogenesis in humans, but also provides genetic testing and counselling in affected families and supports the development of more personalized therapeutic approaches, ultimately improving disease outcomes.

Key words: common variable immune deficiency, whole-exome sequencing, NF-κB2, inborn error of immunity, alternative NF-κB signaling pathway

ÖZET

YAYGIN DEĞİŞKEN İMMÜN YETMEZLİĞİ OLAN MULTİPLEKS BİR AİLEDE YENİ BİR HETEROZİGOT NFKB2 VARYANTININ KARAKTERİZASYONU

Alperen Baran

Moleküler Biyoloji ve Genetik, Yüksek Lisans

Danışman: Serkan Belkaya

Ağustos 2024

Yaygın değişken immün yetmezlik (YDİY), düşük serum immunoglobulin seviyeleri (IgG ve IgA ve/veya IgM) ve tekrarlayan enfeksiyonlara, otoimmün ve malign hastalıklara karşı artan duyarlılık ile karakterize edilen karmaşık bir primer immün yetmezliktir. Geniş klinik karakterizasyona rağmen, YDİY'nin altında yatan genetik nedenler birçok durumda belirsiz kalmakta ve bu durum hem tanıyı hem de tedaviyi zorlaştırmaktadır. Çalışmamızda, hem baba hem de iki oğlunun YDİY'den etkilendiği multipleks bir ailede detaylı bir genetik araştırma gerçekleştirdik. Bu ailedeki YDİY'nin doğuştan gelen monogenik kusurlarını bulmak amacıyla hastalıktan etkilenen iki aile üyesinde tüm ekzom dizilime yaptık. Tüm hastalarda bulunan ancak sağlıklı annede bulunmayan, otozomal dominant kalıtım moduna ve tam penetransa uygun olarak NF-κB2 proteinini kodlayan NFKB2 geninde yeni bir heterozigot yanlış anlamlı varyant (NM_001322934.2:c.2602T>A:p.Y868N) keşfettik. Bu varyantın NF-κB2'nin ifadesi ve fonksiyonu üzerinde etkisini karakterize etmek için, aşırı ifade sistemleri ve hastaların hücrelerini kullanarak çeşitli biyokimyasal ve fonksiyonel çalışmalar gerçekleştirdik. p.Y868N varyantının, p100'den aktif p52'nin oluşumunu engellediğini ve bu nedenle p100 birikimine yol açtığını gösterdik. Bu birikim, IκBδ'nin inhibe edici aktivitesinde fonksiyon kazancı ve p52'nin transkripsiyonel

aktivitesinde fonksiyon kaybı ile sonuçlandı. Bu sonuçlar, NFKB2 mutasyonu ile hastalardaki YDİY arasında nedensel bir bağlantı olduğunu öne sürdü. Bulgularımız, YDİY'nin genetik spektrumunu daha da genişletmekte ve tüm ekzom dizilime gibi yeni nesil dizileme teknolojilerinin YDİY'li hastaların tanısal değerlendirilmesine dahil edilmesinin önemini vurgulamaktadır. YDİY'nin genetik olarak incelenmesi, sadece insanlarda hastalığın patogenezini anlamamızı geliştirmekle kalmaz, aynı zamanda etkilenen ailelerde genetik test ve danışmanlık sağlamaya yardımcı olur ve daha kişiselleştirilmiş tedavi yaklaşımlarının geliştirilmesini destekler, nihayetinde hastalık sonuçlarını iyileştirir.

Anahtar kelimeler: yaygın değişken immün yetmezlik, tüm ekzom dizilime, NF-κB2, doğuştan bağışıklık hatası, alternatif NF-κB sinyalizasyon yolağı

ACKNOWLEDGMENTS

Firstly, I would like to express my deepest gratitude to my advisor, Dr. Serkan Belkaya, for his patience and guidance throughout my graduate studies. His support has played a crucial role in shaping my skills as a scientist, and I am deeply thankful for the productive environment he cultivated in our lab. His extensive knowledge and experience have been invaluable, and I could not have achieved this level of dedication without his exceptional supervision and encouragement.

I am deeply indebted to Dr. Şengül Beyaz for her valuable contributions to my thesis. Her insights and suggestions have added depth to my research, and I am grateful for the time and expertise she generously shared.

I would like to express my appreciation to committee members, Dr. Pınar Önal and Dr. Emel Timuçin for their feedback and contributions in completion of this thesis. I also thank my labmate, Yücehan Yılmaz Yazıcı, for his help on the analysis of WES data.

I would like to express my greatest gratitude to Aysima Altılgan Lülecioğlu, my labmate and dear friend, who has been an unwavering source of support throughout this journey. From conducting experiments side by side to sharing every success and setback, she was always there, ready to lend a helping hand or offer a kind word. Her knowledge and wisdom guided me through many challenges, and I am endlessly grateful for the countless questions she patiently answered. I would also like to extend my deepest and most heartfelt gratitude to Beste Uygur, who has been far more than just an assistant during my undergraduate years. She taught me the essential experimental techniques during my undergraduate years, ensuring that I entered my master's studies with a solid foundation. Thanks to her excellent teaching, I began my master's journey well-prepared and confident in my skills. Beyond that, she became a

true friend and like a sister to me, offering unwavering support throughout my entire master's journey. She was always there, providing me with wise counsel and guiding me with such care and insight. Her advice was invaluable, and her encouragement gave me the strength to keep going, even in the most challenging times. The depth of her support goes beyond words, and I am profoundly grateful to have had her by my side through it all. I am deeply thankful to my friends Zeynep Güneş Tepe Demir and Servin Bagheralmoosavi for their unwavering emotional support. They have been my steadfast pillars through every high and low, creating lasting memories I will always cherish. I am also deeply thankful to my friend Tunahan Çalıkoğlu for his cheerful demeanor and unwavering positivity, which have made this journey more bearable and left us with unforgettable memories.

I would like to express my deepest and heartfelt thanks to my mother, whose unwavering love and sacrifice have been the true pillars of my journey. She has given everything, both materially and emotionally, without hesitation, to support me. I would not be where I am today without her endless devotion and strength. She is the most important and cherished person in my life, and I am forever grateful for all she has done for me.

TABLE OF CONTENT

LIST OF TABLES

LIST OF FIGURES

ABBREVIATIONS

ACMG	American College of Medical Genetics and Genomics
AD	Autosomal Dominant
AF	Allele Frequency
AFB	Allele Frequency Browser
AMP	Association For Molecular Pathology
APS	Ammonium Persulphate
BAFF	B Cell Activating Factor
BAFF-R	B Cell Activating Factor Receptor
BCA	Bicinchoninic Acid
BSA	Bovine Serum Albumin
CADD	Combined Annotation-Dependent Depletion
CR2	Complement Receptor 2
CVID	Common Variable Immune Deficiency
DMEM	Dulbecco's Modified Eagle Medium
DMSO	Dimethyl sulfoxide
DNA	Deoxyribonucleic acid
DP	Depth Coverage
dPBS	Dulbecco’s Phosphate-Buffered Saline
DTT	Dithiothreitol
ECL	Enhanced Chemiluminescence
EDTA	Ethylenediaminetetraacetic Acid
FBS	Fetal Bovine Serum

Fwd	Forward
GAPDH	Glyceraldehyde 3-Phosphate Dehydrogenase
GDI	Gene Damaging İndex
gDNA	Genomic DNA
GFP	Green Fluorescent Protein
GLILD	Granulomatous Lymphocytic Interstitial Lung Disease
gnomAD	The genome aggregation database
GOF	Gain-Of-Function
GQ	Genotype Quality
GWAS	Genome-Wide Association Studies
HCl	Hydrochloric Acid
HET	Heterozygous
ICOS	Inducible T Cell Co-Stimulator
IEIs	Inborn Errors Of Immunity
Ig	Immunoglobulin
IgRT	Immunoglobulin Replacement Therapy
IKK	IκB kinase
IκBδ	Inhibitor of kappa B delta
IKZF1	IKAROS Family Zinc Finger 1
IL-1	Interleukin-1
IL-21	Interleukin-21
IRF2BP2	Interferon Regulatory Factor 2 Binding Protein 2
ITB	Inoue Transformation Buffer
IUIS	International Union of Immunological Societies

LB	Lysogeny broth
LOF	Loss-Of-Function
LRBA	LPS responsive beige-like anchor protein
LTβ	Lymphotoxin β
LTβR	Triggers Including Lymphotoxin B Receptor
miRs	microRNAs
MS4A1	Membrane-Spanning 4-Domains Subfamily A Member 1
MQ	Mapping Quality
NaOH	Sodium Hydroxide
NF-κB	Nuclear Factor Kappa B
NFKB1	Nuclear Factor Kappa B Subunit 1
NFKB2	Nuclear Factor Kappa B Subunit 2
NGS	Next-Generation Sequencing
NIK	NF-κB Inducing Kinase
NRS	NIK-Responsive Sequence
ORFs	Open Reading Frames
PADs	Predominantly Antibody Deficiencies
PAGE	Polyacrylamide gel electrophoresis
PBMCs	Peripheral Blood Mononuclear Cells
PCR	Polymerase Chain Reaction
PFA	Paraformaldehyde
PID	Primary Immunodeficiency
pLOF	Predicted Loss-of-Function
PolyPhen-2	Polymorphism Phenotyping V2

PVDF	Polyvinylidene Difluoride
QUAL	Overall Quality
RANKL	Receptor activator of NF-κB ligand
RBC	Red Blood Cell
RELA	V-rel Avian Reticuloendotheliosis Viral Oncogene Homolog A
RELB	V-rel Avian Reticuloendotheliosis Viral Oncogene Homolog B
Rev	Reverse
RHD	Rel homology domain
RIPA	Radio İmmunoprecipitation Assay Buffer
RLTK	Renilla Luciferase
RTIs	Respiratory Tract Infections
SARS-CoV-2	Severe Acute Respiratory Syndrome Coronavirus-2
SBDS	Shwachman–Bodian-Diamond Syndrome
SDM	Site-Directed Mutagenesis
SDS	Sodium Dodecyl Sulfate
SEAP	Secreted Alkaline Phosphatase
SEC61A1	SEC61 Translocon Alpha 1 Subunit
SIFT	Sorting Intolerant From Tolerant
TBE	Tris Borate EDTA Buffer
TBS	Tris-Buffered Saline
TEMED	N,N,N',N'-Tetramethyl Ethylenediamine
TGP	Turkish Genome Project Data Sharing Portal
Th cells	Helper T Cells
TNF	Tumor necrosis factor

TNFRSF13B	Tumor Necrosis Factor Receptor Superfamily Member 13B
TNFRSF13C	Tumor Necrosis Factor Receptor Superfamily Member 13C
Tregs	Regulatory T Cells
WES	Whole-Exome Sequencing
WGS	Whole-Genome Sequencing
WT	Wild-Type

CHAPTER 1

Introduction

1.1. Common Variable Immune Deficiency

Human inborn errors of immunity (IEIs), also known as primary immunodeficiency (PID) disorders, are a heterogeneous group of inherited diseases, in which the immune system components are absent or dysfunctional[1–5]. Monogenic inborn errors result in the loss or gain of function of the affected gene[2,5]. They can be autosomal or X-linked, and inherited in dominant or recessive manner, with complete or incomplete penetrance[2,5]. Clinically, IEIs present with phenotypes, such as increased susceptibility to infections, autoimmunity, pituitary gland disorders, autoinflammation, allergy, bone marrow failure, and/or malignancy[2,3,5,6]. A total of 485 genetic disorders have been reported so far in patients with IEI[2]. The phenotypic classification of all these conditions, categorized based on the clinical and laboratory characteristics of the patients, has been periodically revised by the International Union of Immunological Societies (IUIS) in line with the genotypic catalog since 2013[2]. Currently, IEIs are classified into 10 categories, each of which has subcategories based on the overlapping phenotypes[7]. The third category consists of Predominantly Antibody Deficiencies (PADs)[2]. PADs are a broad range of disorders that are the most common category of all IEIs, due to defects in various genes crucial for B cell development[2,6]. In this category, the subcategory with hypogammaglobulinemia and B cell counts more than 1% constitutes the Common Variable Immune Deficiency (CVID) phenotype[2].

CVID is a disorder defined by the defect in the differentiation of B cells into plasma cells, leading to impaired immunoglobulin (Ig) production[8,9,10]. CVID is a genetically heterogenous group of PAD disorders, as it is caused by different genetic defects[11]. This condition is characterized by (i) severe reduction in the serum levels of at least two Ig isotypes: IgG, and IgA and/or IgM, (ii) inadequate/absent antibody responses upon infections or immunization, and (iii) lack of other defined causes of immunological abnormalities[12–14] . It is critical to fulfill the defined criteria for accurate diagnosis of CVID, which are as follows[11,12];

At least one of the following: Increased predisposition to infectious diseases, autoimmune disorder, Granulomatous disease, lymphoproliferation, or presence of a family member affected with PIDs, and fulfilling all the criteria listed below;

- Significant decrease of IgG accompanied by a reduction in IgA and/or IgM levels on at least two measurements more than 3 weeks apart (at least 2 standard deviations below the normal levels for age).
- At least one of the following: Impaired antibody response to vaccinations (in patients with IgG >100 mg/dL, responses to T-dependent or T-independent antigens should be measured and unresponsiveness to at least one type should be demonstrated) and/or inadequate levels of isohemagglutinins, or decreased levels of switched memory B cells (<70% of normal levels for age).
- Excluding other primary or secondary causes of hypogammaglobulinemia is crucial (e.g., infections, drugs, monogenic defects, such as Ataxia telangiectasia, Combined or severe-combined immunodeficiency, Hyper-IgM syndromes, X-linked agammaglobulinemia, X-linked lymphoproliferative disorder, metabolic disorders, etc., chromosomal anomalies, protein loss, and malignancy).

- Diagnosis can be made after the 4th year of life, even if the onset of symptoms is earlier.
- No evidence for significant T-cell depletion, which is defined as (i) CD4 counts per microliter as <300 for 2-6 years, <250 for 6-12 years, <200 for >12 years of age, (ii) percentages of naive CD4 T cells as <25% for 2-6 years, <20% for 6-16 years, <10% for >16 years of age, (iii) absence of T cell proliferation.

CVID is still diagnosed by exclusion due to variable clinical presentation and laboratory findings[11,10]. The phenotype, which has been termed "variable" due to its diverse clinical presentations, varies from simply bacterial infections to a severe disease mimicking combined immunodeficiency[11,15]. Clinical symptoms and laboratory abnormalities may manifest at any age, from early childhood to the elderly, but more common during the second and third decades of life, and their onsets are not always concurrent[11]. For CVID, five distinct clinical manifestations have generally been described, including infections only (no disease-related complications), autoimmune disorder, polyclonal lymphocytic infiltration, enteropathy, and lymphoid malignancy[16]. These phenotypes were re-evaluated and refined following the investigation of large CVID cohorts, and categorized as four phenotypes (autoimmune cytopenia, enteropathy, infection, and polyclonal lymphoproliferation)[15]. Thus, when evaluating the clinical picture of a patient with recently diagnosed CVID, two complications—infectious (no disease-related complications) and noninfectious (disease-related complications)—must be taken into account[10].

1.1.1. Clinical Manifestations

The most prevalent symptomatic PID disorder, CVID, can present with wide range of clinical manifestations, from recurrent infections to malignancy[11,17,10]. The following

clinical symptoms might develop in patients as initial signs of the disease or as the disease progresses.

1.1.1.1. Infections

The most frequent clinical signs of CVID are recurrent infections. An anamnesis of acute or chronic sinopulmonary infections, such as pneumonia, otitis, and sinusitis, is present in the majority of CVID patients. The most frequently affected sites are the upper and lower respiratory tracts[17]. Around half of the CVID patients have had recurrent bronchitis, acute and chronic rhinosinusitis, and/or otitis media, while more than half of the patients have developed at least one pneumonia episode[18]. Around 90% of individuals with CVID experience recurrent bacterial infections primarily with encapsulated bacteria, such as *Streptococcus pneumoniae*, *Haemophilus influenzae*, *Staphylococcus aureus*, and *Pseudomonas aeruginosa*[11,17,18]. In contrast, viral, parasitic and fungal infections are uncommon[19]. Infections with viruses, such as Rhinovirus, Adenovirus, Herpes Simplex Virus, Varicella Zoster Virus, Enterovirus, and Human Papillomavirus, may be more recurrent and/or persistent in CVID patients, whereas severe infections upon Severe Acute Respiratory Syndrome Coronavirus-2 (SARS-CoV-2), Epstein-Barr Virus or Cytomegalovirus have also been reported[18,20–23].

The second most common infection site is the gastrointestinal tract[19]. Gastrointestinal system infections caused by pathogens, such as Human Herpes Virus-6, Hepatitis B/C Viruses, Norovirus, Giardia lamblia, *Salmonella spp.*, *Helicobacter pylori*, and *Campylobacter jejuni* can lead to problems, such as chronic active gastritis, chronic or intermittent diarrhea, hepatitis, enteropathy, malabsorption, and weight loss[21,22]. In addition to respiratory and gastrointestinal tract infections, conjunctivitis, septic arthritis, osteomyelitis, meningitis, cutaneous infections, and genitourinary tract infections are

reported for CVID[10,17,19]. Ureaplasma and mycoplasma, uncommon pathogens, can cause arthritis, genitourinary tract, and lung infections in patients[17]. Fungal infections are also less common, but candidiasis, invasive aspergillosis, and opportunistic *Pneumocystis jirovecii* pneumonia can be observed in affected individuals[18,19].

1.1.1.2. Lung Diseases

Chronic lung disease represents one of the major complications of CVID, and bronchiectasis in particular is a frequent condition, affecting approximately 51% of patients[24,25]. Bronchiectasis and interstitial lung disease are two different forms of chronic lung disease that can arise from severe, recurrent, and chronic pulmonary infections[18,24,26]. The hallmarks of bronchiectasis are thickened bronchial walls and dilated bronchi[27]. Although past chronic infection is the most prevalent underlying cause, the majority of cases are classified as idiopathic[27]. Chronic cough, phlegm, and recurrent infections of the respiratory tract are the most prevalent symptoms[27]. Granulomatous lymphocytic interstitial lung disease (GLILD) is a unique clinico-radio-pathological interstitial lung disease that affects patients with CVID, is related to a lung granuloma or lymphocytic infiltration, and is considered in patients when other causes have been ruled out[28]. A multisystem granulomatous/inflammatory disease, including splenomegaly, lymphadenopathy, and/or a hepatic disorder, even when not symptomatic, can be observed in conjunction with GLILD[28].

1.1.1.3. Granulomatous and lymphoproliferative disorders

Granulomatous and lymphoproliferative disorders are serious and common non-infectious complications in CVID patients[22,29]. Granulomatous disease seen in CVID is characterized by granuloma formation, which is non-caseificated and clusters of inflammatory cells, in

various tissues and organs, such as lungs, lymph nodes, and spleen[11,30–32]. In addition, bone marrow, brain, eyes, gastrointestinal system, kidney, liver, and/or skin may be affected[33–36]. Up to 40% of CVID patients experienced polyclonal lymphadenopathy[29]. Clinically, abnormal lymphocyte proliferation characterized by lymphoid hyperplasia or lymphocytic inflammation, splenomegaly, and lymphadenopathy are other common presentations of CVID[22,37,38]. Two typical findings in lymph nodes and other lymphoid tissues are characterized by the absence of plasma cells and the presence of ill-defined germinal centers[39]. Although its cause and implications are still unclear, splenomegaly is a common symptom in CVID patients, and histological examination of splenectomy material has revealed granulomatous lesions[11,40,41]. The coexistence of autoimmune cytopenia, granulomatous disorder, and lymphadenopathy is strongly related to splenomegaly in CVID[16,42,43].

1.1.1.4. Autoimmune disorders

Autoimmune disorders are an important and complex aspect of CVID, affecting approximately 20-30% of patients[18,22]. However, the pathogenic pathways driving autoimmunity in CVID are still uncertain. The most frequent autoimmune complications in CVID are autoimmune hematological disorders (immune thrombocytopenic purpura, hemolytic anemia, and Evans syndrome), and in almost half of these individuals, hematological autoimmune disease occurs prior to or concurrently with the diagnosis of CVID[43–47]. Seronegative rheumatoid arthritis affects 1 to 10% of individuals, but systemic lupus erythematosus is very rare (less than 1%)[48,49]. Other autoimmune disorders documented in CVID are autoimmune thyroiditis, vitiligo, pernicious anemia, arthritis, psoriasis, autoimmune hepatitis, primary biliary cholangitis, and disorders like connective tissue diseases[43,45,47,50].

1.1.1.5. Gastrointestinal infections and other gastrointestinal disorders

There are three primary categories of gastrointestinal manifestations in CVID: infectious, autoimmune or inflammatory, and malignant[17]. The most common gastrointestinal symptom in patients with CVID is chronic diarrhea, affecting approximately 20-60% of patients with/without accompanying malabsorption and weight loss[17,51–54]. Exclusion of infections upon Giardia lamblia, Salmonella, Campylobacter, Cytomegalovirus, Norovirus, or *Clostridium difficile* is crucial in those patients[55–57]. Around 20-30% of individuals have intestinal inflammatory complications[55,58]. Inflammatory bowel diseases or colitis cause persistent inflammation in the gastrointestinal tract, with symptoms including abdominal pain, diarrhea, and weight loss in CVID patients[59]. Nodular lymphoid hyperplasia and lymphoid follicles are observed, both of which are endoscopic characteristics[17]. An intestinal biopsy reveals hyperplastic crypts, and villous atrophy/flattening that are indicative of an enteropathy resembling celiac disease[17,60]. CVID-related autoimmune enteropathy can lead to malabsorption and nutrient deficiencies[61,62]. Another gastrointestinal manifestation of CVID is autoimmune gastritis, which can damage the parietal cells required for vitamin B12 absorption, leading to pernicious anemia[51,63–65].

Hepatomegaly with elevated liver enzymes is common in CVID[11]. The most prevalent causes of hepatic problems are nodular regenerative hyperplasia and cirrhosis, and portal hypertension can develop in some of these patients[66–68]. In addition, hepatitis B and C infections, autoimmune hepatitis, cholestasis, and primary biliary cholangitis are reported in CVID patients[69,70].

1.1.1.6. Allergic diseases

It is thought that patients with CVID and selective IgA deficiency carry a higher risk of developing atopic conditions due to mucosal immune defects and immune dysregulation[71]. In CVID, allergic respiratory diseases, such as asthma, rhinitis, or rhinosinusitis, occur less frequently than selective IgA and IgG subgroup deficiency[72]. In the various CVID cohorts, the prevalence of allergic diseases[72] varies from 12 to 42%[71,73–75]. These disorders include asthma, allergic diseases, atopic dermatitis, urticaria[71,73,74].

1.1.1.7. Dermatologic manifestations

CVID patients can have both infectious and non-infectious dermatologic conditions[76]. Dermatological manifestations include conditions, such as dermatitis-like lesions, skin infections (candidiasis, abscesses, furunculosis, cellulitis, impetigo), recurrent herpes labialis, oral aphthous ulcers, and urticaria, have been seen in patients with CVID[77].

1.1.1.8. Malignancy

CVID patients are more likely to develop malignancies of all types compared to the general population. Lymphomas are the most prevalent type of malignancy in CVID[11,78]. CVID patients, who are with lymphoproliferative disease, have an increased risk of developing lymphoid malignancies[22,38]. In addition, patients with CVID carry higher risk of gastric malignancies[78–80].

1.1.2. Epidemiology

Prevalence of CVID is between 1 in 10,000 and 1 in 100,000 individuals worldwide, with geographic variability, possibly due to differences in awareness of the disease, diagnostic criteria, and reporting practices across different regions[11,81–87]. In 2019, the numbers of CVID cases in the Dominican Republic and USA were 1 and 4,833, respectively[88]. The prevalence of CVID is 1.4/100,000 in Turkey, 1.3/100,000 in the United Kingdom, and

0.7/100,000 in France[86]. Compared to Africa and Asia, North America, Europe, and Australia have relatively higher observed prevalence[82,88,89]. Additional factors, such as life style, geographic location, and access to healthcare, significantly influence the epidemiology of CVID[11,90–92].

The onset age of CVID is quite diverse, ranging from early childhood to late adulthood, with the peak incidence in the first to third decades of life[16,42]. Both genders are equally affected, though some studies suggest a slight female predominance in adults and male predominance in children[42,93]. Variable clinical presentation may explain why CVID remains under-recognized worldwide. Recent breakthroughs in diagnostic procedures, together with increasing awareness among healthcare professionals, will result in earlier diagnosis and better management of CVID.

1.1.3. Etiopathogenesis of CVID

The etiopathogenesis of CVID is complex and multifactorial, and still not well understood. It can be stated that genetic, epigenetic, and environmental factors and the interplay between them contribute to the complexity and heterogeneity of clinical findings[10,94,95]. Several factors/mechanisms underlying the CVID are mentioned below.

1.1.3.1. Environmental Factors

Environmental influences are also thought to play a significant role in the development and progression of CVID[87,96,97]. Environmental factors include infectious agents, exposure to pollutants and chemicals, dietary factors, microbial translocation, and stress[98–100]. Factors, such as infectious agents, particularly viruses, may trigger or exacerbate the condition in genetically predisposed individuals[101]. Chronic infections can cause immune dysregulation and impaired Ig production[16]. Additionally, there is emerging evidence that

the gut microbiome may modulate immune system functioning and contribute to the pathogenesis of CVID[96,99,102–104]. In addition to infections, autoimmunity and hyperinflammation in CVID indicate an underlying peripheral and central immune tolerance mechanism dysfunction, which might be caused by a combination of environmental and genetic factors[105].

1.1.3.2. Epigenetic Factors

Epigenetic mechanisms play an important role in regulating gene expression and have been implicated in the pathogenesis of CVID[94,96,106]. Mechanisms, such as DNA methylation, histone and chromatin modifications, and non-coding RNAs, especially microRNAs (miRs), may modulate the functions of the immune system without any changes in the genetic sequence[95,107–110]. Studies showed that altered demethylation, particularly in genes crucial for B cell processes and signaling, during B cell differentiation contributes to impaired B cell function and maturation in CVID[111–113]. In addition to DNA methylation modifications and non-coding RNAs, transcriptional changes and defects in chromatin accessibility have been associated with CVID phenotypes using multi-omics approaches[106,114]. For example, miRs have roles in the pathogenesis of CVID[115,116]. Esfahani et al (2021) found that CVID patients without a known genetic defect, overexpression of miR-125b-5p leads to decreased expression of the *BLIMP1* and *IRF4* genes, which in turn impairs the terminal differentiation of B cells[116].

1.1.3.3. Immunological Defects

The pathophysiology of CVID is still not fully understood, but can be proposed as a defect in the ability of B cells to differentiate into plasma cells[117]. CVID is characterized by

impaired antibody responses to infections and vaccines. This impairment might be caused by inherent B-cell abnormalities or errors in the interactions between B cells and T-helper cells[118,119]. Impaired somatic hypermutation, class switching, and plasma cell differentiation are possible underlying abnormalities that resulting hypogammaglobulinemia[120].

- **B cell Dysfunction:** The lack of B cell function is the defining feature of CVID[121–123,123,124]. Although most CVID patients have normal B cell counts, they often have decreased memory B cells and isotype-switched memory B cells, and increased $CD21^{low}$ B cells[125,126]. Despite having an intact B-cell receptor and the capability to produce IgM in certain activation stages, $CD21^{low}$ B cells are distinct from other B cells and may be polyreactive[126,127]. CD73, another B cell marker, is lacking in naive, IgM memory, and switched memory B cells of CVID patients, but is required in class switch recombination[128]. There is a decrease in somatic hypermutation in CD27+ cells and a reduction in the variety of the naive CD27- B cell pool[125,129]. In addition, there are also reports B cell abnormalities in CVID started at the pro-B cell stage of development since patients also have clonally expanded unmutated B cells[125,129].
- **T cell Dysfunction:** CVID patients often display T cell abnormalities, including decreased counts of T cells, regulatory T cells (Tregs), impaired proliferative response to antigens and mitogens, altered production of cytokines, and impaired T cell help for B cell antibody production[118,126,130]. This suggests that T-cell defects may contribute to the pathogenesis of CVID in certain cases[126]. Additionally, this dysfunction also affects T cells and is particularly concentrated on Tregs and helper T cells (Th cells)[130,131]. In CVID, the number and function of Tregs are often

reduced, contributing to the disruption of immune homeostasis and the development of autoimmunity[97,132].

1.1.3.4. Genetic Factors

In 1968, it was discovered that CVID had a hereditary component, and the first monogenetic defect, which was identified in Inducible T cell co-stimulator (*ICOS*) was reported in 2003[133,134]. CVID can also be a polygenic disease with a complex inheritance pattern[135]. This complexity is further compounded by disturbances related to transcription and epigenetics[135]. The development of genome-wide association studies (GWAS) and next-generation sequencing (NGS) has proven very beneficial for rare diseases, such as IEI[135,136]. Various methodologies, such as positional cloning, linkage analysis, candidate gene analysis, and fluorescence in situ hybridization, have been utilized to reveal disease-causing genetic abnormalities[135]. Novel genetic defects were identified in PID patients by whole-exome sequencing (WES) and whole-genome sequencing (WGS) approaches[137–139] . Next-generation sequencing (NGS) technology, including WES and WGS, has become an essential tool in clinical settings for identifying genetic variants linked to various diseases. This technology is particularly valuable in studying a range of conditions, including congenital anomalies, neurological disorders, primary immunodeficiencies, cardiovascular diseases, skeletal abnormalities, and mitochondrial disorders[140–145] . The advantages of reduced costs, rapid analysis, and the ability to obtain extensive genetic data have led to the widespread adoption of NGS in both clinical diagnostics and translational research[146,147]. It also plays a significant role in elucidating the molecular mechanisms underlying inherited disorders. Furthermore, WES/WGS is useful for family screening and genetic counseling[135]. Discovery of the genetic mutations

causing PIDs still remains a significant challenge despite recent advancements in NGS[135]. For most individuals, the underlying genetic defect is yet unknown.

A monogenic etiology of CVID is reported in about 20% of cases, typically displaying an autosomal dominant (AD) mode of inheritance[135,148]. Genes listed as associated with CVID in the OMIM database (https://www.omim.org/) are *CD19, CD81, CR2 (CD21), ICOS, IL21, IKZF1, IRF2BP2, LRBA, MS4A1 (CD20), NFKB1, NFKB2, SEC61A1, TNFRSF13B (TACI), TNFRSF13C (BAFFR).* CD19 Molecule (*CD19*) encodes a critical component of the B cell receptor complex essential for B cell activation, and mutations cause severe impairments in B cell function[149]. CD81 Molecule (*CD81*) encodes a tetraspanin protein that is part of the B cell coreceptor complex, enhancing B cell receptor signaling; mutations disrupt B cell activation and antibody production[150,151]. Complement Receptor 2 (*CR2*, also known as *CD21*) encodes a receptor that functions in B cell activation and binds Epstein-Barr virus; mutations impair B cell function[152,153]. *ICOS* encodes a protein that is expressed on the surface of T cells and plays a crucial role in T cell activation and function, particularly in helping B cells during the immune response[154–156]. Mutations in *ICOS* can impair T cell-B cell interactions, leading to defective antibody production and compromised immune function[133,134]. Interleukin-21 (*IL21*) encodes a cytokine central to B cell proliferation and differentiation, and mutations impair B cell function[157]. IKAROS Family Zinc Finger 1 (*IKZF1*) encodes a transcription factor crucial for lymphocyte development, with mutations leading to defects in B cell maturation[158,159]. Interferon Regulatory Factor 2 Binding Protein 2 (*IRF2BP2*) encodes a transcriptional corepressor involved in immune regulation, and mutations can impair immune responses[160,161]. LPS-responsive vesicle trafficking, beach, and anchor protein (*LRBA*) encodes a protein involved in intracellular vesicle trafficking in immune cells, with

mutations causing defective receptor function and impacting B cell survival[143,147,162]. Membrane-Spanning 4-Domains Subfamily A Member 1 (*MS4A1*, also known as *CD20*) encodes a protein involved in B cell activation and proliferation, and mutations impair these processes[149,163,164]. Nuclear Factor Kappa B Subunit 1 (*NFKB1*) encodes a transcription factor regulating immune responses and cell survival, with mutations disrupting B cell development[165,166]. Nuclear Factor Kappa B Subunit 2 (*NFKB2*) encodes a transcription factor essential for B cell maturation; mutations impair B cell survival[167,168]. Inborn defects in *NFKB1* and *NFKB2*, which encode Nuclear factor kappa B subunit 1 (NF-κB1) and 2 (NF-κB2), respectively, are among the most common causes of monogenic CVID[169,170]. SEC61 Translocon Alpha 1 Subunit (*SEC61A1*) encodes a component of the protein translocation channel in the endoplasmic reticulum, where mutations can affect immune cell function[161]. Mutations in Tumor Necrosis Factor Receptor Superfamily Member 13B (*TNFRSF13B*, also known as *TACI*), which encodes a receptor that binds to ligands promoting B cell survival and antibody class switching, lead to defective B cell function[171–174]. Tumor Necrosis Factor Receptor Superfamily Member 13C (*TNFRSF13C*, also known as *BAFF-R*) encodes a receptor critical for B cell survival, where mutations reduce B cell numbers and impair their function.

1.2. NF-κB Signaling Pathways

The NF-κB signaling pathways have pivotal roles in regulating lymphocyte development, proliferation, survival, death and effector responses[165,175,176]. The NF-κB family consists of five related transcription factors: NF-κB1 p50/p105, NF-κB2 p52/p100, RELA, RELB, and c-Rel[177–179]. These transcription factors possess an N-terminal Rel homology domain (RHD) in common, which includes regions responsible for dimerization, IκB binding, and nuclear localization[177,178]. RELA, RELB, and c-Rel possess a C-terminal transcriptional

activation domain, which is not present in p50 and p52[180,181]. As a result, p50 and p52 homodimers act as transcriptional repressors unless they are paired with RELA, RELB, or c-Rel[181,182]. There are two main pathways linked to NF-κB: the canonical and noncanonical pathways[183] (Figure 1.1). The canonical NF-κB pathway activates a wide range of pro-inflammatory and anti-apoptotic genes[184,185]. In contrast, the noncanonical NF-κB pathway is triggered by a specific set of agonists, such as B-cell activating factor (BAFF), CD40 ligand (CD40L), lymphotoxin β (LTβ) and receptor activator of NF-κB ligand (RANKL)[186–188]. This pathway progresses more slowly and plays a crucial role in cellular differentiation and development[165,176,188].

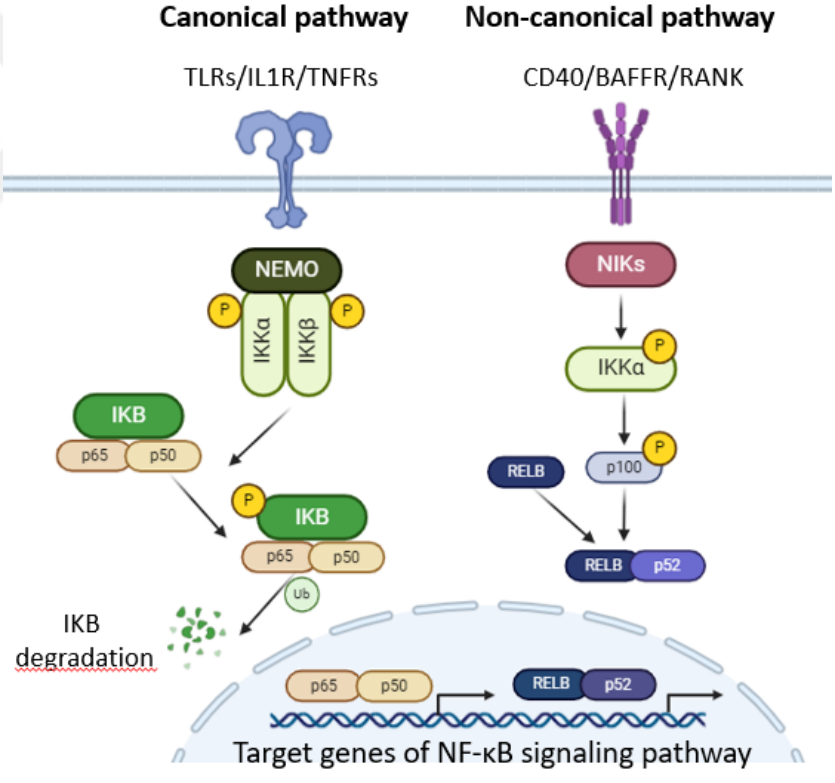

Figure 1.1 Canonical and non-canonical NFκB signaling pathways**.** Canonical pathway is activated by pro-inflammatory signals, leading to IκB degradation and nuclear translocation of NF-κB (p65/p50) to promote inflammation-related gene expression. Non-canonical pathway is triggered by specific TNF receptors (e.g., CD40), resulting in NIK-dependent processing of p100 to p52, which pairs with RELB to regulate immune development genes. Adapted from Peng C. et al., 2020[189]. Created in BioRender.

Pro-inflammatory cytokines, such as Tumor necrosis factor (TNF) and IL-1, microbe-associated molecular patterns, and stress signals can all activate the canonical NF-κB pathway[190–192]. This path utilizes the IκB kinase (IKK) complex, which includes IKKα, IKKβ, and IKKγ[183,193]. When activated, IκB proteins are phosphorylated and degraded, allowing NF-κB dimers (p65-p50) to enter the nucleus and activate genes involved in immunological and inflammatory responses[194–196]. The non-canonical NF-κB pathway is activated by certain TNF receptor family members, such as BAFF receptor (BAFF-R), CD40, and LTβ receptor (LTβR), and does not need IKKβ or IKKγ [186,194,196]. Instead, it relies on NF-κB-inducing kinase (NIK) and IKKα. In resting cells, unprocessed p100 interacts with IκBδ through its C-terminal inhibitory domain, forming high-molecular weight "kappaBsome" complexes sequestering RELB and other NF-κB subunits, which thereby results in the inhibition of DNA-binding activity of NF-κB proteins (referred to as IκBδ regulatory function)[18,197] Upon activation of non-canonical pathway, NIK phosphorylates IKKα, which in turn phosphorylates the NF-κB2 precursor p100, resulting in the proteasomal degradation of p100 and processing into p52[168,187,188,198,199]. The resultant p52-RelB dimers go to the nucleus and control genes required for maturation of medullary thymic epithelial cells, lymphoid organ development, and B cell immunity[187,194,200,201].

The primary distinctions between these routes are their activation triggers, participating components, and regulatory targets, with the canonical pathway causing immediate and temporary responses and the non-canonical pathway linked with longer-term immune system development[168]. Dysregulation of both pathways can cause disorders such as CVID, where defective NF-κB signaling leads to weak immune responses and increased susceptibility to infections and autoimmune problems[183,194,202,203]. Investigating these

pathways is crucial for designing therapies to regulate NF-κB activity, potentially enhancing immune function and patient outcomes in disorders like CVID[185]. Alterations in NF-κB2 activity can have a substantial influence on immunological competence, as demonstrated in illnesses such as CVID, where dysregulation contributes to symptoms such as defective immunoglobulin production and aberrant lymphocyte function[169,204–206]. These modifications emphasize the gene's function in immunological homeostasis and the potential consequences of its disruption, such as increased susceptibility to infections and autoimmune disorders.

1.3. Aim of the study

CVID is the most frequent type of symptomatic PID and characterized by a wide variability in symptoms, from recurrent infections to autoimmunity, allergy, lymphoproliferation, malignancy, and pituitary insufficiency. Along with the lack of a clear understanding of the underlying causes of CVID, the precise causes underlying why symptoms vary so much from person to person are mostly unclear. Therefore, the diagnosis of these patients is often delayed due to variable clinical presentations. In majority of cases, the genetic cause remains unknown. However, advancements in NGS technologies have facilitated the identification of genes linked to both autosomal recessive and dominant forms of CVID. In our study, we focus on a multiplex family affected with CVID, aiming to identify genetic defects using WES and to perform comprehensive biochemical and functional characterization of the identified candidate disease-causing monogenic variant.

CHAPTER 2

Materials and Methods

2.1. Materials

All materials used in this study are listed in the sections below.

2.1.1. Cell culture media, solutions and recombinant protein

Table 2.1 Cell culture media, solutions and recombinant protein

Liquid consumable	**Catalog Number**	**Manufacturer**
Cell Culture Water Pyrogen free	L0970-500	Biowest, USA
Dimethyl sulphoxide	A3672-0100	AppliChem, USA
DMEM High Glucose w/L-glutamine wo/Sodium pyruvate	L0102-500	Biowest, USA
Dulbecco's PBS (dPBS) w/o Ca2+ & Mg2+	02-023-1A	Biological Industries, Israel
Fetal Bovine Serum, European Grade, South America origin	BI0-007-1A	Biological Industries, Israel
Lymphoprep™ Density Gradient Medium, Sterile, pH 6.3 - 7.3, Liquid	7801	STEMCELL Technologies, USA
Opti-MEM™ I Reduced Serum Medium	31985062	Thermo Scientific, USA
RBC Lysis solution 10X	01-888-1B	Biolegend, USA
RPMI 1640 w/stable glutamine	L0498-500	Biowest, USA
Trypsin-EDTA 1X Solution	L0930-100	Biowest, USA
Recombinant Human CD40L (TNFSF5) (carrierfree)	591704	Biolegend, USA

2.1.2. Contents of buffers

Table 2.2 Contents of buffers

Buffer	**Contents**	**Amount**

10X TBS	1M Tris HCl pH 7.5 5M NaCl ddH_2O	100 mL 300 mL 600 mL
1X TBS-T	10X TBS Tween-20 ddH_2O	100 mL 900 mL 1 mL
10X Running buffer	Tris base Glycine 20% SDS ddH_2O	30 g 144 g 50 mL complete to 1 L
10X Transfer buffer	Tris base Glycine ddH_2O	30 g 144 g complete to 1 L
1X Transfer buffer	10X Transfer buffer %100 Methanol ddH_2O	110 mL 165 mL 825 mL
2X RIPA Lysis buffer	NaCl EDTA Triton X-100 Sodium deoxycholate SDS 1M Tris-HCl, pH 7.6 ddH_2O	0.88 g 0.15 g 1 g 1 g 0.1 g 2.5 mL complete to 100 mL
Complete RIPA Lysis buffer	2X RIPA Lysis buffer 7X Protease inhibitor ddH_2O	700 µL 200 µL 500 µL
PBS-EDTA solution	dPBS solution EDTA solution	1 L 1 mL
1.5 M Tris-HCl pH 8.8	Tris base ddH_2O Adjust pH with HCl ddH_2O	6.06 g 60 mL … complete to 100 mL
0.5M Tris-HCl pH 6.8	Tris base ddH_2O Adjust pH with HCl ddH_2O	12.11 g 80 mL … complete to 100 mL
20% SDS solution	Sodium dodecyl sulphate ddH_2O	2 g complete to 100 mL
10% APS solution	APS ddH_2O	1 g complete to 10 mL
Mild Stripping Buffer	Glycine SDS Tween-20 ddH_2O Adjust pH to 2.2 with HCl ddH_2O	7.5 g 0.5 g 5 mL 400 mL … complete to 500 mL
5% Stacking gel	ddH_2O 40% Bis-acrylamide	4.2 mL 623 µL

	0.5 M Tris-HCl pH 6.8 20% SDS 10% APS TEMED	630 µL 25 µL 50 µL 5 µL
12% Separating gel	ddH2O 40% Bis-acrylamide 1.5 M Tris-HCl pH 8.8 20% SDS 10% APS TEMED	4.3 mL 3 mL 2.5 mL 50 µL 100 µL 4 µL
ITB Buffer	$MnCl_2$ 4 H_2O $CaCl_2$ 2 H_2O KCl PIPES (0.5 M, pH 6.7) ddH_2O	10.88 g 2.20 g 18.65 g 20 mL complete to 1 L
1% Agarose gel	Agarose (Biomax) 0.5X TBE buffer SafeView Classic	1 g 100 mL 5 µL
5X TBE buffer	Tris base Boric acid 0.5M EDTA pH:8.0 ddH_2O	27 g 13.75 g 10 mL complete to 500 mL
LB Broth Medium	NaCl Tryptone Yeast extract ddH_2O	4 g 4 g 2 g 400 mL
LB Agar Medium	NaCl Tryptone Yeast extract Agar ddH_2O 100 mg/mL Ampicillin (if applicable)	4 g 4 g 2 g 6 g 400 mL 400 µL

2.1.3. Chemicals and reagents

Table 2.3 Chemicals and reagents

Product name	**Catalog Number**	**Manufacturer**
Agar	05039-500G	Sigma Aldrich, USA
Agarose (Biomax)	BHE500	Prona, USA

Ammonium persulphate (APS)	7727-54-0	Sigma Aldrich, USA
Ampicillin sodium salt	BP1760-25	Fisher Bioreagents, USA
Acrylamide: Bis-Acrylamide 37.5:1 (40% Solution/Electrophoresis)	BP1410-1	Fisher Bioreagents, USA
Boric acid powder	302177	Carlo Erba, Germany
Bovine Serum Albumin (BSA)	BSA-1T	Capricorn, USA
cOmplete™, Mini, EDTA-free Protease Inhibitor Cocktail	11836170001	Roche, USA
DTT (dithiothreitol)	R0861	Thermo Scientific, USA
Ethanol	32221	Sigma Aldrich, USA
Ethylenediaminetetraaceti c Acid (EDTA)	E-5134	Sigma Aldrich, USA
Glycerol	15524	Sigma Aldrich, USA
Glycine	GLN001.1	BioShop, Canada
Hydrochloric acid (HCl)	30712-2.5L	Sigma Aldrich, USA
Isopropanol	100995	Sigma Aldrich, USA
Lipofectamine 3000 Transfection Kit	L3000-008	Thermo Scientific, USA
Mounting Medium	50011	Ibidi, Germany
Methanol	24229-2.5L-R	Sigma Aldrich, USA

N,N,N',N'-Tetramethyl ethylenediamine (TEMED)	1610801	BioRad, USA
NaCl	31434-1KG-R	Sigma Aldrich, USA
Orange G Sodium Salt (High Purity Grade)	E783-50G	Amresco, USA
Polyjet™ In Vitro DNA Transfection Reagent	SL100688	SignaGen Laboratories, USA
Ponceau S	C.I 27195	Applichem, USA
SafeView Classic	G108	ABM, USA
Skimmed Milk	-	Pınar, TR
Sodium deoxycholate	302-95-4	Sigma Aldrich, USA
Sodium dodecyl sulphate	822050	Merck, USA
Sodium hydroxide (NaOH)	O6203	Sigma Aldrich, USA
Triton X-100	A1694.0250	Applichem, USA
Trizma Base	T1503	Sigma Aldrich, USA
Tryptone	48647.02	Serva, Germany
Tween-20	777	Ambresco/VWR, USA
XT Sample Buffer, 4X	1610791	BioRad, USA
Yeast extract	1.037.530.500	Merck, USA

2.1.4. Antibodies

Table 2.4 Antibodies

Antibody	**Clone or Catalog Number**	**Company**	**Purpose**
Alexa Fluor® 488 anti- DYKDDDDK Tag Antibody	637317	Biolegend, USA	Immunofluorescence
Anti-FLAG	M2	Sigma-Aldrich, USA	Immunoblotting
Anti-GFP	JL-8	Clontech, Japan	Immunoblotting
Anti-Human GAPDH	1E6D9	Proteintech, USA	Immunoblotting
Anti-NFKB2(p100/p52)	Sc-7386	Santa Cruz, USA	Immunoblotting
DAPI	422801	Biolegend, USA	Immunofluorescence
Goat anti-Mouse IgG	72-8062-M001	Tonbo Biosciences, USA	Immunoblotting

2.1.5. Enzymes and enzyme buffers

Table 2.5 Enzyme and enzyme buffers

Enzyme	**Catalog #**	**Manufacturer**
XhoI	R0146S	NEB, USA
EcoRI-HF	R3101S	NEB, USA
SalI-HF	R3138S	NEB, USA
XbaI	R0145S	NEB, USA
Q5® High-Fidelity DNA Polymerase	M0491S	NEB, USA
5X Q5 Reaction Buffer	B9027S	NEB, USA
T4 DNA Ligase	M0202S	NEB, USA
Taq DNA Polymerase	LSG-EP0406	Thermo Scientific, USA
rCutSmart buffer	B6004S	NEB, USA

T4 DNA Ligase Reaction Buffer	B0202S	NEB, USA
10X Taq Buffer with $(NH_4)_2SO_4$	-	Thermo Scientific, USA
$MgCl_2$	-	Thermo Scientific, USA
dNTP-Set (Na salt) - 100mM	M3015.4125	Genaxxon Bioscience, Germany

2.1.6. Plasmids

All constructed plasmid maps were shown in the Appendix C.

Table 2.6 Plasmids

Plasmid	**Antibiotic Resistance**	**Manufacturer**
pcDNA3.1(+)	Ampicillin	Invitrogen, USA
pCI-neo-N-3xFLAG	Ampicillin	Promega, USA
pCI-neo-C-3xFLAG	Ampicillin	Promega, USA
pNiFty-SEAP	Ampicillin	Invivogen, USA
pRL-TK	Ampicillin	Promega, USA
pNF-κB-Firefly-Luc	Ampicillin	Promega, USA

2.1.7. Primers

Table 2.7 Primers

Primer	**Sequence**	**Purpose**
NFKB2_Y868N_Fwd	CCCTGGAAGGTGGATCTG	Sanger sequencing (Y868N)
NFKB2_Y868N_Rev	TTGAAATAGGTGGGGACGC	Sanger sequencing (Y868N)
NFKB2_XbaI_Fwd	CAGTCTAGAATGGAGAGTTGCTACAACCC	Cloning (pCI-Neo-N3xFlag)
NFKB2_SalI_Rev	GATGTCGACTCAGTGCACCTGAGGCTG	Cloning (pCI-Neo-N3xFlag)
NFKB2_Y868N_Fwd	GGAAGACAGTGCGAACGGGAGCCAGTC	SDM (pCI-Neo-N3xFlag)

NFKB2_Y868N_Rev	GACTGGCTCCCGTTCGCACTGTCTTCC	SDM (pCI-Neo-N3xFlag)
NFKB2_Seq1_Fwd	CCTGAAGCCAGTCATCTCCC	Sanger Sequencing (NFKB2 ORF)
NFKB2_Seq1_Rev	GGGAGATGACTGGCTTCAGG	Sanger Sequencing (NFKB2 ORF)
NFKB2_Seq2_Fwd	CTACTCGACTACGGCGTCAC	Sanger Sequencing (NFKB2 ORF)
NFKB2_Seq2_Rev	GTGACGCCGTAGTCGAGTAG	Sanger Sequencing (NFKB2 ORF)
NFKB2_Seq3_Fwd	CTGAAGGCTGGTGCTGACATC	Sanger Sequencing (NFKB2 ORF)
NFKB2_Seq3_Rev	GATGTCAGCACCAGCCTTCAG	Sanger Sequencing (NFKB2 ORF)
NFKB2_R853X_SalI_Rev	GATGTCGACTCAGGTTTCTGGACCCCTCAG	Cloning (pCI-Neo-N3xFlag)
NFKB2_R635X_SalI_Rev	GATGTCGACTCATCCCCCCTGCCGCTCTG	Cloning (pCI-Neo-N3xFlag)
Relb_EcoRI_Fwd	CTGAGAATTCATGCTTCGGTCTGGGCC	Cloning (pcDNA3.1(+))
Relb_XbaI_Rev	GATTCTAGACTACGTGGCTTCAGGCCC	Cloning (pcDNA3.1(+))
RelB_Seq1_Fwd	CATCGAGCTCCGGGATTGTG	Sanger Sequencing (RelB ORF)
RelB_Seq1_Rev	CACAATCCCGGAGCTCGATG	Sanger Sequencing (RelB ORF)
RelB_Seq2_Fwd	CCATTGCCTTTCACGTACCTG	Sanger Sequencing (RelB ORF)
RelB_Seq2_Rev	CAGGTACGTGAAAGGCAATGG	Sanger Sequencing (RelB ORF)
NIK_EcoRI_Fwd	GTACGAATTCATGGCAGTGATGGAAATGGC	Cloning (pcDNA3.1(+))
NIK_XhoI_Rev	TATCCTCGAGTTAGGGCCTGTTCTCCAGC	Cloning (pcDNA3.1(+))

NIK_Seq1_Fwd	CAGGAGGATGAGTCTCCAC	Sanger Sequencing (NIK ORF)
NIK_Seq2_Rev	GTGGAGACTCATCCTCCTG	Sanger Sequencing (NIK ORF)
NIK_Seq3_Fwd	GCGGCTGGAAGTATTTCG	Sanger Sequencing (NIK ORF)
NIK_Seq4_Rev	CGAAATACTTCCAGCCGC	Sanger Sequencing (NIK ORF)
NIK_Seq5_Fwd	GAGAGAGCTTTCGCCAAGG	Sanger Sequencing (NIK ORF)
NIK_Seq6_Rev	CCTTGGCGAAAGCTCTCTC	Sanger Sequencing (NIK ORF)
SV40-poly(A)-signal_Rev	GCATTCTAGTTGTGGTTTGTCC	Colony PCR (pCI-Neo-N-3xFlag)
VP1.5 Ext	CGGGACTTTCCAAAATGTCGT	Colony PCR (pCI-Neo-N-3xFlag)
BGH-Reverse	GGCACCTTCCAGGGTCAAGG	Colony PCR (pcDNA3.1(+))
NFKB2_405-900aa_EcoRI_Fwd	GTATGAATTCATGGCGCAGATG GCCGCCACGG	Cloning (pCI-Neo-C3xFlag)
NFKB_405-900aa_XbaI_Rev	GATTCTAGAGGGTGCACCTGAG GCTGGGGG	Cloning (pCI-Neo-C3xFlag)
NFKB2_R853X_400-853aa_XbaI_Rev	GATTCTAGAGGGGTTTCTGGAC CCCTCAGCAG	Cloning (pCI-Neo-C3xFlag)

2.1.8. Kits

Table 2.8 Kits

Kit	Catalog Number	Manufacturer
BCA Protein Assay Kit	T9300A	TaKaRa Bio, USA
Secreted Alkaline Phosphatase Reporter Gene Assay Kit (Luminescence)	600260	Cayman, USA

The Dual-Glo® Luciferase Assay System	E2920	Promega, USA
WesternBright ECL HRP substrate kit	K-12045-D50	Advansta, USA
WizPrep Gel/PCR Purification Mini Kit	W70050-300	Wizbiosolutions Inc. Republic of Korea
WizPrep™ gDNA Mini Kit (Blood)	W71050-100	Wizbiosolutions Inc. Republic of Korea
WizPrep™ Plasmid DNA Mini Kit	W70050-100	Wizbiosolutions Inc. Republic of Korea

2.1.9. Equipment

Table 2.9 Equipment

Equipment	**Model**	**Manufacturer**
AmershamTM Luminescent Image Analyzer	AmershamTM Imager 600	GE Healthcare Life Sciences, USA
Centrifuge	Eppendorf 5415 R	Eppendorf, USA
Centrifuge	Universal 320	Hettich, Germany
Heat Block	Type 17600 Dri-Bath	Thermolyne, USA
Confocal Microscope	Leica SP8	Leica Microsystems, Germany
Liquid Nitrogen Refrigerator	LS4800	Worthington Industries, USA

Microplate Reader	SynergyTM HT	BioTek, Tr
NanoDrop Microvolume UV-Vis Spectrophotometer	NanoDrop One	Thermo Scientific, USA
pH meter	S-610L	Peak Instruments, USA
Spectrophotometer	UV-5100	SOIF, China
Thermal cycler	2720 Thermal cycler	Applied Biosystems, USA
Thermal cycler	TC-512	Techne, USA
ZX3 Advanced Vortex Mixer	F202A0176	VELP Scientifica, Italy

2.1.10. Other materials

Table 2.10 Other materials

Product	**Catalog #**	**Manufacturer**
1 mL syringe	70575	Ayset, Tr
BD Vacutainer® Heparin Tubes	367874	BD Biosciences, USA
Cryovials, 2 mL	122263	Greiner, USA
GeneRuler 1 kb DNA Ladder	SM0311	Thermo Scientific, USA
Hemocytometer Neubauer	C962010	Marienfeld Superior, Germany
Mini-PROTEAN Tetra Handcast Systems	1658007FC	BioRad, USA

Molecular Biology grade water	01-869-1B	Biological Industries, Israel
Mr. Frosty™ Freezing Container	5100-0001	Thermo Scientific, USA
Prime-Step Prestained Broad Range Protein Ladder	773302	BioLegend, USA
WesternBright PVDF-FL membrane roll, 0.45 µm, 26 cm x 3.3 m	L-08025-001	Advansta, USA

2.2. Methods

2.2.1. Patient recruitment and ethics

Oral and written informed consents were obtained from the patients and healthy donors, and clinical information and biological samples from the patients were collected by the clinician. This study was conducted in accordance with the institutional, local, and national ethical guidelines, and with the 1964 Helsinki Declaration and its later amendments or comparable ethical standards. The study was approved by the İhsan Doğramacı Bilkent University Ethics Committee (#2022_04_28_01).

2.2.2. Genomic DNA isolation from whole blood

2.2.2.1. Red blood cell lysis

Whole blood samples taken using blood collection tubes containing heparin were delivered to the laboratory on the same day for processing. First, approximately 1 mL of blood was carefully transferred into 15 mL volume conical centrifuge tubes. To these tubes, 9 mL of 1X red blood cell (RBC) lysis solution was added and the samples were inverted to mix thoroughly. This mixture was incubated at RT for 20 min. After the incubation period, the samples were separated by centrifugation at 400 g for 5 min at RT.

The resulting supernatants were carefully removed and the remaining pellets were resuspended with 3 mL of 1X RBC lysis solution. After this process, the pellets were incubated for another 10 min at RT and centrifuged at 400 g for 10 min at RT. Supernatants were removed again and pellets were resuspended with 1 mL of 1X RBC lysis solution. The cells were then transferred to 1.5 mL centrifuge tubes and centrifuged at 13,000 rpm for 1 min. The supernatants were removed once again and the remaining pellets were made ready for immediate use for genomic DNA (gDNA) isolation.

2.2.2.2. gDNA isolation

WizPrep™ gDNA Mini Kit (Blood) kit was used for gDNA isolation. Pellets obtained from RBC lysis were resuspended with 200 µL of 1X dPBS, followed by the addition of 200 µL of GB Buffer and 20 µL of Proteinase K, which we mixed by vortexing. The mixture was incubated at 56 ℃ for 10 min, and we inverted the tube every 5 min. Subsequently, 200 µL of 100% ethanol was added to the sample lysates, and we briefly vortexed the mixture. The mixture was then applied to a Spin Column connected to a 2 mL Collection tube and centrifuged for 1 min at 13,000 rpm. The Spin Column was transferred to a new Collection tube, and we discarded the flow-through. The Spin Column was then washed with 500 µL of W1 Buffer and centrifuged for 1 min at 13,000 rpm, followed by another wash with 500 µL of W2 Buffer (with added ethanol) and centrifugation for 1 min at 13,000 rpm. We discarded the flow-through, and the Spin Column was centrifuged for an additional 2 min at 13,000 rpm. For elution, the Spin Column was connected to a new 1.5 mL tube, and we added 80 µL of Elution Buffer, incubated it at room temperature for 1 min, and centrifuged for 1 min at 13,000 rpm. We then removed and discarded the spin columns, and the concentration of purified gDNA collected in 1.5 mL centrifuge tubes was measured with a NanoDrop™ One/OneC

Microvolume UV-Vis Spectrophotometer. The resulting purified gDNAs were stored at −20 °C for later use.

2.2.3. Peripheral blood mononuclear cell isolation

Whole blood was placed in blood collection tubes containing heparin in volumes ranging from 6 to 10 mL and processed immediately on the same day. These blood samples were transferred to 15 mL conical centrifuge tubes and diluted 1:1 (v/v) with pre-warmed 1x dPBS at RT. Lymphoprep™ Density Gradient Medium was then added to empty 15 mL conical centrifuge tubes with a final ratio of the blood™ mixture of 2:1 (v/v). Diluted blood was carefully placed on top of Lymphoprep™ separation medium and samples were centrifuged at 800 g at RT for 20 min with the deceleration setting at zero. As a result of this process, four separate layers were formed. Peripheral blood mononuclear cells (PBMCs) in the cloudy layer were removed using sterile Pasteur pipettes and moved into 15 mL conical centrifuge tubes supplemented with 3 mL of Wash medium containing 2% FBS. These tubes were filled with 14 mL of Wash medium. The samples containing PBMCs were centrifuged at 250 g for 10 min and then the supernatants were removed. PBMCs were counted with a hemocytometer after washing in 8 mL of Wash medium. The samples were then centrifuged again at 250 g for 10 min and the supernatants were removed. PBMC aliquots were resuspended in freezing medium (FBS + 10% DMSO) at a density of $5x10^6$ cells/mL and incubated overnight at -80 °C. Transferred to cryovials for cryopreservation using the Frosty™ Freezing Container. The next day, the cryopreserved vials were placed in a liquid nitrogen tank for later use.

2.2.4. Genetic analysis

2.2.4.1. Whole-exome sequencing

gDNA isolated from the peripheral blood of the patients were used for whole-exome sequencing (WES). WES including library preparation, raw sequencing-data collection, alignment with the reference human genome (GRCh37), variant calling and annotations were performed by a service provider, Genoks, Turkey, as previously described[207]. The allele frequency (AF) values were obtained from the public genome databases: gnomAD[208], Bravo[209], UK Biobank-Allele Frequency Browser (AFB)[210], Turkish Genome Project Data Sharing Portal (TGP) (https://tgd.tuseb.gov.tr/), which includes genome data of more than 500 healthy individuals from Turkey. WES data variant filtering was performed with the help of Yılmaz Yücehan Yazıcı.

2.2.4.2. Interpretation of variants

Prediction of the damaging impact of variants was performed utilizing various algorithms including AlphaMissense[211], Combined annotation-dependent depletion (CADD) v1.7[212], MutationTaster[213], Polymorphism Phenotyping v2 (PolyPhen-2)[212], and Sorting intolerant from tolerant (SIFT)[214]. Variant significance related to the human health was obtained from the ClinVar database (https://www.ncbi.nlm.nih.gov/clinvar/). OMIM (https://www.omim.org/) database was used to obtain clinical significance of the variants. Variant clinical interpretation was performed following the American College of Medical Genetics and Genomics (ACMG) and the Association for Molecular Pathology (AMP) guidelines[207].

2.2.4.3. Sanger sequencing of gDNA

Sanger confirmation of the *NFKB2* mutation status in the patients and their family members was done by amplification of approximately 300 bp region encompassing the p.Y868N mutation on their gDNAs. Primers used in this reaction are listed in Table 2.7.

PCR amplicons were purified using WizPrep™ Gel/PCR Purification Mini Kit. Sanger sequencing of PCR products was performed by the service provider, Macrogen (Europe).

2.2.5 Generation of NFKB2 constructs

2.2.5.1 Generation of NFKB2 constructs and site-directed mutagenesis

Generation of desired constructs was performed with the help of Aysima Atılgan Lülecioğlu. The human canonical *NFKB2* (NM_001322934.2) open reading frame (ORF) was PCR amplified using cDNA generated from PBMCs. It was cloned in frame with N-terminal 3x DYKDDDDK (FLAG)-tag into the pCI-Neo-N-3xFlag vector through XbaI and SalI sites. Site-directed mutagenesis (SDM) following a modified overlap-extension PCR-based method was used to generate plasmids encoding mutant NF-κB2 as previously described[215]. To generate pCI-Neo-N-3xFlag constructs encoding mutant NF-κB2 (p.Y868N) and truncated NF-κB2 with p.R635X or p.R853X, the wild-type (WT) full-length NF-κB2 (NP_001309863.1, 900 amino acids)-encoding plasmid was used as a PCR template. The NF-κB2 p.Y868N was amplified with NFKB2_XbaI_Fwd/NFKB2_Y868N_Rev, and NFKB2_SalI_Rev/NFKB2_Y868N_Fwd primer pairs. The PCR products were purified with WizPrep™ Gel/PCR Purification Mini Kit. One-step overlap extension PCR was performed to anneal fragments to each other. To confirm the expected sizes of PCR products, agarose gel electrophoresis was performed. The PCR products having orange loading dye at 1X final concentration were loaded into 1% agarose gel and run for 30 min at 120 V. Amersham Imager 600 was used to visualize DNA. The final PCR products were then purified with WizPrep™ Gel/PCR Purification Mini Kit.

The PCR reaction mixture includes 10 µL Q5 Reaction Buffer, 1 µL dNTPs, 5 µL primers, 2 ng of template DNA, and 0.5 µL Q5 High-Fidelity DNA Polymerase and molecular

biology grade water up to 50 µL. The thermocycling conditions involve initial denaturation at 98 °C for 30 sec, followed by 35 cycles of denaturation (98 °C for 10 sec), annealing (60 °C for 30 sec), and extension (72 °C for 1 min 30 sec). The final extension (72 °C for 2 min). One-step overlap extension PCR conditions: 98 °C (30 sec), 60 °C (30 sec), 72°C (2 min), primers were added; then, initial denaturation at 98 °C for 30 sec, followed by 35 cycles of denaturation (98 °C for 10 sec), annealing (60 °C for 30 sec), and extension (72 °C for 1 min 30 sec) and the final extension (72 °C for 2 min).

WT NF-κB2 C-terminal fragment (amino acids 405-900) and mutant fragments with p.Y868N or p.R853X were PCR-amplified on the pCI-Neo-N-3xFlag constructs encoding WT or mutant NF-κB2, and cloned in frame with C-terminal 3x DYKDDDDK (FLAG)-tag into the pCI-Neo-C-3xFlag through EcoRI and XbaI sites. WT NF-κB2 C-terminal fragment and the mutant one with p.Y868N were amplified by using NFKB2_405-900aa_EcoRI_Fwd and NFKB_405-900aa_XbaI_Rev primers. NF-κB2 C-terminal with p.R853X was amplified by NFKB2_405-900aa_EcoRI_Fwd and NFKB2_R853X_400-853aa_XbaI_Rev primers. PCR reaction mix and thermocycling conditions were as described above. Primers used are listed in Table 2.7. The expected size of the PCR products was checked by agarose gel electrophoresis. Then, products were purified using WizPrep™ Gel/PCR Purification Mini Kit.

2.2.5.2 Generation of NIK and RELB constructs

NIK (NM_003954.5) and RELB (NM_006509.4) ORFs were amplified by using cDNA generated from PBMCs. PCR amplicons of NIK and RELB were inserted into the pcDNA3.1(+) vector through EcoRI/XhoI and EcoRI/XbaI sites, respectively. The PCR products were purified using the WizPrep™ Gel/PCR Purification Mini Kit. To confirm the expected sizes of the PCR products, agarose gel electrophoresis was utilized. The PCR

products were mixed with orange loading dye (1X final concentration) and loaded into a 1% agarose gel containing 1X SafeView™ Classic nucleic acid stain. The gel was run for 30 min at 120 V. Visualization of the DNA bands was performed using the Amersham Imager 600. The annealed PCR products were subsequently purified again with the WizPrep™ Gel/PCR Purification Mini Kit.

The PCR reaction to generate NIK ORF mixture includes 10 µL Q5 Reaction Buffer, 1 µL dNTPs, 5 µL primers, 2 ng of template DNA, and 0.5 µL Q5 High-Fidelity DNA Polymerase and molecular biology grade water up to 50 µL. The thermocycling conditions involve initial denaturation at 98 °C for 30 sec, followed by 35 cycles of denaturation (98 °C for 10 sec), annealing (67 °C for 30 sec), and extension (72 °C for 2 min 30 sec), and the final extension (72 °C for 2 min). The PCR reaction to generate RELB ORF mixture includes 10 µL Q5 Reaction Buffer, 1 µL dNTPs, 5 µL primers, 2 ng of template DNA, and 0.5 µL Q5 High-Fidelity DNA Polymerase and molecular biology grade water up to 50 µL. The thermocycling conditions involve initial denaturation at 98 °C for 30 sec, followed by 35 cycles of denaturation (98 °C for 10 sec), annealing (68 °C for 30 sec), and extension (72 °C for 1 min 10 sec), and the final extension (72 °C for 2 min).

2.2.5.3 Restriction enzyme digestion of PCR products and vectors

For pCI-neo-N-3xFLAG with WT or mutant NF-κB2, purified PCR products and 700 ng of the pCI-neo-N-3xFLAG mammalian expression vector were digested with XbaI and SalI enzymes at 37 °C for 3 h. The resulting digested products were purified using the WizPrep™ Gel/PCR Purification Mini Kit. The restriction enzyme reaction mixture consisted of 700 ng of pCI-neo-N-3xFLAG, 5 µL of 10X rCutSmart Buffer, 1 µL each of XbaI and SalI and molecular biology grade water up to 50 µL. For pCI-neo-C-3xFLAG with WT or mutant NF-κB2 C-terminal fragments, purified PCR products and 700 ng of

the pCI-neo-C-3xFLAG was digested with EcoRI and XbaI with the same procedure described above. For NIK and RELB, pcDNA3.1(+) mammalian expression vector and PCR products purified were digested with EcoRI/XhoI and EcoRI/XbaI sites, respectively, as described above.

2.2.5.4 Ligation of digested products

The digested and purified PCR products were ligated into the digested empty mammalian expression vector using T4 DNA Ligase at room temperature for 15 min. The ligation reaction mixture included 1 μL of the digested pCI-neo-N-3xFLAG vector, 3.0 μL of the PCR product, 0.5 μL of T4 DNA Ligase and 0.5 μL of 10X T4 DNA Ligase buffer.

2.2.5.5 Transformation of the ligation products

DH5α competent cells were used for transformation of ligation products. These cells were removed from a glycerol stock by streaking onto an LB agar plate and incubated overnight at 37 °C. Then, a single colony was selected and transferred to LB broth and grown at 37 °C, followed by incubation at 20 °C. When the optical density of the culture reached 0.55, it was divided into two tubes and centrifuged. Cells were resuspended with cold Inoue transformation buffer (ITB). After a second centrifugation, the pellets were mixed and treated with DMSO. The cells were then incubated on ice, aliquoted, snap frozen with liquid nitrogen, and stored at -80 °C. For transformation, ligation products, 5 μL each, were added to 50–60 μL of competent cells. The mixture was incubated on ice for 15 min. After the incubation, tubes were subjected to a heat shock at 42 °C for 45 sec. Afterwards, the tubes were incubated on ice for another 2 min. 800 μL of LB broth medium was added to the tubes and incubated at 37 °C for 45 min with constant shaking. Finally, 100 μL of

the suspension was spread on LB agar plates containing ampicillin and plates were incubated at 37 °C overnight.

2.2.5.6 Screening for positive colonies by PCR

A sterile pipette tip was used to transfer bacteria from single colonies into PCR tubes containing 50 µL of molecular biology grade water. This bacteria-containing water used as a template in colony PCR. The resulting PCR products were mixed with orange loading dye (1X final concentration) and loaded into a 1% agarose gel with 1X SafeView™ Classic nucleic acid stain. The gel was run at 120 V for 30 min. The presence of NFKB2 inserts was confirmed by visualizing bands of the expected size (2700 bp) on the agarose gel. The colonies with inserts were then transferred into 2 mL LB broth containing ampicillin and incubated overnight at 37 ℃ with constant shaking. SV40-poly(A)-signal_Rev and VP1.5 Ext primers were used for pCI-neo-N-3xFLAG and pCI-neo-C-3xFLAG plasmids. BGH-Reverse and VP1.5 Ext were used for pcDNA3.1(+) plasmid. PCR reaction mixture included 2.5 µL Taq buffer, 2 µL MgCl2, 0.5 µL 10mM dNTPs, 1 µL 5 mM forward primer, 1 µL 5 mM reverse primer, 0.125 µL Taq polymerase, 2.5 µL sample, and 15.35 µL molecular biology grade water. PCR conditions: 95 ℃ 5 min initial denaturation, 95 ℃ 30 sec denaturation (30 cycles), 59 ℃ 30 sec annealing (30 cycles), 72 ℃ 3 min extension (30 cycles), 72 ℃ 5 min final extension.

2.2.5.7 Isolation of plasmid DNA

Plasmid DNA was isolated from bacterial cultures using the WizPrep™ Plasmid DNA Mini Kit. Initially, cultured bacteria were transferred to 2 mL microcentrifuge tubes. These tubes were then centrifuged at 13,000 rpm for 1 min, and the supernatant was subsequently discarded. Resuspension of the bacterial pellet was achieved by adding 200

μL of PD1 buffer, which contained RNase. Following this, PD2 buffer was added to the solution, and the tubes were mixed through inversion 10 times. This mixture was then allowed to incubate at room temperature for 2 min. After incubation, PD3 buffer was added to the mix, and the tubes were inverted 10 times. The mixture was centrifuged at 13,000 rpm for 10 min. The supernatant was transferred to a spin column placed within a 2 mL collection tube, which was then centrifuged at 13,000 rpm for 1 min. The flow-through was discarded. Next, 600 μL of wash buffer was added into the spin column and centrifuged at the same speed for 1 min. The flow-through was removed. An additional centrifugation step for 2 min at 13,000 rpm was performed to ensure all residual wash buffer was eliminated. Then, the spin column was transferred to a new microcentrifuge tube. We added 50 μL of elution buffer directly onto the column matrix and allowed it to sit for 5 min at room temperature. The final centrifugation at 13,000 rpm for 1 min was conducted to collect the eluted DNA, which was then measured for concentration using a spectrophotometer and stored at -20 ℃. All plasmid constructs generated were validated by Sanger sequencing, a service provided by Macrogen (Europe). The specific primer sequences utilized are detailed in Table 2.7.

2.2.6. Cell culture

2.2.6.1. Maintenance and propagation of cell lines

PBMCs were separated using Lymphoprep and were subsequently stored long-term in a cryopreserved state. Lymphoblastoid B cells, which were generated with the help of Serkan Belkaya as previously described[215,216], were cultured in RPMI supplemented with 10% FBS. HEK293 cells were cultured in DMEM with High-Glucose supplemented with 10% FBS. Cells in culture were maintained at 37 °C in a humidified incubator with 5% CO_2.

2.2.6.2. Cryopreservation of cells

Once the adherent cells reached confluence, the medium was discarded and the cells were rinsed with dPBS solution. Trypsin-EDTA solution was then used to detach the adherent cells. After trypsinization, we collected the cells with 6 mL of fresh culture media and centrifuged at 300 g for 5 min. After centrifugation was completed, the supernatant was discarded and the cell pellets were resuspended in freezing medium with FBS solution containing 10% (v/v) DMSO. For HEK293 cells, we transferred 1 mL of the cell suspension, containing 7 million cells per mL, into each cryovial. They were incubated overnight at −80 °C in Mr. Frosty Cell Freezing Container. Similarly, Lymphoblastoid B cells in suspension were collected and centrifuged at 300 g for 5 min. After centrifugation, the supernatant was removed and the cell pellets were resuspended in a freezing environment with FBS solution containing 10% (v/v) DMSO. We then transferred 1 mL of Lymphoblastoid B cell suspension, with a density of 10 million cells per mL, into each cryovial. They were stored them overnight at -80 °C in a Mr. Frosty Cell Freezing Container. Finally, we moved the cryovials to liquid nitrogen for long-term storage.

2.2.6.3. Thawing of frozen cell lines

Frozen cells stored in cryovials were removed from the liquid nitrogen tank and rapidly thawed in a 37 °C water bath. We added fresh growth medium to remove thawed cells from freezer storage vials. The cell suspension was then transferred to a 15 mL canonical centrifuge tube and centrifuged at 300 g force for 5 min. After centrifugation, the supernatant was removed and the cell pellet was resuspended in fresh growth medium. The cell suspension was then carefully transferred to a suitable culture flask. Finally, this vial was placed in an incubator set to maintain a temperature of 37 °C and provide an environment containing 5% CO_2 to support the maintenance and growth of the cells.

2.2.6.4. Transient transfection of mammalian cell lines

HEK293 cells were seeded on 24-well plates at a density of 1.5 x 10^5 cells/mL (500 µL/well) and incubated overnight at 37 °C, 5% CO^2. After 16-18 h of incubation, cells with 70%-80% confluency were transfected with either empty vector, WT or mutant NF-κB2 constructs (300 ng), GFP-encoding plasmid (100 ng) for transfection efficiency, and/or NIK-encoding plasmid (100 ng). Plasmids required for transfection were prepared using Polyjet™ reagent and transferred to a centrifuge tube. Dilution was done with 50 µL serum free DMEM. We then added this diluted reagent-serum free DMEM mixture to the diluted plasmids and mixed well by pipetting to ensure that the mixture was homogeneous. The mixture was allowed to incubate at room temperature for 15 min. After this process, we carefully added the diluted transfection complexes dropwise into the wells of a 24-well plate. Cells were incubated for 48 h at 37 °C in a 5% CO environment until required for further procedures. During the transient transfection process, the ratio of reagent to DNA was determined as 1:3; This is equivalent to 3 µL of reagent for every 1 µg of DNA. The total amount of DNA and the volume of transfection reagent were adjusted according to the size of the cell culture plate used in the experiment.

2.2.7. Immunoblotting

2.2.7.1. Cell lysis and protein extraction

HEK293 cells were harvested at 48 h post-transfection and centrifuged at 13,000 rpm for one minute. After removing the supernatant, the cell pellets were resuspended in ice-cold complete RIPA lysis buffer containing protease inhibitor cocktail and cells were lysed by this process. To obtain a homogeneous lysate, cell lysates were processed with 1 mL syringes. Next, we incubated the lysates on ice for 30 min. Lysates were then centrifuged at 13,000 rpm for 20 min at 4 °C. Supernatants containing protein extracts were carefully

transferred to new 1.5 mL centrifuge tubes and stored at −80 °C for further use. Lymphoblastoid B cells in 48-well plates ($2x10^6$ cells/well) were stimulated with CD40L (2 μg/mL) for 4 h. Cells were lysed with 1x RIPA buffer supplemented with the complete protease inhibitor cocktail as described above.

2.2.7.2. Quantification of total protein

Total protein concentration in cell lysates was measured with the TaKaRa BCA Protein Assay Kit. In the first step, cell lysate samples were thawed on ice and then diluted 1:100 (v/v) with Molecular Biology grade water. Bovine serum albumin (BSA) protein standards were prepared as 10 μg/ml, 20 μg/ml, 30 μg/ml, 40 μg/ml, 50 μg/ml, 70 μg/ml and 100 μg/ml. Aliquots of 100 μL of diluted protein samples and BSA standards were transferred to a flat-bottom 96-well plate. Then, 100 μL of Bicinchoninic acid (BCA) solution prepared by mixing Reagent A and Reagent B at a ratio of 1:100 (v/v) was added to each well. The plate was incubated at 37 °C for 1.5 h. After incubation was completed, absorbance values were measured at a wavelength of 620 nm using a Synergy HT Microplate Reader. Standard curves were created using the absorbance values of BSA protein standards and total protein concentrations of protein extracts were calculated based on these curves.

2.2.7.3. Denaturation of protein samples

The desired amount of cell lysate was transferred to 1.5 mL centrifuge tubes. Lysates were mixed with 4X Laemmli sample buffer and 10X DTT. Next, the volume of the samples was adjusted by making up to 30 μL with complete RIPA lysis buffer. Next, the samples were boiled at 95 °C for 5 min. After the boiling process was completed, the samples were used for immunoblotting.

2.2.7.4. SDS-Polyacrylamide gel electrophoresis

SDS-Polyacrylamide gel electrophoresis (SDS-PAGE) was performed using polyacrylamide gels containing 12% SDS. Stacking and separation of polyacrylamide gels were prepared as shown in Table 2.2 using a gel casting apparatus. After polymerization was completed, polyacrylamide gels were placed in vertical electrophoresis cells in a western blot tank filled with 1X Running buffer. Boiled protein samples stored at room temperature were loaded onto polyacrylamide gels. The electrophoresis process was started at 80 V for 20 min and continued by increasing to 120 V for 1.5 h.

2.2.7.5. Wet transfer of proteins onto membrane

Proteins in polyacrylamide gels were transferred to polyvinylidene difluoride (PVDF) membranes using a Wet transfer system. In buckets filled with 1X Transfer buffer, transfer sandwiches were prepared in the following order: one fiber pad, two blotting papers, a PVDF membrane, a polyacrylamide gel, two blotting papers, and another fiber pad. These sandwiches were then placed in transfer cassettes located in the transfer tank. The tank was filled with ice-cold 1X Transfer buffer and placed in an ice container to maintain the low temperature. The wet transfer process was performed at 250 mA for 2 h on ice. After the transfer process was completed, the membranes were stained with Ponceau dye for two min to evaluate the transfer efficiency of the membranes. After staining was completed, membranes were washed with 1X TBS for 5 min. Then, they were blocked with a solution containing 10% skimmed milk for 30 min at room temperature and then washed 3 times with 1X TBS-T for 5 min each.

2.2.7.6. Protein detection

The immunoblotting procedure involves the use of primary and secondary antibodies as described in Table 2.4. Membranes were treated with an anti-NFKB2 antibody and incubated overnight at +4 °C on an orbital shaker. To assess transfection efficiency, membranes were also incubated with an anti-GFP antibody under similar conditions. As a loading control, anti-human GAPDH antibody was used and membranes were incubated on an orbital shaker for 4 h at room temperature. After primary antibody treatment, membranes were washed three times with 1X TBS-T at room temperature, each wash lasting 5 min. Then, membranes were incubated with secondary antibody at room temperature on an orbital shaker for 30 min. After this incubation, membranes were subjected to a series of three additional washes with 1X TBS-T at room temperature, each lasting 5 min. WesternBright® ECL Chemiluminescent HRP Substrate Kit was used for detection. The components of WesternBright ECL were mixed at a ratio of 1:1 and applied to the membranes for 2 min in the dark at room temperature. Detection was performed with Amersham Imager 600.

2.2.7.7. Stripping and re-immunoblotting of blotted membranes

Stripping and re-probing were performed to sequentially stain the membranes with various antibodies. After the first primary antibody was used and detection was performed, the membranes were stripped with Mild Stripping Buffer on an orbital shaker for 10 min at room temperature. After stripping, the membranes were rinsed with 1X TBS-T for 5 min. Then, the membranes were blocked with 10% skimmed milk for 30 min at room temperature. After blocking, the membranes were washed three times with 1X TBS-T for 5 min each. After these steps, the membranes were ready for re-immunoblotting by the previously described method.

2.2.8. Confocal microscopy

HEK293 cells, seeded on coverslips in 6-well plates, were transiently transfected with either WT or mutant NF-κB2 constructs (1125 ng) together with either an empty vector or a NIK-encoding plasmid (375 ng). We fixed the cells with 4% paraformaldehyde (PFA) for 15 min at room temperature at 48 h post-transfection. We then permeabilized them with 0.5% Triton X-100 in PBS for 10 min and blocked with 5% BSA for 30 min at room temperature. We stained the cells overnight at 4 °C in the dark with Alexa Fluor® 488 anti-DYKDDDDK Tag Antibody. Following the staining, we washed the cells and counterstained the nuclei with DAPI. We mounted the coverslips using Anti-Fade Fluorescence Mounting medium and acquired images using a Leica SP8 Confocal Microscope with a 63X objective and immersion oil. The antibodies we used are listed in Table 2.4.

2.2.9. Reporter assays

For the luciferase reporter assay, we seeded HEK293 cells in 96-well plates at a density of 2.5 x 10^5 cells/mL (100 µL/well) and transiently transfected them with either an empty vector, WT or mutant NF-κB2 constructs (60 ng), pNF-κB-Firefly-Luc encoding NF-κB-dependent Firefly luciferase (30 ng), pRL-TK encoding Renilla luciferase (10 ng) as the transfection control, along with either a NIK-encoding plasmid (10 ng) or RELB-encoding plasmid (10 ng). We performed the transfections using Lipofectamine 3000 Transfection Reagent. Plasmids required for transfection were prepared using P3000™ reagent and transferred to a centrifuge tube; Dilution was done with 7.5 µL Opti-MEM. Additionally, in another centrifuge tube, Lipofectamine 3000 reagent transfection reagent was diluted with 7.5 µL of Opti-MEM. We then added this diluted reagent-Opti-MEM mixture to the diluted plasmids and mixed well by pipetting to ensure that the mixture was homogeneous.

Both reagents were performed with a ratio of 1:2 (2 μL of reagent for 1 μg DNA). The mixture was allowed to incubate at room temperature for 20 min. After this process, we carefully added the diluted transfection complexes dropwise into the wells of a 96-well plate. At 48 h post-transfection, we measured the Firefly and Renilla luciferase activities using the Dual-Glo Luciferase Assay System as per the manufacturer's instructions.

For the secreted alkaline phosphatase (SEAP) reporter assay, we seeded HEK293 cells in 96-well plates at a density of 2.5 x 10^5 cells/mL (100 μL/well) and transiently transfected them with either empty vector, WT or mutant NF-κB2 constructs (60 ng), pNiFty-SEAP encoding NF-κB-dependent SEAP (30 ng), and a NIK-encoding plasmid (10 ng), using Lipofectamine 3000 Transfection Reagent as described above. At 48 h post-transfection, we collected the supernatant from each well and lysed the cells for western blotting. We then used the diluted supernatants to measure SEAP activity with the Secreted Alkaline Phosphatase Reporter Gene Assay Kit following the manufacturer's instructions. Briefly, 10 μL of diluted culture supernatants (1:3) were transferred into white opaque 96-well plate and placed at 65 °C for 30 min to inactivate endogenous alkaline phosphatase. Standard dilutions were prepared and 10 μL of diluted standards were transferred into assigned wells. SEAP substrate were added at 50 μL onto each well and incubated at RT for 10 min. Last, we performed luminescence measurements using a BioTek Synergy HT Microplate Reader.

2.2.10. Statistical analysis

Experiment results were plotted and analyzed using GraphPad Prism software. One-way and Two-way ANOVA were used for statistical analyses, for which significance is indicated by asterisks (*, $P < 0.05$, **, $P < 0.01$, ***, $P < 0.001$, and **** p-value < 0.0001), with P values greater than 0.05 considered non-significant (n.s.).

CHAPTER 3

Results

3.1. Clinical characteristics of the patients

We studied a non-consanguineous multiplex family of Turkish origin, in which the two sons (II.1 and II.2) and their father (I.2) were diagnosed with CVID (Figure 3.1). Index patient (P1) was diagnosed with adrenocorticotropic hormone deficiency and CVID at the age of 7. P2 and P3 were diagnosed with CVID at the ages of 13 and 38, respectively, during the family screening following P1's diagnosis. All 3 patients had low serum concentrations of immunoglobulins (IgG, IgM and IgA) along with impaired vaccine responses, fulfilling the diagnostic criteria of CVID. Peripheral immune phenotyping of patients revealed decreased B and CD4+ T memory cells compared to age-matched healthy controls. All 3 patients suffered from severe or recurrent infections, particularly of the respiratory tract, since their childhood. Two of the patients had severe viral infections. P1 developed influenza pneumonia. P2 had frequent episodes of labial herpes simplex infection and developed severe COVID-19 pneumonia. Of note, P2, unlike P1 and P3, did not receive any vaccination against SARS-CoV-2. All 3 patients have been under Immunoglobulin replacement therapy (IgRT) for decades. Antibiotic prophylaxis was also given as the need arose. All patients are alive as of conducting this study. Details of clinical features of the patients are provided in Appendix A.

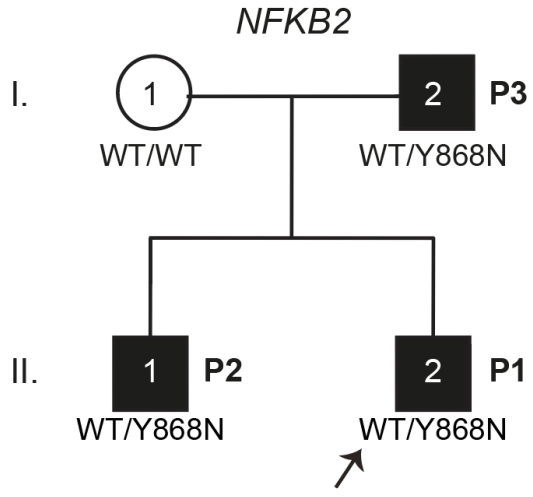

Figure 3.1 A novel heterozygous missense mutation in *NFKB2*. **a** Pedigree of the multiplex family affected with CVID. The patients are shown in black, and the healthy individual is shown in white. The proband is indicated with the arrow. Status of *NFKB2* mutation (p.Y868N) status is shown. WT = wild-type.

3.2. WES data analysis of the patients

Occurrence of CVID in both the father and his two sons has strongly suggested a genetic inheritance. We therefore performed WES on genomic DNA isolated from peripheral blood samples of two patients, P2 (II.1, the elder son) and P3 (I.2, the father), in order to determine whether an inborn monogenic defect might underlie CVID in this multiplex family. There were total 181,560 variants in 23,614 genes and 177,863 variants in 23,562 genes identified in P2 and P3, respectively (Table 3.1). We first filtered out the variant calls with low quality: total depth coverage (DP) less than 10, mapping quality (MQ) score less than 40, genotype quality (GQ) less than 30, or overall quality (QUAL) score less than 60. Heterozygous variants with allele depth to DP ratio lower than 0.25 were also removed. Next, we only selected predicted loss-of-function (pLOF) (frameshift insertion and deletions, stop-gain (nonsense), and essential splice site (± 2 bp from the exon-intron boundary)), start-loss, stop-loss, in-frame insertion and deletions, and missense variants for further analysis.

Table 3.1 Genetic analysis of WES data of the patients

WES analysis	P2 (II.1)	P3 (I.2)
Total	181,560 (23,614)	177,863 (23,562)
Heterozygous variants with AF<0.01% (pLOF, start-loss, stop-loss, in-frame indel, and missense)	131 (129)	125 (124)
Present in both patients	59 (59)	

The number of annotated variations with the number of genes, shown in parenthesis, found in the patient, are shown.

In addition, the variants, which were previously listed as non-pathogenic variants commonly found in the exomes of patients but not in the public genome databases[217], were eliminated. We removed the variants with AF ≥1% in gnomAD v2.1.1, including variants with AF ≥1% in gnomAD subpopulations, including African, Ashkenazi Jewish, Finnish, non-Finnish European, South Asian, East Asian, Latino and other. Common variants (AF ≥1%) in TGP Turkish Genome Project Data Sharing Portal (TGP) (https://tgd.tuseb.gov.tr/), which includes genome data of more than 500 healthy individuals from Turkey, were further excluded. We hypothesized that a monogenic etiology under an autosomal dominant (AD) mode of inheritance with complete penetrance might underlie CVID based on its segregation in the affected family, we focused only on the heterozygous variants. Given that CVID is rare (<1/10,000), we retained heterozygous variants with AF <0.01% in patients. Overall, 131 heterozygous rare variants in 129 genes and 125 heterozygous rare variants in 124 genes were revealed in P2 and P3, respectively (Table 3.1). Among these, 59 variants in 59 different genes were present in both patients (Table 3.1 and Table 3.2).

Table 3.2 Heterozygous rare nonsynonymous variants present in both P2 and P3

Gene	Variation			gnomAD AF		In silico predictions					GDI
	Transcript	HGVS C	HGVS P	v2.1.1	v4.1.0	AM	CADD	MT	PP2	SIFT	
A2ML1	ENST00000299698	c.1361G>A	p.Gly454Asp	-	-	B	B	B	B	B	18.3
ANKDD1B	ENST00000601380	c.1277G>A	p.Arg426His	-	4.56E-06	B	B	B	B	D	14.9
ANKRD28	ENST00000383777	c.913G>A	p.Gly305Arg	-	-	-	D	D	D	D	3.2
C19orf55	ENST00000396908	c.1325T>C	p.Leu442Pro	-	1.25E-06	-	B	B	D	D	7.1
CAPN12	ENST00000328867	c.8C>T	p.Ser3Phe	-	6.20E-07	B	B	B	B	D	9.4
CDC42EP2	ENST00000279249	c.259C>T	p.Arg87Cys	7.96E-06	8.06E-06	B	D	B	D	D	1.7
CRP	ENST00000255030	c.134C>G	p.Thr45Arg	-	-	B	B	B	B	B	1.1
CTBP2	ENST00000309035	c.389C>A	p.Pro130Gln	-	1.86E-06	-	B	B	B	B	28.0
CTNNBIP1	ENST00000377256	c.16G>C	p.Ala6Pro	2.12E-05	2.04E-05	B	D	B	D	B	1.1
DENND1C	ENST00000381480	c.281G>A	p.Cys94Tyr	-	7.44E-06	D	D	B	D	D	6.7
DSCAM	ENST00000400454	c.5860G>A	p.Ala1954Thr	-	3.10E-06	B	B	B	B	B	3.2
EFCAB6	ENST00000262726	c.2860A>G	p.Lys954Glu	-	2.48E-06	B	B	B	B	D	8.8
ETFDH	ENST00000511912	c.1465A>G	p.Lys489Glu	-	1.24E-06	B	D	B	B	B	1.4
EYS	ENST00000370616	c.4510C>G	p.Gln1504Glu	6.50E-06	2.58E-06	B	D	B	B	B	21.0
FARP1	ENST00000376586	c.1520A>G	p.Lys507Arg	3.98E-06	4.34E-06	B	D	B	B	B	5.6
FCRL1	ENST00000368176	c.462A>C	p.Leu154Phe	-	-	B	B	B	B	B	4.7
GNPDA2	ENST00000295448	c.32T>G	p.Leu11Trp	-	-	B	D	B	B	D	0.6
GPR15	ENST00000284311	c.300G>T	p.Arg100Ser	3.98E-05	3.72E-05	D	B	B	B	B	7.0
GPX7	ENST00000361314	c.194G>A	p.Arg65Gln	1.19E-05	7.44E-06	B	D	B	B	B	1.5
GREB1	ENST00000234142	c.3289A>G	p.Thr1097Ala	-	1.25E-06	B	D	B	B	D	20.5
HIP1R	ENST00000253083	c.3091dupC	p.Arg1031fs	1.42E-05	1.98E-05	-	D	D	-	-	5.3
INPP5F	ENST00000361976	c.2746C>A	p.His916Asn	-	3.72E-06	B	B	B	B	B	4.7
ITGA1	ENST00000282588	c.1376A>G	p.Tyr459Cys	3.98E-06	2.48E-06	D	D	-	D	D	11.5
KMT2D	ENST00000301067	c.14315C>T	p.Thr4772Ile	-	-	B	B	B	B	B	6.7
KRTAP10-12	ENST00000400365	c.187T>A	p.Cys63Ser	1.20E-05	1.12E-05	B	B	B	B	D	9.4
LAMC1	ENST00000258341	c.3051A>C	p.Glu1017Asp	-	5.58E-06	D	D	B	D	B	5.6
LSM11	ENST00000286307	c.749T>C	p.Leu250Pro	-	-	B	D	B	D	B	2.3
MANBA	ENST00000226578	c.1517G>A	p.Ser506Asn	1.59E-05	7.44E-06	D	D	D	D	D	6.6
MISP	ENST00000215582	c.1961C>T	p.Ala654Val	4.01E-06	1.86E-06	A	D	B	D	D	5.3
MYO10	ENST00000513610	c.5098A>G	p.Met1700Val	8.02E-06	1.86E-06	B	B	B	B	B	19.4
MYOF	ENST00000359263	c.3838C>G	p.Pro1280Ala	8.07E-06	4.96E-06	A	D	B	D	D	8.4
NFKB2	ENST00000369966	c.2602T>A	p.Tyr868Asn	-	-	D	D	B	D	B	1.7
NLRP4	ENST00000301295	c.801G>C	p.Lys267Asn	1.19E-05	8.05E-06	D	B	B	D	D	1.8
NUDT12	ENST00000230792	c.941A>G	p.His314Arg	2.05E-05	9.35E-06	D	D	D	B	D	2.1
NUMB	ENST00000355058	c.1834C>G	p.Pro612Ala	-	-	B	B	B	B	B	2.5
OR4C46	ENST00000328188	c.788T>C	p.Leu263Ser	1.60E-05	1.31E-05	B	B	B	B	D	22.3
OSBPL9	ENST00000371710	c.1083G>T	p.Leu361Phe	7.97E-06	4.96E-06	-	D	B	B	B	2.2
PDCD6IP	ENST00000457054	c.794A>G	p.Gln265Arg	4.01E-06	3.10E-06	-	D	D	D	D	19.8
PHLPP1	ENST00000262719	c.1259C>A	p.Pro420Gln	-	-	B	B	B	B	D	4.8
PLEKHA7	ENST00000531066	c.2017C>T	p.Arg673Trp	1.77E-05	1.18E-05	B	D	D	D	D	6.0
PTPRF	ENST00000359947	c.1789A>C	p.Ile597Leu	-	6.23E-07	B	B	B	B	B	3.5
SBDS	ENST00000246868	c.657A>C	p.Glu219Asp	3.19E-05	6.20E-07	B	B	B	B	B	2.9
SCAMP5	ENST00000562212	c.656C>T	p.Ala219Val	-	6.32E-07	-	D	D	D	B	0.3
SEC16A	ENST00000313050	c.4670C>T	p.Ala1557Val	1.22E-05	4.78E-05	D	D	B	D	D	7.9
SENP3	ENST00000429205	c.681G>T	p.Arg227Ser	2.05E-05	2.48E-05	B	B	B	B	B	1.0
SETX	ENST00000372169	c.3341T>C	p.Ile1114Thr	2.84E-05	3.22E-05	B	B	B	B	B	7.4
SPPL2A	ENST00000261854	c.974G>A	p.Cys325Tyr	-	-	D	D	D	D	D	4.0
SUSD1	ENST00000374264	c.1327G>T	p.Ala443Ser	3.98E-05	3.90E-05	B	B	B	B	B	2.5
TGS1	ENST00000260129	c.387T>A	p.His129Gln	-	6.50E-07	B	B	B	B	B	7.6
TMF1	ENST00000543976	c.2105C>T	p.Ala702Val	-	3.72E-06	-	D	B	D	D	5.3
TRIM41	ENST00000315073	c.169G>C	p.Asp57His	-	-	B	D	B	B	D	7.1
TRPC3	ENST00000379645	c.580A>G	p.Ile194Val	-	1.24E-06	-	D	B	D	D	1.9
TTN	ENST00000589042	c.51703C>T	p.Arg17235Trp	1.22E-05	9.95E-06	-	D	B	-	-	42.9
TULP4	ENST00000367097	c.685G>A	p.Glu229Lys	-	6.20E-07	D	D	B	D	D	4.9
UNCX	ENST00000316333	c.827C>T	p.Pro276Leu	-	1.50E-06	B	D	B	D	D	1.1
USP39	ENST00000323701	c.56C>A	p.Ser19Tyr	-	-	B	D	B	B	D	3.1
VPS13C	ENST00000261517	c.3745G>T	p.Val1249Phe	-	6.20E-07	B	D	B	D	D	12.1
ZFYVE16	ENST00000338008	c.2621A>G	p.Asp874Gly	3.98E-06	1.86E-06	D	D	B	D	D	3.9
ZNF23	ENST00000357254	c.230A>T	p.Glu77Val	-	-	B	D	B	D	B	1.4

Ensembl transcript IDs are provided. HGVS: Human Genome Variation Society, c: coding DNA sequence, p: protein sequence. Gene damaging index (GDI) represents mutation-load of genes, ranging from 0.0001 to 42.91 (from the least to the most)[218]. The variant was considered damaging if its CADD score was higher than 20. AM: AlphaMissense, MT: MutationTaster2021, PP2: PolyPhen-2, A: Ambiguous, B: Benign, D: Damaging

3.3. Search for candidate disease-causing variants in the multiplex family with CVID

We next undertook a biased approach and searched for variants in a panel of genes previously associated with CVID[202,219,220]. This panel consisted of 514 genes listed in Appendix B. We found that both patients carried a heterozygous variant (NM_001322934.2:c.2602T>A:p.Y868N) in *NFKB2* encoding NF-κB2, which is involved in the alternative NF-κB pathway (Table 3.2). Sanger sequencing confirmed the familial segregation of the *NFKB2*:p.Y868N variant with CVID (Figure 3.2). It was heterozygous in both the two sons (II.1, P2 and II.2, P1) and the father (I.2, P3), but wild-type (WT) in the healthy mother (I.1) (Figure 3.2). This was consistent with our hypothesis of AD inheritance with complete penetrance.

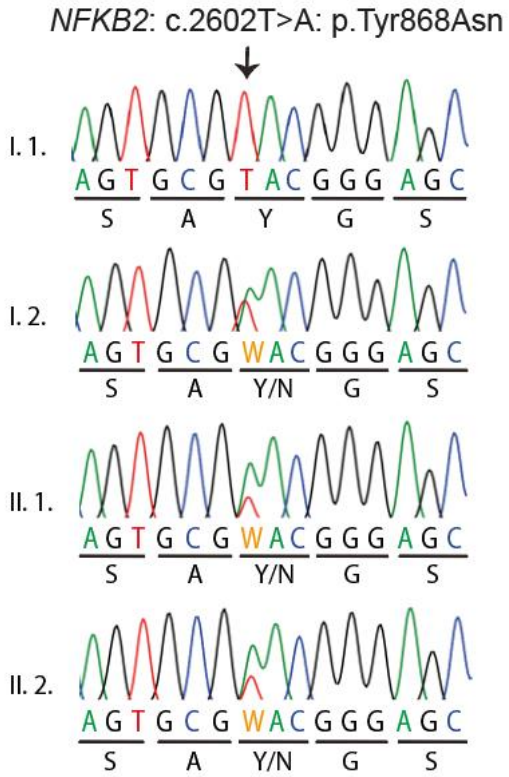

Figure 3.2 Familial segregation of the p.Y868N with the disease and its heterozygous state in the patients were confirmed by Sanger sequencing.

Of note, we also found that P2 and P3 had a heterozygous missense mutation in Shwachman–Bodian-Diamond syndrome (*SBDS*) gene, in which mutations have been proposed to be associated with CVID in some cases[221]. However, this *SBDS* variant, predicted to be benign, was not present in P1 and the mother, not consistent with the segregation of the disease in the family, confirmed by Sanger sequencing (data not shown). Overall, we did not reveal any other candidate disease-causing variants in genes, which can cause inborn errors of immunity under AD mode of inheritance, in the patients. The p.Y868 is a highly conserved residue across various species, which is located in the NIK-responsive sequence (NRS) of the protein (Figure 3.3). A missense variant at this location, p.Y868C, has been previously linked to CVID[169], however the p.Y868N is novel (not previously associated with any disease) and not listed in public genome databases. We also assessed the predicted damaging impact of

this variant using various in silico algorithms. AlphaMissense, CADD, and PolyPhen-2 and predicted p.Y868N as damaging, but it was benign by MutationTaster and SIFT (Table 3.2). Finally, *NFKB2*:p.Y868N was interpreted as likely disease-causing in this family based on the ACMG-AMP variant classification criteria (PM1, PM2, PM5, and PP1)[207].

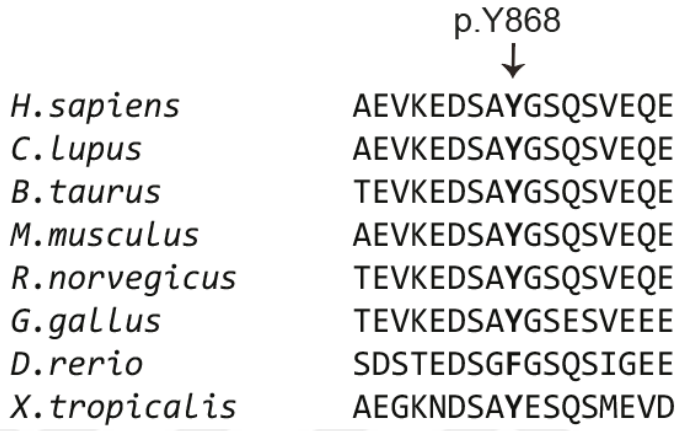

Figure 3.3 Conservation of the p.Y868 residue, highlighted in bold, across various species. (Source: NCBI HomoloGene).

3.4. Impact of the p.Y868N on NF-κB2 expression and its nuclear localization

Following activation of the alternative NF-κB2 pathway, NIK-mediated phosphorylation of the NF-κB2 precursor p100 (amino acids 1–900) culminates in p100 processing to form the transcriptionally active p52 (amino acids 1–405) and subsequent translocation of p52 and its heterodimerization partner, RELB, into the nucleus[168]. We sought to characterize the impact of the p.Y868N variant on the processing of the p100 precursor to generate p52. We therefore generated full-length ORF constructs, which encode wild-type (WT) and mutant NF-κB2 with p.Y868N with an in-frame N-terminal 3xFLAG tag. We also generated mutant NF-κB2 constructs with previously reported morbid mutations: p.R635* or p.R853*. We transiently transfected HEK293 with either empty vector, WT or mutant NF-κB2 constructs, along with a GFP-encoding plasmid for transfection efficiency and/or NIK-

encoding plasmid. When over-expressed together with NIK, the p.Y868N led to a severely impaired generation of p52 compared to the WT (Figure 3.4). The p.R635* and p.R853* caused abolished processing of p100 into p52, consistent with previous findings[222] (Figure 3.4).

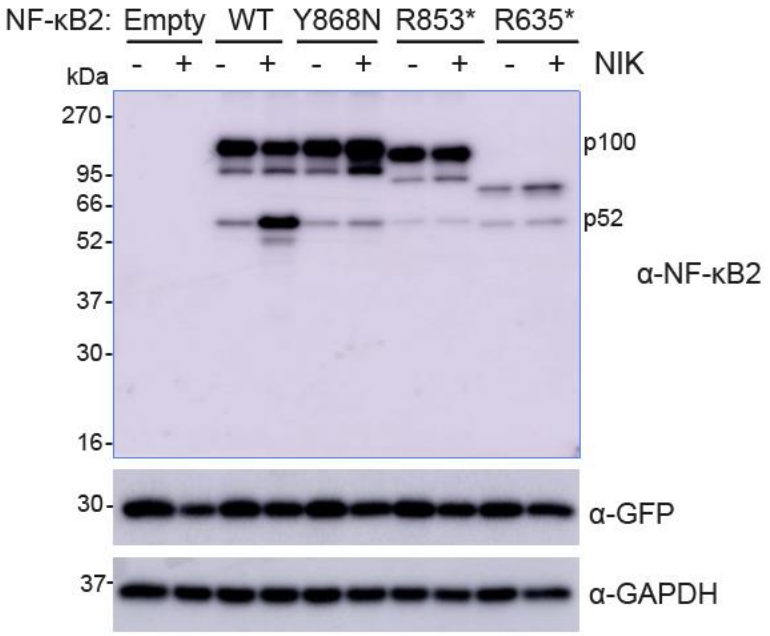

Figure 3.4 Impact of p.Y868N on NF-κB2 expression in vitro. Representative immunoblot images showing expression levels of NF-κB2 (p100/p52) in whole cell lysates (25 µg protein/lane) from HEK293 cells transiently transfected with empty, WT or mutant NF-κB2, along with a GFP encoding plasmid and/or a plasmid encoding NIK. Immunoblotting was performed using anti-NF-κB2 antibody. The membranes were then stripped and reblotted with anti-GFP and anti-GAPDH, serving as transfection efficiency and loading controls, respectively. Expected molecular weights: NF-κB2 p100: ~100 kDa, NF-κB2 p52: ~52 kDa, GFP: ~ 27 kDa, GAPDH: ~ 36 kDa.

Moreover, we tested the impact of the p.Y868N variant on the subcellular localization of NF-κB2 by confocal microscopy. HEK293 cells were transiently transfected with either WT or mutant NF-κB2 constructs along with the NIK-encoding plasmid. At 48 h post-transfection, the cells were fixed, permeabilized, and stained with anti-Flag Tag Antibody. Nuclei were counterstained with DAPI. While the WT NF-κB2

demonstrated nuclear translocation, the p.Y868N variant was not detected in the nucleus when over-expressed together with NIK (Figure 3.5).

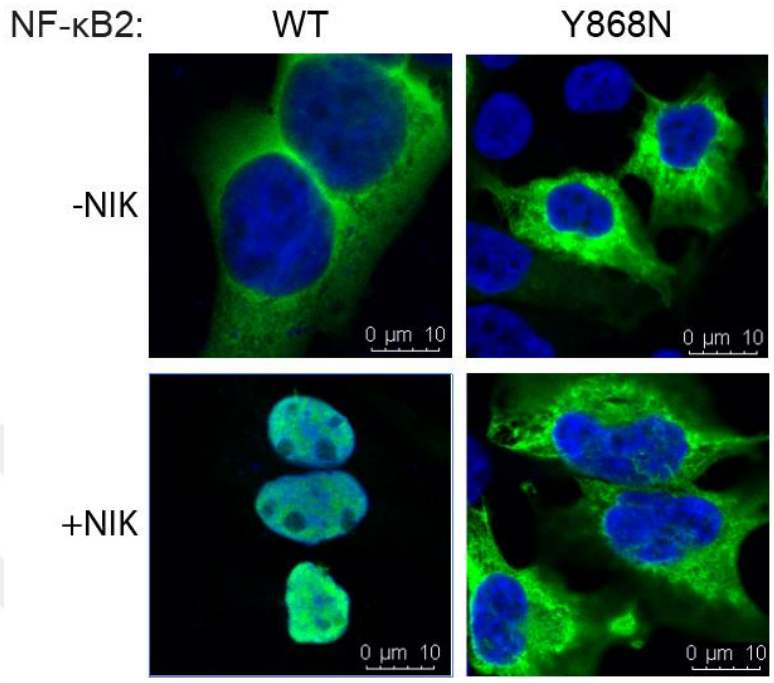

Figure 3.5 Impact of p.Y868N on subcellular localization of NF-κB2. Representative confocal fluorescence microscopy images showing subcellular localization of WT and mutant NF-κB2 when transiently over-expressed in HEK293 with or without NIK. Blue shows the nucleus stained by DAPI. Green shows NF-κB2 stained by anti-FLAG antibody.

Finally, we assessed the formation of p52 from the NF-κB2 p100 precursor in patients' cells. Lymphoblastoid B cells generated from PBMCs of patients and healthy controls were stimulated with CD40L, followed by cell lysis and immunoblotting. We found that processing of p100 into p52 was abolished in the patients' cells in comparison with the healthy controls (Figure 3.6). To sum up, these findings demonstrated that the p.Y868N variant is a deleterious allele, causing impaired generation of p52 from the NF-κB2 p100 precursor.

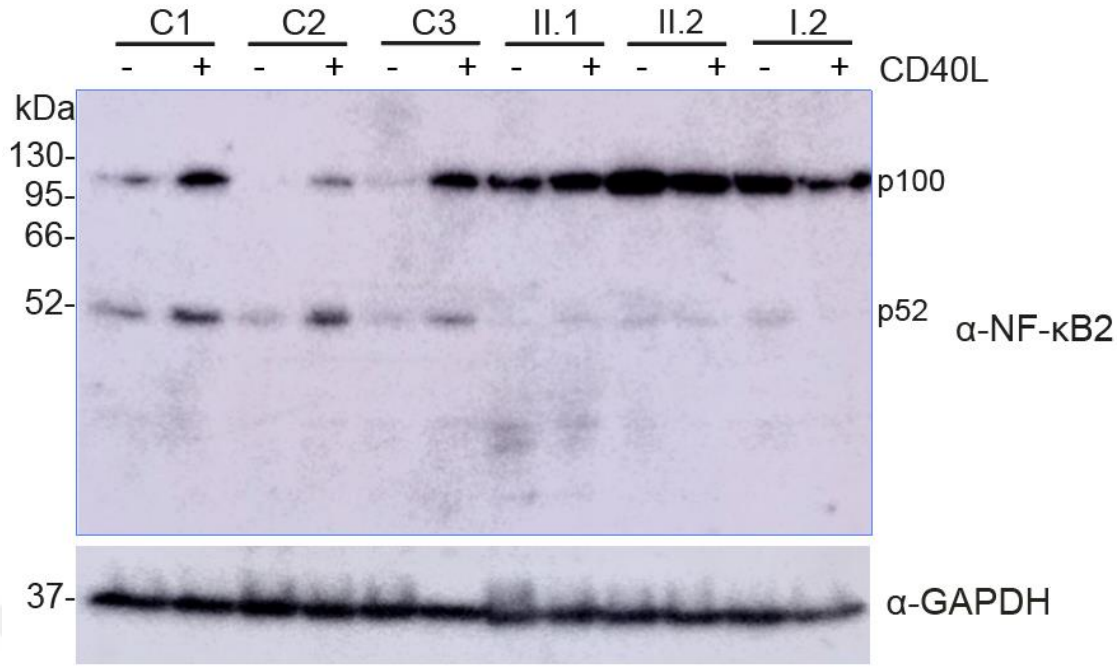

Figure 3.6 Impact of p.Y868N on NF-κB2 expression in patients' cells. Representative immunoblot images showing NF-κB2 (p100/p52) expression in whole cell lysates (45 µg protein/lane) from Lymphoblastoid B cells derived from three healthy donors and patients upon treatment with or without CD40L. Immunoblotting was performed using the anti-NF-κB2 antibody. The membranes were then stripped and reblotted with anti-GAPDH as the loading control. Expected molecular weights: NF-κB2 p100: ~100 kDa, NF-κB2 p52: ~52 kDa, GAPDH: ~ 36 kDa.

3.5. Impact of the p.Y868N on NF-κB2 function

We next aimed to determine the impact of the p.Y868N variant on NF-κB2 function. We utilized a recently described p52-dependent luciferase reporter assay to assess the κB transcriptional activity in vitro[222]. Briefly, HEK293 cells were transiently transfected with a plasmid encoding NF-κB-dependent Firefly luciferase, Renilla luciferase plasmid, NIK-encoding plasmid, RELB-encoding plasmid, and either an empty vector, WT or mutant NF-κB2 constructs. When over-expressed together with NIK and RELB, the WT NF-κB2 had around 76% decrease in κB-dependent luciferase activity, however the p.Y868N variant led to approximately 50% repression in comparison with the empty vector (Figure 3.7). Known loss-of-function (LOF) and gain-of-function (GOF) variants of p52, p.R853* and p.R635*, were also tested in the

same assay. These variants, p.R853* and p.R635*, led to lower (~35%) and higher (~83%) repression, respectively, compared to the empty vector, consistent with the previous findings[222] (Figure 3.7).

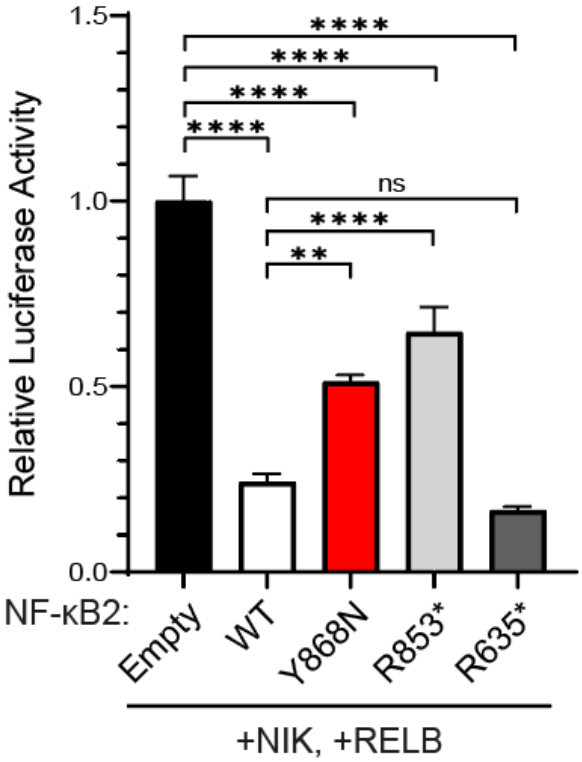

Figure 3.7 Impact of p.Y868N on NF-κB2 function in vitro. Relative luciferase activity (Firefly/Renilla) normalized to the empty vector in HEK293 cells at 48 h upon transient transfection with NFκB-driven Firefly luciferase and Renilla luciferase (as transfection efficiency control) plasmids, vectors encoding NIK and RELB, and either empty vector, WT, or mutant NF-κB2. Empty vector was set as 1. Data are the mean ± SEM of five independent experiments performed in duplicates. (ns: non-significant, * p-value < 0.05, ** p-value < 0.01, *** p-value < 0.001, **** p-value < 0.0001; One-way ANOVA followed by Tukey's post-hoc test)

Moreover, we generated constructs encoding the C-terminal fragment (amino acids 405-900) of WT and mutant NF-κB2. We found that the expression of C-terminal fragment of WT NF-κB2 in HEK293 cells was reduced due to its proteasomal degradation, when transiently transfected together with NIK in HEK293 cells (Figure 3.8).

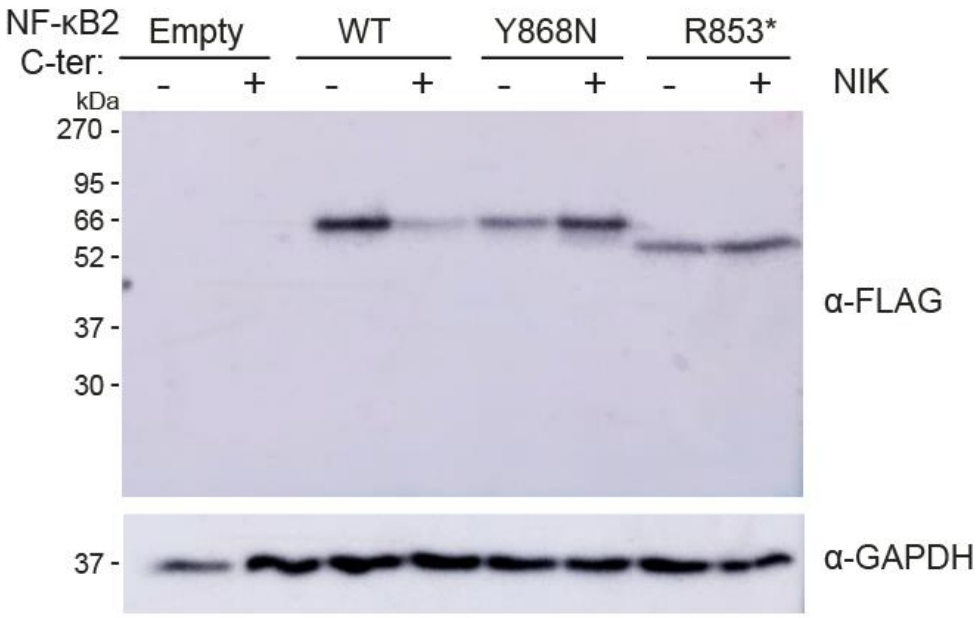

Figure 3.8 Impact of p.Y868N on expression of NF-κB2 C-terminal fragment in vitro. Representative immunoblot images showing expression levels of WT and mutant NF-κB2 C-terminal fragment (amino acids 405-900) in whole cell lysates (10 μg protein/lane). HEK293 cells were transiently transfected with NFκB-driven secreted alkaline phosphatase (SEAP) plasmid and either empty vector, WT, or mutant NF-κB2 C-terminal fragment (amino acids 405-900) in the presence or absence of a plasmid encoding NIK. At 48 h post-transfection, cell lysates were processed for immunoblotting in Figure 3.8 and supernatants were utilized for measurement of SEAP activity in Figure 3.9. Immunoblotting was performed using anti-FLAG antibody. The membranes were then stripped and reblotted with anti-GAPDH as the loading control. Expected molecular weights: NF-κB2 C-terminal fragment: ~ 57 kDa and GAPDH: ~ 36 kDa.

We also utilized luciferase- and SEAP-based p52-dependent reporter assays in HEK293 cells and showed that over-expression of the C-terminal fragment of WT NF-κB2 with NIK had no repression on NF-κB-dependent transcriptional activity compared to the empty vector (Figure 3.9A-B). On the other hand, the C-terminal fragment of p.Y868N NF-κB2 was not degraded when over-expressed with NIK, similar to the p.R853* morbid allele, which exhibits p52 LOF and IκBδ GOF activities. These findings were consistent with previous findings[222]. Both the p.Y868N and p.R853* variants exhibited transcriptional repressive activity using luciferase- and SEAP-based reporter assays performed in HEK293 cells (Figure 3.9).

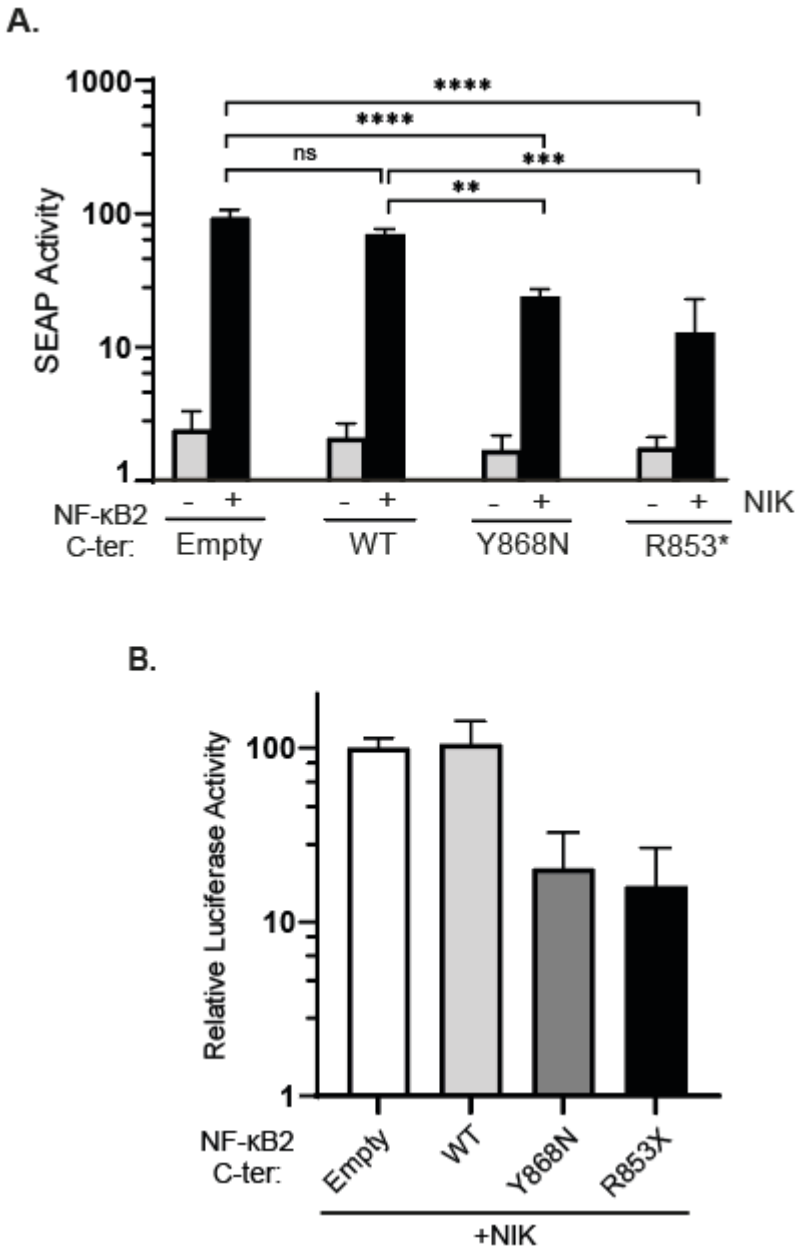

Figure 3.9 Impact of p.Y868N on function of NF-κB2 C-terminal fragment in vitro. A. HEK293 cells were transiently transfected with NFκB-driven secreted alkaline phosphatase (SEAP) plasmid and either empty vector, WT, or mutant NF-κB2 C-terminal fragment (amino acids 405-900) in the presence or absence of a plasmid encoding NIK. At 48 h post-transfection, cell lysates were processed for immunoblotting in Figure 3.8 and supernatants were utilized for measurement of SEAP activity in Figure 3.9. Data are the mean ± SEM of three independent experiments. (ns: non-significant, * p-value < 0.05, ** p-value < 0.01, *** p-value < 0.001, **** p-value < 0.0001; Two-way ANOVA followed by Tukey's post-hoc test). B. Relative luciferase activity (Firefly/Renilla) normalized to the empty vector in HEK293 cells at 48 h upon transient transfection with NFKB-driven Firefly luciferase and Renilla luciferase (as transfection efficiency control) plasmids, and either empty vector, WT, or mutant NF-KB2 C-terminal fragment (amino acids 405-900) in the presence of a plasmid encoding NIK. Empty vector was set as 100. Data are the mean ± SEM of two independent experiments performed in duplicates.

Furthermore, we assessed the dose-dependent impact of p.Y868N variant on the processing of WT NF-κB2 precursor p100 to form p52 in transiently transfected HEK293 cells. We found a dose-dependent inhibition of WT p100 processing into p52 with increasing concentrations of p.Y868N NF-κB2, similar to the p.R853* (Figure 3.10), as expected[222]. In conclusion, these results demonstrated that the novel p.Y868N is a LOF allele in NF-κB transcriptional activity due to impaired p52 generation from p100. The p.Y868N allele also exhibits GOF in IκBδ regulatory function since the accumulation of unprocessed p100 leads to increased inhibitory action of IκBδ.

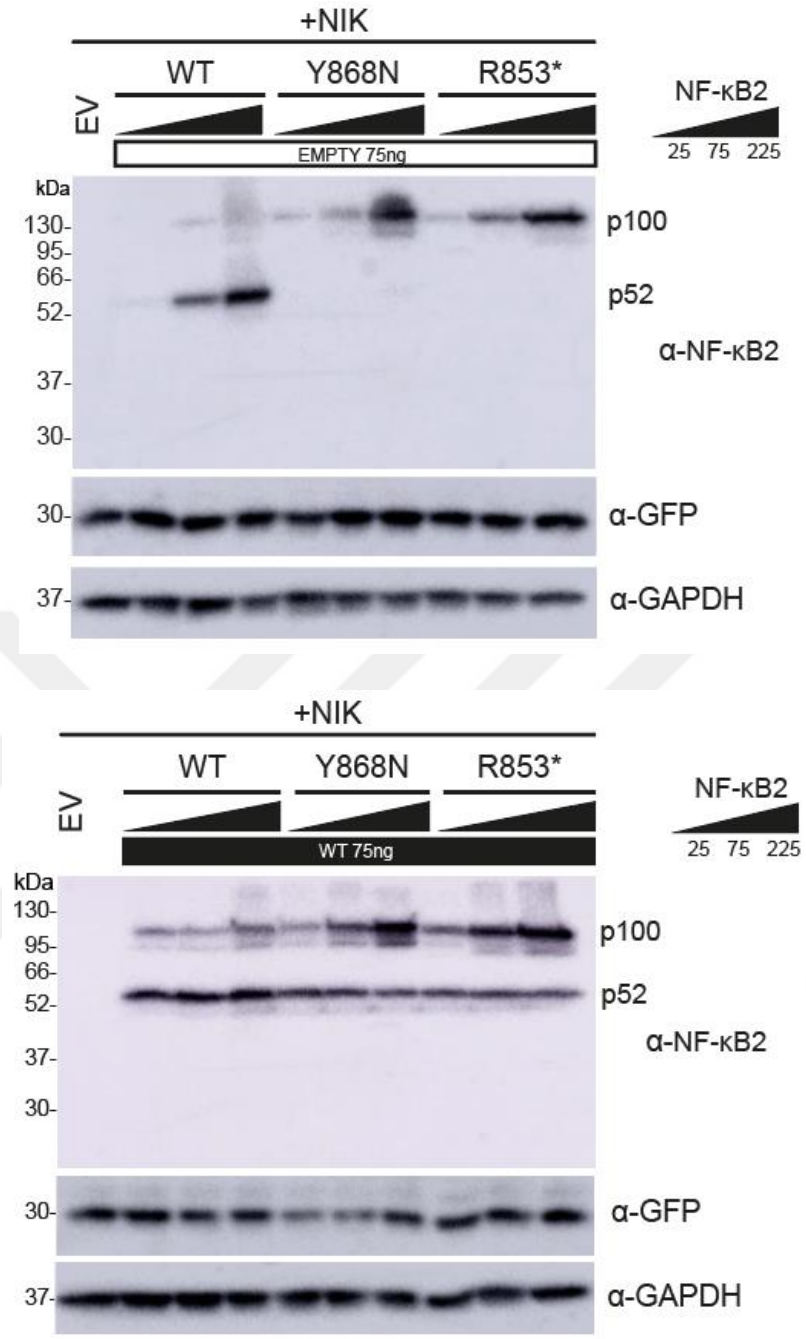

Figure 3.10 Dose-dependent impact of p.Y868N on WT NF-κB2. Representative immunoblot images showing expression levels of NF-κB2 (p100/p52) in whole cell lysates (25 μg protein/lane) from HEK293 cells transiently transfected with plasmids encoding NIK, and various amounts of WT or NF-κB2 mutants, together with constant amounts of empty vector (top panel) or WT NF-κB2 (bottom panel). Immunoblotting was performed using anti-NF-κB2 antibody. The membranes were then stripped and reblotted with anti-GFP and anti-GAPDH as transfection efficiency and loading controls, respectively. Expected molecular weights: NF-κB2 p100: ~100 kDa, NF-κB2 p52: ~52 kDa, GFP: ~27 kDa, GAPDH: ~36 kDa.

CHAPTER 4

Discussion

We herein report the discovery of a private heterozygous missense variant, p.Y868N, in *NFKB2* by WES in a multiplex family, in which two siblings and their father were diagnosed with CVID. This diagnosis was established based on the consistently low levels of serum immunoglobulins, specifically IgG, IgM, and IgA, coupled with impaired responses to vaccinations, and a recurrent history of infectious diseases. These clinical manifestations were documented during a comprehensive family screening that was conducted decades ago. Further laboratory investigations of peripheral blood samples revealed that the affected individuals exhibited a marked reduction in the populations of memory lymphocytes, which are critical components of the adaptive immune system against recurrent infections. Inborn errors of NF-κB1 and NF-κB2 are among the most common causes of monogenic CVID[169,170]. The canonical NF-κB1 pathway is involved in the regulation of inflammatory responses, whereas the alternative NF-κB2 pathway regulates maturation of medullary thymic epithelial cells, lymphoid organogenesis, survival and development of B lymphocytes[168]. There have been at least 40 different pathogenic mutations reported in *NFKB2*[222]. The p.Y868N is a novel variant, which has not been previously associated with CVID or is not listed in public genome databases including recently released Turkish Genome Portal. This mutation affects an evolutionary conserved amino acid residue, on which a different missense mutation, p.Y868C, is known to cause CVID[169]. Y868 is found between the sites S866 and S870, which are phosphorylated by NIK on NF-κB2 precursor p100, crucial for processing of p100 into active p52[168]. Tyrosine to Asparagine substitution at amino acid position 868 is

predicted to be damaging by many *in silico* prediction algorithms tested. We showed by Sanger sequencing that the p.Y868N segregates with the disease among family members, confirming an AD mode of inheritance with complete penetrance. Together with these findings, p.Y868N is interpreted as likely disease-causing based on ACMG-AMP classification criteria.

To characterize the molecular and cellular impact of the p.Y868N variant on NF-κB2, we carried out an extensive series of biochemical and functional studies using overexpression systems and patients' cells. Overall, our findings indicated that the p.Y868N variant results in a LOF activity related to the generation of the p52 subunit, thereby impairing its role in transcriptional repression. Additionally, it shows a GOF effect by enhancing the inhibitory activity of IκBδ. These findings were consistent with that two previously-reported mutations at the same residue, p.Y868C and p.Y868*, were LOF in p52 activity and GOF in IκBδ regulatory function[222]. Similar to previously reported CVID cases with NFKB2 variants that display both p52 LOF and IκBδ GOF activities[222], two of our patients experienced severe or recurrent viral diseases including influenza pneumonia in P1, and severe COVID-19 pneumonia and frequent episodes of labial herpes simplex infection in P2. Overall, our findings expand the genotypic and phenotypic spectrum of human NF-κB2 deficiency.

Increased viral susceptibility in individuals with inborn errors of the alternative NF-κB pathway was attributed to impaired central T cell tolerance, leading to generation of autoantibodies against type I interferon (IFN)s[222]. Preexisting neutralizing autoantibodies against type I IFNs have been identified as underlying culprit in individuals who developed severe forms of COVID-19 pneumonia, herpesvirus diseases, influenza pneumonia, Middle East respiratory syndrome, adverse reactions to the yellow fever live-attenuated vaccine, and West Nile virus encephalitis[222,223,231–

[233,224,224–230]. Presence of autoantibodies that neutralize IFN-α2 and IFN-ω have been reported in patients with p52 LOF and IκBδ GOF *NFKB2* variants, who were unvaccinated against SARS-CoV-2 and developed severe/critical COVID-19 pneumonia[222]. We did not assess the presence of anti-type I IFN autoantibodies in the patients in this thesis work, however detection of neutralizing autoantibody activity against type I IFNs in our patients' plasma samples may explain severe or recurrent viral diseases developed in our patients, P1 and P2. All three patients have received IgRT for decades, yet they have continued to suffer from infections, particularly of the upper respiratory tract, presumed to be mostly due to viruses. The variability among three related patients in susceptibility, frequency and severity of viral infections can be attributed to age, environmental factors such as lifestyle, or perhaps presence or absence of neutralizing autoantibodies against type I IFNs.

Early diagnosis is of great importance in CVID, which is the most common symptomatic primary immunodeficiency disease in the adult age group and is characterized by impaired and/or insufficient immunoglobulin production. CVID disorders, which are not a single disease but an umbrella diagnosis, can occur under the influence of many genetic defects. Although specific genetic/molecular defects have been identified in some patients, the underlying causes have not yet been determined in the vast majority of patients. Although it may be familial, displaying autosomal recessive or autosomal dominant inheritance, it may also occur sporadically. Clinical findings are important for the definitive diagnosis of CVID, especially the characteristics and frequency of infections are a warning sign for clinicians. Yet, diagnosis can still be delayed for clinical presentations with infectious complications and especially for the manifestations with non-infectious symptoms. Early diagnosis of these patients is vital for early treatment. Because early

immunoglobulin treatment and prophylaxis for infections prevent chronic complications and increase the life quality of patients. Moreover, genetic diagnosis paves the way for patient-specific treatments such as gene therapies. In addition, genetic diagnosis is of great importance for the patients as well as their relatives. Family screening should be performed during diagnosis, keeping in mind that there may be patients in the same family, who have been overlooked/undiagnosed or who have different clinical phenotypes. Considering that CVID diagnosis is more common in the 2nd and 3rd decades of life, genetic counseling is especially important for patients of reproductive age. In this respect, human genetic studies are important even in patients, who have already been diagnosed by meeting the CVID diagnostic criteria and receiving treatment. In geographical regions where consanguineous marriages are common, genetic testing and premarital counseling should be considered for individuals who have familial CVID history. In summary, elucidation of the genetic and molecular pathways underlying CVID will greatly contribute to the dissection of clinical phenotypes, which will enable the development/implementation of patient-specific follow-up and treatments.

CHAPTER 5

Conclusion and Future Perspectives

In this study, we investigated the monogenic basis of CVID in a multiplex Turkish family by performing WES analysis on the genomic DNA of two affected family members. Our findings revealed a novel heterozygous variant (p.Y868N) in *NFKB2*, which encodes a key regulator in the alternative NF-κB pathway. Our results showed that the *NFKB2*: c.2602T>A:p.Y868N variant is a CVID-causing allele. NF-κB2 with p.Y868N is LOF for p52 and GOF for IκBδ regulatory activities. Our discovery of this novel pathogenic variant in *NFKB2* expands the spectrum of known genetic mutations associated with CVID and underscores the importance of the alternative NF-κB pathway in immune regulation in humans. These insights have potential implications for the diagnosis and management of CVID in affected individuals. Further investigation of variability among clinical symptoms of individuals with pathogenic variants in *NFKB2* will provide valuable insights into the genotype-phenotype correlation in CVID. Additionally, expanding the study to larger cohorts and different populations may help to identify other rare variants contributing to CVID and related immunodeficiencies. Future studies should also focus on elucidating the molecular mechanisms underlying the impaired NF-κB2 processing caused by the p.Y868N variant. Transcriptomic and proteomic approaches could be employed to further dissect the functional consequences of this variant in relevant cell types, such as B and T cells, in patients. Another future direction would be to assess autoantibodies that neutralize type I IFNs in patients' plasma samples, which may underlie severe or recurrent viral diseases in our patients. Moreover, exploring potential therapeutic strategies to modulate NF-κB2 activity, including small molecules or gene therapy

approaches, could offer new avenues for treating CVID patients with *NFKB2* mutations. In summary, our study provides significant insights into the genetic basis of CVID and highlights the importance of the alternative NF-κB pathway in immune homeostasis.

REFERENCES

1. Seidel MG, Kindle G, Gathmann B, et al. The European Society for Immunodeficiencies (ESID) Registry Working Definitions for the Clinical Diagnosis of Inborn Errors of Immunity. *J Allergy Clin Immunol Pract*. 2019;7(6):1763-1770. doi:10.1016/j.jaip.2019.02.004

2. Bousfiha A, Moundir A, Tangye SG, et al. The 2022 Update of IUIS Phenotypical Classification for Human Inborn Errors of Immunity. *J Clin Immunol*. 2022;42(7):1508-1520. doi:10.1007/s10875-022-01352-z

3. Wang JJF, Dhir A, Hildebrand KJ, et al. Inborn errors of immunity in adulthood. *Allergy, Asthma Clin Immunol*. 2024;20(1):6. doi:10.1186/s13223-023-00862-8

4. Notarangelo LD, Bacchetta R, Casanova JL, Su HC. Human inborn errors of immunity: An expanding universe. *Sci Immunol*. 2020;5(49). doi:10.1126/sciimmunol.abb1662

5. Bousfiha A, Jeddane L, Picard C, et al. Human Inborn Errors of Immunity: 2019 Update of the IUIS Phenotypical Classification. *J Clin Immunol*. 2020;40(1):66-81. doi:10.1007/s10875-020-00758-x

6. Fathi N, Nirouei M, Salimian Rizi Z, et al. Clinical, Immunological, and Genetic Features in Patients with NFKB1 and NFKB2 Mutations: a Systematic Review. *J Clin Immunol*. 2024;44(7):160. doi:10.1007/s10875-024-01763-0

7. Tangye SG, Al-Herz W, Bousfiha A, et al. Human Inborn Errors of Immunity: 2022 Update on the Classification from the International Union of Immunological Societies Expert Committee. *J Clin Immunol*. 2022;42(7):1473-1507. doi:10.1007/s10875-022-01289-3

8. Sanchez LA, Maggadottir SM, Pantell MS, et al. Two Sides of the Same Coin: Pediatric-Onset and Adult-Onset Common Variable Immune Deficiency. *J Clin Immunol*. 2017;37(6):592-602. doi:10.1007/s10875-017-0415-5

9. Huq ME, Bhatnagar NK, Hostoffer RW. Hypogammaglobulinemia. In: ; 2024.

10. Pescador Ruschel MA, Vaqar S. Common Variable Immunodeficiency. In: ; 2024.

11. Bonilla FA, Barlan I, Chapel H, et al. International Consensus Document (ICON): Common Variable Immunodeficiency Disorders. *J Allergy Clin Immunol Pract*. 2016;4(1):38-59. doi:10.1016/j.jaip.2015.07.025

12. Seidel MG, Kindle G, Gathmann B, et al. The European Society for Immunodeficiencies (ESID) Registry Working Definitions for the Clinical Diagnosis of Inborn Errors of Immunity. *J Allergy Clin Immunol Pract*. 2019;7(6):1763-1770. doi:10.1016/j.jaip.2019.02.004

13. Filion CA, Taylor-Black S, Maglione PJ, Radigan L, Cunningham-Rundles C. Differentiation of Common Variable Immunodeficiency From IgG Deficiency. *J Allergy Clin Immunol Pract*. 2019;7(4):1277-1284. doi:10.1016/j.jaip.2018.12.004

14. Salzer U, Warnatz K, Peter H. Common variable immunodeficiency - an update. *Arthritis Res Ther*. 2012;14(5):223. doi:10.1186/ar4032

15. Chapel H, Lucas M, Patel S, et al. Confirmation and improvement of criteria for clinical phenotyping in common variable immunodeficiency disorders in replicate cohorts. *J Allergy Clin Immunol*. 2012;130(5):1197-1198.e9. doi:10.1016/j.jaci.2012.05.046

16. Chapel H, Lucas M, Lee M, et al. Common variable immunodeficiency disorders: division into distinct clinical phenotypes. *Blood*. 2008;112(2):277-286. doi:10.1182/blood-2007-11-124545

17. Jolles S. The Variable in Common Variable Immunodeficiency: A Disease of Complex Phenotypes. *J Allergy Clin Immunol Pract*. 2013;1(6):545-556. doi:10.1016/j.jaip.2013.09.015

18. Patuzzo G, Barbieri A, Tinazzi E, et al. Autoimmunity and infection in common variable immunodeficiency (CVID). *Autoimmun Rev*. 2016;15(9):877-882. doi:10.1016/j.autrev.2016.07.011

19. Zainaldain H, Rizvi FS, Rafiemanesh H, et al. Infectious Complications Reporting in Common Variable Immunodeficiency: A Systematic Review and Meta-analysis. *Oman Med J*. 2020;35(4):e157-e157. doi:10.5001/omj.2020.64

20. Kainulainen L, Vuorinen T, Rantakokko-Jalava K, Österback R, Ruuskanen O. Recurrent and persistent respiratory tract viral infections in patients with primary hypogammaglobulinemia. *J Allergy Clin Immunol*. 2010;126(1):120-126. doi:10.1016/j.jaci.2010.04.016

21. Al-Hakim A, Kacar M, Savic S. The Scope and Impact of Viral Infections in Common Variable Immunodeficiency (CVID) and CVID-like Disorders: A Literature Review. *J Clin Med*. 2024;13(6):1717. doi:10.3390/jcm13061717

22. Więsik-Szewczyk E, Jahnz-Różyk K. From infections to autoimmunity: Diagnostic challenges in common variable immunodeficiency. *World J Clin Cases*. 2020;8(18):3942-3955. doi:10.12998/wjcc.v8.i18.3942

23. Quinti I, Lougaris V, Milito C, et al. A possible role for B cells in COVID-19? Lesson from patients with agammaglobulinemia. *J Allergy Clin Immunol*. 2020;146(1):211-213.e4. doi:10.1016/j.jaci.2020.04.013

24. Ramzi N, Jamee M, Bakhtiyari M, et al. Bronchiectasis in common variable immunodeficiency: A systematic review and meta-analysis. *Pediatr Pulmonol*. 2020;55(2):292-299. doi:10.1002/ppul.24599

25. Mooney D, Edgar D, Einarsson G, Downey D, Elborn S, Tunney M. Chronic lung disease in common variable immune deficiency (CVID): A pathophysiological role for microbial and non-B cell immune factors. *Crit Rev Microbiol*. 2017;43(4):508-519. doi:10.1080/1040841X.2016.1268568

26. Patrawala M, Cui Y, Peng L, et al. Pulmonary Disease Burden in Primary Immune Deficiency Disorders: Data from USIDNET Registry. *J Clin Immunol*.

2020;40(2):340-349. doi:10.1007/s10875-019-00738-w

27. Quast TM, Self AR, Browning RF. Diagnostic Evaluation of Bronchiectasis. *Disease-a-Month*. 2008;54(8):527-539. doi:10.1016/j.disamonth.2008.05.001

28. Hurst JR, Verma N, Lowe D, et al. British Lung Foundation/United Kingdom Primary Immunodeficiency Network Consensus Statement on the Definition, Diagnosis, and Management of Granulomatous-Lymphocytic Interstitial Lung Disease in Common Variable Immunodeficiency Disorders. *J Allergy Clin Immunol Pract*. 2017;5(4):938-945. doi:10.1016/j.jaip.2017.01.021

29. Ho H en, Cunningham-Rundles C. Non-infectious Complications of Common Variable Immunodeficiency: Updated Clinical Spectrum, Sequelae, and Insights to Pathogenesis. *Front Immunol*. 2020;11. doi:10.3389/fimmu.2020.00149

30. Morimoto Y, Routes JM. Granulomatous disease in common variable immunodeficiency. *Curr Allergy Asthma Rep*. 2005;5(5):370-375. doi:10.1007/s11882-005-0008-x

31. Ardeniz Ö, Cunningham-Rundles C. Granulomatous disease in common variable immunodeficiency. *Clin Immunol*. 2009;133(2):198-207. doi:10.1016/j.clim.2009.05.001

32. Timmermans WMC, van Laar JAM, van Hagen PM, van Zelm MC. Immunopathogenesis of granulomas in chronic autoinflammatory diseases. *Clin Transl Immunol*. 2016;5(12). doi:10.1038/cti.2016.75

33. Misbah SA, Spickett GP, Esiri MM, et al. Recurrent intra-cranial granulomata presenting as space-occupying lesions in a patient with common variable immunodeficiency. *Postgrad Med J*. 1992;68(799):359-362. doi:10.1136/pgmj.68.799.359

34. Mechanic LJ. Granulomatous Disease in Common Variable Immunodeficiency. *Ann Intern Med*. 1997;127(8_Part_1):613. doi:10.7326/0003-4819-127-8_Part_1-199710150-00005

35. LIN J, LIEBHABER M, ROBERTS R, DYER Z, STIEHM E. Etanercept treatment of cutaneous granulomas in common variable immunodeficiency. *J Allergy Clin Immunol*. 2006;117(4):878-882. doi:10.1016/j.jaci.2006.01.034

36. Bouvry D, Mouthon L, Brillet PY, et al. Granulomatosis-associated common variable immunodeficiency disorder: a case-control study versus sarcoidosis. *Eur Respir J*. 2013;41(1):115-122. doi:10.1183/09031936.00189011

37. Costagliola G, Consolini R. Lymphadenopathy at the crossroad between immunodeficiency and autoinflammation: An intriguing challenge. *Clin Exp Immunol*. 2021;205(3):288-305. doi:10.1111/cei.13620

38. Yakaboski E, Fuleihan RL, Sullivan KE, Cunningham-Rundles C, Feuille E. Lymphoproliferative Disease in CVID: a Report of Types and Frequencies from a US Patient Registry. *J Clin Immunol*. 2020;40(3):524-530. doi:10.1007/s10875-020-00769-8

39. Unger S, Seidl M, Schmitt-Graeff A, et al. Ill-Defined Germinal Centers and Severely Reduced Plasma Cells are Histological Hallmarks of Lymphadenopathy in Patients with Common Variable Immunodeficiency. *J Clin Immunol*. 2014;34(6):615-626. doi:10.1007/s10875-014-0052-1

40. Gompels Mm, Hodges E, Lock Rj, et al. Lymphoproliferative disease in antibody deficiency: a multi-centre study. *Clin Exp Immunol*. 2003;134(2):314-320. doi:10.1046/j.1365-2249.2003.02253.x

41. Tran H, Nourse J, Hall S, Green M, Griffiths L, Gandhi MK. Immunodeficiency-associated lymphomas. *Blood Rev*. 2008;22(5):261-281. doi:10.1016/j.blre.2008.03.009

42. Gathmann B, Mahlaoui N, Gérard L, et al. Clinical picture and treatment of 2212 patients with common variable immunodeficiency. *J Allergy Clin Immunol*. 2014;134(1):116-126.e11. doi:10.1016/j.jaci.2013.12.1077

43. Wehr C, Kivioja T, Schmitt C, et al. The EUROclass trial: defining subgroups in common variable immunodeficiency. *Blood*. 2008;111(1):77-85. doi:10.1182/blood-2007-06-091744

44. Resnick ES, Moshier EL, Godbold JH, Cunningham-Rundles C. Morbidity and mortality in common variable immune deficiency over 4 decades. *Blood*. 2012;119(7):1650-1657. doi:10.1182/blood-2011-09-377945

45. Maglione PJ. Autoimmune and Lymphoproliferative Complications of Common Variable Immunodeficiency. *Curr Allergy Asthma Rep*. 2016;16(3):19. doi:10.1007/s11882-016-0597-6

46. Chawla S, Barman P, Tyagi R, et al. Autoimmune Cytopenias in Common Variable Immunodeficiency Are a Diagnostic and Therapeutic Conundrum: An Update. *Front Immunol*. 2022;13. doi:10.3389/fimmu.2022.869466

47. Agarwal S, Cunningham-Rundles C. Autoimmunity in common variable immunodeficiency. *Ann Allergy, Asthma Immunol*. 2019;123(5):454-460. doi:10.1016/j.anai.2019.07.014

48. Fernández-Castro M, Mellor-Pita S, Citores MJ, et al. Common Variable Immunodeficiency in Systemic Lupus Erythematosus. *Semin Arthritis Rheum*. 2007;36(4):238-245. doi:10.1016/j.semarthrit.2006.09.005

49. Swierkot J, Lewandowicz-Uszynska A, Chlebicki A, et al. Rheumatoid arthritis in a patient with common variable immunodeficiency:difficulty in diagnosis and therapy. *Clin Rheumatol*. 2006;25(1):92-94. doi:10.1007/s10067-005-1141-6

50. Mucke J, Cornet A, Witte T, Schneider M. Association of common variable immunodeficiency and rare and complex connective tissue and musculoskeletal diseases. A systematic literature review. *Clin Exp Rheumatol*. 2022;40(5):40-45. doi:10.55563/clinexprheumatol/bbuvih

51. Agarwal S, Mayer L. Pathogenesis and treatment of gastrointestinal disease in antibody deficiency syndromes. *J Allergy Clin Immunol*. 2009;124(4):658-664.

doi:10.1016/j.jaci.2009.06.018

52. Washington K, Stenzel TT, Buckley RH, Gottfried MR. Gastrointestinal Pathology in Patients with Common Variable Immunodeficiency and X-Linked Agammaglobulinemia. *Am J Surg Pathol*. 1996;20(10):1240-1252. doi:10.1097/00000478-199610000-00010

53. Daniels JA, Lederman HM, Maitra A, Montgomery EA. Gastrointestinal Tract Pathology in Patients With Common Variable Immunodeficiency (CVID). *Am J Surg Pathol*. 2007;31(12):1800-1812. doi:10.1097/PAS.0b013e3180cab60c

54. Pecoraro A, Nappi L, Crescenzi L, D'Armiento FP, Genovese A, Spadaro G. Chronic Diarrhea in Common Variable Immunodeficiency: a Case Series and Review of the Literature. *J Clin Immunol*. 2018;38(1):67-76. doi:10.1007/s10875-017-0461-z

55. Agarwal S, Mayer L. Gastrointestinal manifestations in primary immune disorders. *Inflamm Bowel Dis*. 2010;16(4):703-711. doi:10.1002/ibd.21040

56. Sanchez DA, Rotella K, Toribio C, Hernandez M, Cunningham-Rundles C. Characterization of infectious and non-infectious gastrointestinal disease in common variable immunodeficiency: analysis of 114 patient cohort. *Front Immunol*. 2023;14. doi:10.3389/fimmu.2023.1209570

57. Woodward J, Gkrania-Klotsas E, Kumararatne D. Chronic norovirus infection and common variable immunodeficiency. *Clin Exp Immunol*. 2017;188(3):363-370. doi:10.1111/cei.12884

58. Kainulainen L, Nikoskelainen J, Ruuskanen O. Diagnostic findings in 95 Finnish patients with common variable immunodeficiency. *J Clin Immunol*. 2001;21(2):145-149. doi:10.1023/A:1011012023616

59. van Schewick CM, Nöltner C, Abel S, et al. Altered Microbiota, Impaired Quality of Life, Malabsorption, Infection, and Inflammation in CVID Patients With Diarrhoea. *Front Immunol*. 2020;11. doi:10.3389/fimmu.2020.01654

60. Malamut G, Verkarre V, Suarez F, et al. The Enteropathy Associated With Common Variable Immunodeficiency: The Delineated Frontiers With Celiac Disease. *Am J Gastroenterol*. 2010;105(10):2262-2275. doi:10.1038/ajg.2010.214

61. Azizi G, Abolhassani H, Asgardoon MH, et al. Autoimmunity in common variable immunodeficiency: epidemiology, pathophysiology and management. *Expert Rev Clin Immunol*. 2017;13(2):101-115. doi:10.1080/1744666X.2016.1224664

62. van Wanrooij RLJ, Bontkes HJ, Neefjes-Borst EA, Mulder CJ, Bouma G. Immune-mediated enteropathies: From bench to bedside. *J Autoimmun*. 2021;118:102609. doi:10.1016/j.jaut.2021.102609

63. Kalha I, Sellin JH. Common variable immunodeficiency and the gastrointestinal tract. *Curr Gastroenterol Rep*. 2004;6(5):377-383. doi:10.1007/s11894-004-0053-y

64. Lenti MV, Rugge M, Lahner E, et al. Autoimmune gastritis. *Nat Rev Dis Prim*. 2020;6(1):56. doi:10.1038/s41572-020-0187-8

65. Rustgi SD, Bijlani P, Shah SC. Autoimmune gastritis, with or without pernicious anemia: epidemiology, risk factors, and clinical management. *Therap Adv Gastroenterol*. 2021;14:175628482110387. doi:10.1177/17562848211038771

66. Ward C, Lucas M, Piris J, Collier J, Chapel H. Abnormal liver function in common variable immunodeficiency disorders due to nodular regenerative hyperplasia. *Clin Exp Immunol*. 2008;153(3):331-337. doi:10.1111/j.1365-2249.2008.03711.x

67. Fuss IJ, Friend J, Yang Z, et al. Nodular Regenerative Hyperplasia in Common Variable Immunodeficiency. *J Clin Immunol*. 2013;33(4):748-758. doi:10.1007/s10875-013-9873-6

68. Malamut G, Ziol M, Suarez F, et al. Nodular regenerative hyperplasia: The main liver disease in patients with primary hypogammaglobulinemia and hepatic abnormalities. *J Hepatol*. 2008;48(1):74-82. doi:10.1016/j.jhep.2007.08.011

69. Xiao X, Miao Q, Chang C, Gershwin ME, Ma X. Common variable immunodeficiency and autoimmunity – an inconvenient truth. *Autoimmun Rev*. 2014;13(8):858-864. doi:10.1016/j.autrev.2014.04.006

70. Song J, Lleo A, Yang GX, et al. Common Variable Immunodeficiency and Liver Involvement. *Clin Rev Allergy Immunol*. 2018;55(3):340-351. doi:10.1007/s12016-017-8638-z

71. Yazdani R, Heydari A, Azizi G, Abolhassani H, Aghamohammadi A. Asthma and Allergic Diseases in a Selected Group of Patients With Common Variable Immunodeficiency. *J Investig Allergol Clin Immunol*. 2016;26(3):209-211. doi:10.18176/jiaci.0062

72. Aghamohammadi A, Cheraghi T, Gharagozlou M, et al. IgA Deficiency: Correlation Between Clinical and Immunological Phenotypes. *J Clin Immunol*. 2009;29(1):130-136. doi:10.1007/s10875-008-9229-9

73. Yıldız E, Çölkesen F, Arslan S, Evcen R, Sadi Aykan F, Kılınç M. Allergic Diseases as a Clinical Phenotype Marker in Patients with Common Variable Immunodeficiency</bold>. *Int Arch Allergy Immunol*. 2023;184(10):1047-1055. doi:10.1159/000530901

74. Agondi RC, Barros MT, Rizzo L V., Kalil J, Giavina-Bianchi P. Allergic asthma in patients with common variable immunodeficiency. *Allergy*. 2010;65(4):510-515. doi:10.1111/j.1398-9995.2009.02211.x

75. El-Sayed ZA, El-Ghoneimy DH, Ortega-Martell JA, et al. Allergic manifestations of inborn errors of immunity and their impact on the diagnosis: A worldwide study. *World Allergy Organ J*. 2022;15(6):100657. doi:10.1016/j.waojou.2022.100657

76. Zarezadeh Mehrabadi A, Aghamohamadi N, Abolhassani H, Aghamohammadi A,

Rezaei N, Yazdani R. Comprehensive Assessment of Skin Disorders in Patients with Common Variable Immunodeficiency (CVID). *J Clin Immunol*. 2022;42(3):653-664. doi:10.1007/s10875-022-01211-x

77. de Wit J, Brada RJK, van Veldhuizen J, Dalm VASH, Pasmans SGMA. Skin disorders are prominent features in primary immunodeficiency diseases: A systematic overview of current data. *Allergy*. 2019;74(3):464-482. doi:10.1111/all.13681

78. Kiaee F, Azizi G, Rafiemanesh H, et al. Malignancy in common variable immunodeficiency: a systematic review and meta-analysis. *Expert Rev Clin Immunol*. 2019;15(10):1105-1113. doi:10.1080/1744666X.2019.1658523

79. Leone P, Vacca A, Dammacco F, Racanelli V. Common Variable Immunodeficiency and Gastric Malignancies. *Int J Mol Sci*. 2018;19(2):451. doi:10.3390/ijms19020451

80. Yazdani R, Habibi S, Sharifi L, et al. Common Variable Immunodeficiency: Epidemiology, Pathogenesis, Clinical Manifestations, Diagnosis, Classification, and Management. *J Investig Allergol Clin Immunol*. 2020;30(1):14-34. doi:10.18176/jiaci.0388

81. Bethune C, Egner W, Garcez T, et al. British Society for Immunology/United Kingdom Primary Immunodeficiency Network consensus statement on managing non-infectious complications of common variable immunodeficiency disorders. *Clin Exp Immunol*. 2019;196(3):328-335. doi:10.1111/cei.13272

82. Ameratunga R, Longhurst H, Lehnert K, Steele R, Edwards ESJ, Woon ST. Are All Primary Immunodeficiency Disorders Inborn Errors of Immunity? *Front Immunol*. 2021;12. doi:10.3389/fimmu.2021.706796

83. Ameratunga R, Woon ST. Perspective: Evolving Concepts in the Diagnosis and Understanding of Common Variable Immunodeficiency Disorders (CVID). *Clin Rev Allergy Immunol*. 2020;59(1):109-121. doi:10.1007/s12016-019-08765-6

84. Odnoletkova I, Kindle G, Quinti I, et al. The burden of common variable immunodeficiency disorders: a retrospective analysis of the European Society for Immunodeficiency (ESID) registry data. *Orphanet J Rare Dis*. 2018;13(1):201. doi:10.1186/s13023-018-0941-0

85. Westh L, Mogensen TH, Dalgaard LS, et al. Identification and Characterization of a Nationwide Danish Adult Common Variable Immunodeficiency Cohort. *Scand J Immunol*. 2017;85(6):450-461. doi:10.1111/sji.12551

86. Selenius JS, Martelius T, Pikkarainen S, et al. Unexpectedly High Prevalence of Common Variable Immunodeficiency in Finland. *Front Immunol*. 2017;8. doi:10.3389/fimmu.2017.01190

87. Chapel H, Cunningham-Rundles C. Update in understanding common variable immunodeficiency disorders (CVIDs) and the management of patients with these conditions. *Br J Haematol*. 2009;145(6):709-727. doi:10.1111/j.1365-2141.2009.07669.x

88. Weifenbach N, Schneckenburger AAC, Lötters S. Global Distribution of Common Variable Immunodeficiency (CVID) in the Light of the UNDP Human Development Index (HDI): A Preliminary Perspective of a Rare Disease. *J Immunol Res*. 2020;2020:1-8. doi:10.1155/2020/8416124

89. Modell V, Orange JS, Quinn J, Modell F. Global report on primary immunodeficiencies: 2018 update from the Jeffrey Modell Centers Network on disease classification, regional trends, treatment modalities, and physician reported outcomes. *Immunol Res*. 2018;66(3):367-380. doi:10.1007/s12026-018-8996-5

90. Byrd GS, Edwards CL, Kelkar VA, et al. Recruiting Intergenerational African American Males for Biomedical Research Studies: A Major Research Challenge. *J Natl Med Assoc*. 2011;103(6):480-487. doi:10.1016/S0027-9684(15)30361-8

91. Gathmann B, Grimbacher B, Beauté J, et al. The European internet-based patient and research database for primary immunodeficiencies: results 2006–2008. *Clin Exp Immunol*. 2009;157(Supplement_1):3-11. doi:10.1111/j.1365-2249.2009.03954.x

92. Wood P, Stanworth S, Burton J, et al. Recognition, clinical diagnosis and management of patients with primary antibody deficiencies: a systematic review. *Clin Exp Immunol*. 2007;149(3):410-423. doi:10.1111/j.1365-2249.2007.03432.x

93. Janssen LMA, van der Flier M, de Vries E. Lessons Learned From the Clinical Presentation of Common Variable Immunodeficiency Disorders: A Systematic Review and Meta-Analysis. *Front Immunol*. 2021;12. doi:10.3389/fimmu.2021.620709

94. Li J, Wei Z, Li YR, et al. Understanding the genetic and epigenetic basis of common variable immunodeficiency disorder through omics approaches. *Biochim Biophys Acta - Gen Subj*. 2016;1860(11):2656-2663. doi:10.1016/j.bbagen.2016.06.014

95. Rae W. Indications to Epigenetic Dysfunction in the Pathogenesis of Common Variable Immunodeficiency. *Arch Immunol Ther Exp (Warsz)*. 2017;65(2):101-110. doi:10.1007/s00005-016-0414-x

96. Jørgensen SF, Fevang B, Aukrust P. Autoimmunity and Inflammation in CVID: a Possible Crosstalk between Immune Activation, Gut Microbiota, and Epigenetic Modifications. *J Clin Immunol*. 2019;39(1):30-36. doi:10.1007/s10875-018-0574-z

97. Gereige JD, Maglione PJ. Current Understanding and Recent Developments in Common Variable Immunodeficiency Associated Autoimmunity. *Front Immunol*. 2019;10. doi:10.3389/fimmu.2019.02753

98. Chaari A, Bendriss G, Zakaria D, McVeigh C. Importance of Dietary Changes During the Coronavirus Pandemic: How to Upgrade Your Immune Response. *Front Public Heal*. 2020;8. doi:10.3389/fpubh.2020.00476

99. Berbers RM, Nierkens S, van Laar JM, Bogaert D, Leavis HL. Microbial

Dysbiosis in Common Variable Immune Deficiencies: Evidence, Causes, and Consequences. *Trends Immunol*. 2017;38(3):206-216. doi:10.1016/j.it.2016.11.008

100. Franza L, Cianci R. Pollution, Inflammation, and Vaccines: A Complex Crosstalk. *Int J Environ Res Public Health*. 2021;18(12):6330. doi:10.3390/ijerph18126330

101. Abolhassani H, Sagvand BT, Shokuhfar T, Mirminachi B, Rezaei N, Aghamohammadi A. A review on guidelines for management and treatment of common variable immunodeficiency. *Expert Rev Clin Immunol*. 2013;9(6):561-575. doi:10.1586/eci.13.30

102. Jørgensen SF, Trøseid M, Kummen M, et al. Altered gut microbiota profile in common variable immunodeficiency associates with levels of lipopolysaccharide and markers of systemic immune activation. *Mucosal Immunol*. 2016;9(6):1455-1465. doi:10.1038/mi.2016.18

103. Andersen I, Jørgensen S. Gut inflammation in CVID: causes and consequences. *Expert Rev Clin Immunol*. 2022;18(1):31-45. doi:10.1080/1744666X.2021.2008241

104. Fiedorová K, Radvanský M, Bosák J, et al. Bacterial but Not Fungal Gut Microbiota Alterations Are Associated With Common Variable Immunodeficiency (CVID) Phenotype. *Front Immunol*. 2019;10. doi:10.3389/fimmu.2019.01914

105. Podjasek JC, Abraham RS. Autoimmune Cytopenias In Common Variable Immunodeficiency. *Front Immunol*. 2012;3. doi:10.3389/fimmu.2012.00189

106. Rodríguez-Cortez VC, del Pino-Molina L, Rodríguez-Ubreva J, López-Granados E, Ballestar E. Dissecting Epigenetic Dysregulation of Primary Antibody Deficiencies. *J Clin Immunol*. 2016;36(S1):48-56. doi:10.1007/s10875-016-0267-4

107. Wu H, Deng Y, Feng Y, et al. Epigenetic regulation in B-cell maturation and its dysregulation in autoimmunity. *Cell Mol Immunol*. 2018;15(7):676-684. doi:10.1038/cmi.2017.133

108. Rodriguez-Cortez VC, Hernando H, de la Rica L, Vento R, Ballestar E. Epigenomic Deregulation in the Immune System. *Epigenomics*. 2011;3(6):697-713. doi:10.2217/epi.11.99

109. Moroney JB, Chupp DP, Xu Z, Zan H, Casali P. Epigenetics of the antibody and autoantibody response. *Curr Opin Immunol*. 2020;67:75-86. doi:10.1016/j.coi.2020.09.004

110. Campos-Sanchez E, Martínez-Cano J, del Pino Molina L, López-Granados E, Cobaleda C. Epigenetic Deregulation in Human Primary Immunodeficiencies. *Trends Immunol*. 2019;40(1):49-65. doi:10.1016/j.it.2018.11.005

111. Aggarwal V, Banday AZ, Jindal AK, Das J, Rawat A. Recent advances in elucidating the genetics of common variable immunodeficiency. *Genes Dis*.

2020;7(1):26-37. doi:10.1016/j.gendis.2019.10.002

112. del Pino-Molina L, Rodríguez-Ubreva J, Torres Canizales J, et al. Impaired CpG Demethylation in Common Variable Immunodeficiency Associates With B Cell Phenotype and Proliferation Rate. *Front Immunol*. 2019;10. doi:10.3389/fimmu.2019.00878

113. Rodríguez-Cortez VC, del Pino-Molina L, Rodríguez-Ubreva J, et al. Monozygotic twins discordant for common variable immunodeficiency reveal impaired DNA demethylation during naïve-to-memory B-cell transition. *Nat Commun*. 2015;6(1):7335. doi:10.1038/ncomms8335

114. Rodríguez-Ubreva J, Arutyunyan A, Bonder MJ, et al. Single-cell Atlas of common variable immunodeficiency shows germinal center-associated epigenetic dysregulation in B-cell responses. *Nat Commun*. 2022;13(1):1-18. doi:10.1038/s41467-022-29450-x

115. Babaha F, Yazdani R, Shahkarami S, et al. Evaluation of miR-210 expression in common variable immunodeficiency: patients with unsolved genetic defect. *Allergol Immunopathol (Madr)*. 2021;49(2):84-93. doi:10.15586/aei.v49i2.39

116. Hamidi Esfahani Z, Yazdani R, Shahkarami S, et al. Evaluation of MicroRNA-125b-5p and Transcription Factors BLIMP1 and IRF4 Expression in Unsolved Common Variable Immunodeficiency Patients. *Iran J Allergy, Asthma Immunol*. Published online December 12, 2021. doi:10.18502/ijaai.v20i6.8021

117. Jeevarathnum AC, Van Niekerk A, Kriel J, Green RJ. Common variable immunodeficiency disorders: What generalists should know. *African J Thorac Crit Care Med*. 2021;27(3):112. doi:10.7196/AJTCCM.2021.v27i3.228

118. Fekrvand S, Khanmohammadi S, Abolhassani H, Yazdani R. B- and T-Cell Subset Abnormalities in Monogenic Common Variable Immunodeficiency. *Front Immunol*. 2022;13. doi:10.3389/fimmu.2022.912826

119. Romberg N, Le Coz C. Common variable immunodeficiency, cross currents, and prevailing winds. *Immunol Rev*. 2024;322(1):233-243. doi:10.1111/imr.13291

120. Cunningham-Rundles C. The many faces of common variable immunodeficiency. *Hematol Am Soc Hematol Educ Progr*. 2012;2012:301-305. doi:10.1182/asheducation-2012.1.301

121. Groth C, Dräger R, Warnatz K, et al. Impaired up-regulation of CD70 and CD86 in naive (CD27−) B cells from patients with common variable immunodeficiency (CVID). *Clin Exp Immunol*. 2002;129(1):133-139. doi:10.1046/j.1365-2249.2002.01883.x

122. van de Ven AAJM, Compeer EB, van Montfrans JM, Boes M. B-cell Defects in Common Variable Immunodeficiency: BCR signaling, Protein Clustering and Hardwired Gene Mutations. *Crit Rev Immunol*. 2011;31(2):85-98. doi:10.1615/CritRevImmunol.v31.i2.10

123. Sharifi L, Mirshafiey A, Rezaei N, et al. The role of toll-like receptors in B-cell

development and immunopathogenesis of common variable immunodeficiency. *Expert Rev Clin Immunol*. 2016;12(2):195-207. doi:10.1586/1744666X.2016.1114885

124. Yu JE, Zhang L, Radigan L, Sanchez-Ramon S, Cunningham-Rundles C. TLR-Mediated B Cell Defects and IFN-α in Common Variable Immunodeficiency. *J Clin Immunol*. 2012;32(1):50-60. doi:10.1007/s10875-011-9602-y

125. Cunningham-Rundles C. Common variable immune deficiency: Dissection of the variable. *Immunol Rev*. 2019;287(1):145-161. doi:10.1111/imr.12728

126. Salzer U, Unger S, Warnatz K. Common variable immunodeficiency (CVID): exploring the multiple dimensions of a heterogeneous disease. *Ann N Y Acad Sci*. 2012;1250(1):41-49. doi:10.1111/j.1749-6632.2011.06377.x

127. Isnardi I, Ng YS, Menard L, et al. Complement receptor 2/CD21− human naive B cells contain mostly autoreactive unresponsive clones. *Blood*. 2010;115(24):5026-5036. doi:10.1182/blood-2009-09-243071

128. Schena F, Volpi S, Faliti CE, et al. Dependence of Immunoglobulin Class Switch Recombination in B Cells on Vesicular Release of ATP and CD73 Ectonucleotidase Activity. *Cell Rep*. 2013;3(6):1824-1831. doi:10.1016/j.celrep.2013.05.022

129. Roskin KM, Simchoni N, Liu Y, et al. IgH sequences in common variable immune deficiency reveal altered B cell development and selection. *Sci Transl Med*. 2015;7(302). doi:10.1126/scitranslmed.aab1216

130. Azizi G, Rezaei N, Kiaee F, et al. T-Cell Abnormalities in Common Variable Immunodeficiency. *J Investig Allergol Clin Immunol*. 2016;26(4):233-243. doi:10.18176/jiaci.0069

131. Yu GP, Chiang D, Song SJ, et al. Regulatory T cell dysfunction in subjects with common variable immunodeficiency complicated by autoimmune disease. *Clin Immunol*. 2009;131(2):240-253. doi:10.1016/j.clim.2008.12.006

132. Azizi G, Hafezi N, Mohammadi H, et al. Abnormality of regulatory T cells in common variable immunodeficiency. *Cell Immunol*. 2017;315:11-17. doi:10.1016/j.cellimm.2016.12.007

133. Kamin RM, Fudenberg HH, Douglas SD. A genetic defect in “acquired” agammaglobulinemia. *Proc Natl Acad Sci*. 1968;60(3):881-885. doi:10.1073/pnas.60.3.881

134. Grimbacher B, Hutloff A, Schlesier M, et al. Homozygous loss of ICOS is associated with adult-onset common variable immunodeficiency. *Nat Immunol*. 2003;4(3):261-268. doi:10.1038/ni902

135. Kienzler AK, Hargreaves CE, Patel SY. The role of genomics in common variable immunodeficiency disorders. *Clin Exp Immunol*. 2017;188(3):326-332. doi:10.1111/cei.12947

136. Orange JS, Glessner JT, Resnick E, et al. Genome-wide association identifies diverse causes of common variable immunodeficiency. *J Allergy Clin Immunol*. 2011;127(6):1360-1367.e6. doi:10.1016/j.jaci.2011.02.039

137. Dickinson RE, Griffin H, Bigley V, et al. Exome sequencing identifies GATA-2 mutation as the cause of dendritic cell, monocyte, B and NK lymphoid deficiency. *Blood*. 2011;118(10):2656-2658. doi:10.1182/blood-2011-06-360313

138. Liu L, Okada S, Kong XF, et al. Gain-of-function human STAT1 mutations impair IL-17 immunity and underlie chronic mucocutaneous candidiasis. *J Exp Med*. 2011;208(8):1635-1648. doi:10.1084/jem.20110958

139. Li FY, Chaigne-Delalande B, Kanellopoulou C, et al. Second messenger role for Mg2+ revealed by human T-cell immunodeficiency. *Nature*. 2011;475(7357):471-476. doi:10.1038/nature10246

140. Brlek P, Bulić L, Bračić M, et al. Implementing Whole Genome Sequencing (WGS) in Clinical Practice: Advantages, Challenges, and Future Perspectives. *Cells*. 2024;13(6):504. doi:10.3390/cells13060504

141. Choi M, Scholl UI, Ji W, et al. Genetic diagnosis by whole exome capture and massively parallel DNA sequencing. *Proc Natl Acad Sci*. 2009;106(45):19096-19101. doi:10.1073/pnas.0910672106

142. Hakim A, Zhang X, DeLisle A, et al. Clinical utility of genomic analysis in adults with idiopathic liver disease. *J Hepatol*. 2019;70(6):1214-1221. doi:10.1016/j.jhep.2019.01.036

143. Retterer K, Juusola J, Cho MT, et al. Clinical application of whole-exome sequencing across clinical indications. *Genet Med*. 2016;18(7):696-704. doi:10.1038/gim.2015.148

144. Wortmann SB, Koolen DA, Smeitink JA, den van Heuvel L, Rodenburg RJ. Whole exome sequencing of suspected mitochondrial patients in clinical practice. *J Inherit Metab Dis*. 2015;38(3):437-443. doi:10.1007/s10545-015-9823-y

145. Posey JE, Rosenfeld JA, James RA, et al. Molecular diagnostic experience of whole-exome sequencing in adult patients. *Genet Med*. 2016;18(7):678-685. doi:10.1038/gim.2015.142

146. Sanford Kobayashi EF, Dimmock DP. Better and faster is cheaper. *Hum Mutat*. 2022;43(11):1495-1506. doi:10.1002/humu.24422

147. Warr A, Robert C, Hume D, Archibald A, Deeb N, Watson M. Exome Sequencing: Current and Future Perspectives. *G3 Genes|Genomes|Genetics*. 2015;5(8):1543-1550. doi:10.1534/g3.115.018564

148. Abolhassani H, Aghamohammadi A, Fang M, et al. Clinical implications of systematic phenotyping and exome sequencing in patients with primary antibody deficiency. *Genet Med*. 2019;21(1):243-251. doi:10.1038/s41436-018-0012-x

149. van Zelm MC, Reisli I, van der Burg M, et al. An Antibody-Deficiency Syndrome

Due to Mutations in the CD19 Gene. *N Engl J Med*. 2006;354(18):1901-1912. doi:10.1056/NEJMoa051568

150. van Zelm MC, Smet J, Adams B, et al. CD81 gene defect in humans disrupts CD19 complex formation and leads to antibody deficiency. *J Clin Invest*. 2010;120(4):1265-1274. doi:10.1172/JCI39748

151. Küppers R. CD81 as target for B cell lymphomas. *J Exp Med*. 2019;216(7):1469-1470. doi:10.1084/jem.20190733

152. Kovács KG, Mácsik-Valent B, Matkó J, Bajtay Z, Erdei A. Revisiting the Coreceptor Function of Complement Receptor Type 2 (CR2, CD21); Coengagement With the B-Cell Receptor Inhibits the Activation, Proliferation, and Antibody Production of Human B Cells. *Front Immunol*. 2021;12. doi:10.3389/fimmu.2021.620427

153. Thiel J, Kimmig L, Salzer U, et al. Genetic CD21 deficiency is associated with hypogammaglobulinemia. *J Allergy Clin Immunol*. 2012;129(3):801-810.e6. doi:10.1016/j.jaci.2011.09.027

154. Mahajan S, Cervera A, MacLeod M, et al. The role of ICOS in the development of CD4 T cell help and the reactivation of memory T cells. *Eur J Immunol*. 2007;37(7):1796-1808. doi:10.1002/eji.200636661

155. Yong PFK, Salzer U, Grimbacher B. The role of costimulation in antibody deficiencies: ICOS and common variable immunodeficiency. *Immunol Rev*. 2009;229(1):101-113. doi:10.1111/j.1600-065X.2009.00764.x

156. Liu Z, Liu S, Zhang Y, et al. Distinct roles of ICOS and CD40L in human T-B cell adhesion and antibody production. *Cell Immunol*. 2021;368:104420. doi:10.1016/j.cellimm.2021.104420

157. Rahe MC, Murtaugh MP. Interleukin-21 Drives Proliferation and Differentiation of Porcine Memory B Cells into Antibody Secreting Cells. Renukaradhya GJ, ed. *PLoS One*. 2017;12(1):e0171171. doi:10.1371/journal.pone.0171171

158. Hoshino A, Picard BH, Polychronopoulou S, et al. Loss-of-phosphorylation of IKZF1 results in gain-of-function associated with immune dysregulation. *J Allergy Clin Immunol*. 2024;154(1):229-236.e2. doi:10.1016/j.jaci.2024.01.029

159. Kirstetter P, Thomas M, Dierich A, Kastner P, Chan S. Ikaros is critical for B cell differentiation and function. *Eur J Immunol*. 2002;32(3):720. doi:10.1002/1521-4141(200203)32:3<720::AID-IMMU720>3.0.CO;2-P

160. Keller MD, Pandey R, Li D, et al. Mutation in IRF2BP2 is responsible for a familial form of common variable immunodeficiency disorder. *J Allergy Clin Immunol*. 2016;138(2):544-550.e4. doi:10.1016/j.jaci.2016.01.018

161. Ramalho-Oliveira R, Oliveira-Vieira B, Viola JPB. IRF2BP2: A new player in the regulation of cell homeostasis. *J Leukoc Biol*. 2019;106(3):717-723. doi:10.1002/JLB.MR1218-507R

162. Jaramillo CM, Trujillo-Vargas CM. LRBA in the endomembrane system. *Colomb Med*. 2018;49(3):236-243. doi:10.25100/cm.v49i3.3802

163. van de Ven AAJM, Compeer EB, Bloem AC, et al. Defective calcium signaling and disrupted CD20–B-cell receptor dissociation in patients with common variable immunodeficiency disorders. *J Allergy Clin Immunol*. 2012;129(3):755-761.e7. doi:10.1016/j.jaci.2011.10.020

164. Sathkumara HD, De Silva NR, Handunnetti S, De Silva AD. Genetics of common variable immunodeficiency: role of transmembrane activator and calcium modulator and cyclophilin ligand interactor. *Int J Immunogenet*. 2015;42(4):239-253. doi:10.1111/iji.12217

165. Beınke S, Ley Sc. Functions of NF-κB1 and NF-κB2 in immune cell biology. *Biochem J*. 2004;382(2):393-409. doi:10.1042/BJ20040544

166. Hoffmann A, Baltimore D. Circuitry of nuclear factor κB signaling. *Immunol Rev*. 2006;210:171-186. doi:10.1111/j.0105-2896.2006.00375.x

167. Kuehn HS, Niemela JE, Sreedhara K, et al. Novel nonsense gain-of-function NFKB2 mutations associated with a combined immunodeficiency phenotype. *Blood*. 2017;130(13):1553-1564. doi:10.1182/blood-2017-05-782177

168. Sun SC. The non-canonical NF-κB pathway in immunity and inflammation. *Nat Rev Immunol*. 2017;17(9):545-558. doi:10.1038/nri.2017.52

169. Klemann C, Camacho-Ordonez N, Yang L, et al. Clinical and Immunological Phenotype of Patients With Primary Immunodeficiency Due to Damaging Mutations in NFKB2. *Front Immunol*. 2019;10. doi:10.3389/fimmu.2019.00297

170. Bogaert DJA, Dullaers M, Lambrecht BN, Vermaelen KY, De Baere E, Haerynck F. Genes associated with common variable immunodeficiency: one diagnosis to rule them all? *J Med Genet*. 2016;53(9):575-590. doi:10.1136/jmedgenet-2015-103690

171. Castigli E, Wilson SA, Garibyan L, et al. TACI is mutant in common variable immunodeficiency and IgA deficiency. *Nat Genet*. 2005;37(8):829-834. doi:10.1038/ng1601

172. Martinez-Gallo M, Radigan L, Almejún MB, Martínez-Pomar N, Matamoros N, Cunningham-Rundles C. TACI mutations and impaired B-cell function in subjects with CVID and healthy heterozygotes. *J Allergy Clin Immunol*. 2013;131(2):468-476. doi:10.1016/j.jaci.2012.10.029

173. Poodt AEJ, Driessen GJA, De Klein A, Van Dongen JJM, Van Der Burg M, De Vries E. TACI mutations and disease susceptibility in patients with common variable immunodeficiency. *Clin Exp Immunol*. 2009;156(1):35-39. doi:10.1111/j.1365-2249.2008.03863.x

174. Campagnoli MF, Garelli E, Baravalle V, et al. A TACI Mutation in a Patient with Autoimmune Lymphoproliferative Syndrome. *Blood*. 2006;108(11):3881-3881. doi:10.1182/blood.V108.11.3881.3881

175. Perkins ND. Integrating cell-signalling pathways with NF-κB and IKK function. *Nat Rev Mol Cell Biol*. 2007;8(1):49-62. doi:10.1038/nrm2083

176. Hayden MS, Ghosh S. NF-κB in immunobiology. *Cell Res*. 2011;21(2):223-244. doi:10.1038/cr.2011.13

177. Guo Q, Jin Y, Chen X, et al. NF-κB in biology and targeted therapy: new insights and translational implications. *Signal Transduct Target Ther*. 2024;9(1):53. doi:10.1038/s41392-024-01757-9

178. Oeckinghaus A, Ghosh S. The NF- B Family of Transcription Factors and Its Regulation. *Cold Spring Harb Perspect Biol*. 2009;1(4):a000034-a000034. doi:10.1101/cshperspect.a000034

179. Valiño-Rivas L, Gonzalez-Lafuente L, Sanz AB, Poveda J, Ortiz A, Sanchez-Niño MD. NF-κB Family. In: *Encyclopedia of Signaling Molecules*. Springer International Publishing; 2018:3466-3475. doi:10.1007/978-3-319-67199-4_220

180. Fliegauf M, Kinnunen M, Posadas-Cantera S, et al. Detrimental NFKB1 missense variants affecting the Rel-homology domain of p105/p50. *Front Immunol*. 2022;13. doi:10.3389/fimmu.2022.965326

181. Solan NJ, Miyoshi H, Carmona EM, Bren GD, Paya C V. RelB Cellular Regulation and Transcriptional Activity Are Regulated by p100. *J Biol Chem*. 2002;277(2):1405-1418. doi:10.1074/jbc.M109619200

182. Ghosh G, Wang VYF. Origin of the Functional Distinctiveness of NF-κB/p52. *Front Cell Dev Biol*. 2021;9. doi:10.3389/fcell.2021.764164

183. Liu T, Zhang L, Joo D, Sun SC. NF-κB signaling in inflammation. *Signal Transduct Target Ther*. 2017;2(1):17023. doi:10.1038/sigtrans.2017.23

184. Shih VFS, Tsui R, Caldwell A, Hoffmann A. A single NFκB system for both canonical and non-canonical signaling. *Cell Res*. 2011;21(1):86-102. doi:10.1038/cr.2010.161

185. Yu H, Lin L, Zhang Z, Zhang H, Hu H. Targeting NF-κB pathway for the therapy of diseases: mechanism and clinical study. *Signal Transduct Target Ther*. 2020;5(1):209. doi:10.1038/s41392-020-00312-6

186. Iacobazzi D, Convertini P, Todisco S, Santarsiero A, Iacobazzi V, Infantino V. New Insights into NF-κB Signaling in Innate Immunity: Focus on Immunometabolic Crosstalks. *Biology (Basel)*. 2023;12(6):776. doi:10.3390/biology12060776

187. Sun S. The noncanonical NF-κB pathway. *Immunol Rev*. 2012;246(1):125-140. doi:10.1111/j.1600-065X.2011.01088.x

188. Sun SC. Non-canonical NF-κB signaling pathway. *Cell Res*. 2011;21(1):71-85. doi:10.1038/cr.2010.177

189. Peng C, Ouyang Y, Lu N, Li N. The NF-κB Signaling Pathway, the Microbiota,

and Gastrointestinal Tumorigenesis: Recent Advances. *Front Immunol*. 2020;11. doi:10.3389/fimmu.2020.01387

190. Perkins ND, Gilmore TD. Good cop, bad cop: the different faces of NF-κB. *Cell Death Differ*. 2006;13(5):759-772. doi:10.1038/sj.cdd.4401838

191. Karin M, Ben-Neriah Y. Phosphorylation Meets Ubiquitination: The Control of NF-κB Activity. *Annu Rev Immunol*. 2000;18(1):621-663. doi:10.1146/annurev.immunol.18.1.621

192. Lawrence T. The Nuclear Factor NF- B Pathway in Inflammation. *Cold Spring Harb Perspect Biol*. 2009;1(6):a001651-a001651. doi:10.1101/cshperspect.a001651

193. Adli M, Merkhofer E, Cogswell P, Baldwin AS. IKKα and IKKβ Each Function to Regulate NF-κB Activation in the TNF-Induced/Canonical Pathway. Herrera-Estrella A, ed. *PLoS One*. 2010;5(2):e9428. doi:10.1371/journal.pone.0009428

194. Shih VFS, Tsui R, Caldwell A, Hoffmann A. A single NFκB system for both canonical and non-canonical signaling. *Cell Res*. 2011;21(1):86-102. doi:10.1038/cr.2010.161

195. MaruYama T. The nuclear IκB family of proteins controls gene regulation and immune homeostasis. *Int Immunopharmacol*. 2015;28(2):836-840. doi:10.1016/j.intimp.2015.03.053

196. Hayden MS, Ghosh S. Shared Principles in NF-κB Signaling. *Cell*. 2008;132(3):344-362. doi:10.1016/j.cell.2008.01.020

197. Fusco AJ, Mazumder A, Wang VYF, Tao Z, Ware C, Ghosh G. The NF-κB subunit RelB controls p100 processing by competing with the kinases NIK and IKK1 for binding to p100. *Sci Signal*. 2016;9(447). doi:10.1126/scisignal.aad9413

198. Zhang T, Ma C, Zhang Z, Zhang H, Hu H. NF-κB signaling in inflammation and cancer. *MedComm*. 2021;2(4):618-653. doi:10.1002/mco2.104

199. Gardam S, Brink R. Non-Canonical NF-κB Signaling Initiated by BAFF Influences B Cell Biology at Multiple Junctures. *Front Immunol*. 2014;4. doi:10.3389/fimmu.2013.00509

200. Bonizzi G, Bebien M, Otero DC, et al. Activation of IKKα target genes depends on recognition of specific κB binding sites by RelB:p52 dimers. *EMBO J*. 2004;23(21):4202-4210. doi:10.1038/sj.emboj.7600391

201. Sasaki Y, Iwai K. Roles of the NF-κB Pathway in B-Lymphocyte Biology. In: ; 2015:177-209. doi:10.1007/82_2015_479

202. Peng XP, Caballero-Oteyza A, Grimbacher B. Common Variable Immunodeficiency: More Pathways than Roads to Rome. *Annu Rev Pathol Mech Dis*. 2023;18(1):283-310. doi:10.1146/annurev-pathmechdis-031521-024229

203. Dabbah-Krancher G, Snow AL. Mistuned NF-κB signaling in lymphocytes:

lessons from relevant inborn errors of immunity. *Clin Exp Immunol*. 2023;212(2):117-128. doi:10.1093/cei/uxad006

204. Fryback DG. A program for training and feedback about probability estimation for physicians. *Comput Methods Programs Biomed*. 1986;22(1):27-33. doi:10.1016/0169-2607(86)90090-8

205. Lindsley AW, Qian Y, Valencia CA, Shah K, Zhang K, Assa'ad A. Combined Immune Deficiency in a Patient with a Novel NFKB2 Mutation. *J Clin Immunol*. 2014;34(8):910-915. doi:10.1007/s10875-014-0095-3

206. Kuehn HS, Bernasconi A, Niemela JE, et al. A Nonsense N –Terminus NFKB2 Mutation Leading to Haploinsufficiency in a Patient with a Predominantly Antibody Deficiency. *J Clin Immunol*. 2020;40(8):1093-1101. doi:10.1007/s10875-020-00842-2

207. Richards S, Aziz N, Bale S, et al. Standards and guidelines for the interpretation of sequence variants: A joint consensus recommendation of the American College of Medical Genetics and Genomics and the Association for Molecular Pathology. *Genet Med*. 2015;17(5):405-424. doi:10.1038/gim.2015.30

208. Karczewski KJ, Francioli LC, Tiao G, et al. The mutational constraint spectrum quantified from variation in 141,456 humans. *Nature*. 2020;581(7809):434-443. doi:10.1038/s41586-020-2308-7

209. Taliun D, Harris DN, Kessler MD, et al. Sequencing of 53,831 diverse genomes from the NHLBI TOPMed Program. *Nature*. 2021;590(7845):290-299. doi:10.1038/s41586-021-03205-y

210. Li S, Carss KJ, Halldorsson B V, Cortes A, Consortium UBWGS. Whole-genome sequencing of half-a-million UK Biobank participants. *medRxiv*. Published online 2023:2023.12.06.23299426. https://www.medrxiv.org/content/10.1101/2023.12.06.23299426v1%0Ahttps://www.medrxiv.org/content/10.1101/2023.12.06.23299426v1.abstract

211. Cheng J, Novati G, Pan J, et al. Accurate proteome-wide missense variant effect prediction with AlphaMissense. *Science (80-).* 2023;381(6664). doi:10.1126/science.adg7492

212. Adzhubei I, Jordan DM, Sunyaev SR. Predicting Functional Effect of Human Missense Mutations Using PolyPhen-2. *Curr Protoc Hum Genet*. 2013;76(1). doi:10.1002/0471142905.hg0720s76

213. Steinhaus R, Proft S, Schuelke M, Schwarz JM, Seelow D, Cooper DN. MutationTaster2021. 2021;49(April):446-451.

214. Vaser R, Adusumalli S, Leng SN, Sikic M, Ng PC. SIFT missense predictions for genomes. *Nat Protoc*. 2016;11(1):1-9. doi:10.1038/nprot.2015.123

215. Belkaya S, Michailidis E, Korol CB, et al. Inherited IL-18BP deficiency in human fulminant viral hepatitis. *J Exp Med*. 2019;216(8):1777-1790. doi:10.1084/jem.20190669

216. Durandy A, Hivroz C, Mazerolles F, et al. Abnormal CD40-mediated activation pathway in B lymphocytes from patients with hyper-IgM syndrome and normal CD40 ligand expression. *J Immunol*. 1997;158(6):2576-2584.

217. Maffucci P, Bigio B, Rapaport F, et al. Blacklisting variants common in private cohorts but not in public databases optimizes human exome analysis. *Proc Natl Acad Sci*. 2019;116(3):950-959. doi:10.1073/pnas.1808403116

218. Itan Y, Shang L, Boisson B, et al. The human gene damage index as a gene-level approach to prioritizing exome variants. *Proc Natl Acad Sci*. 2015;112(44):13615-13620. doi:10.1073/pnas.1518646112

219. Maffucci P, Filion CA, Boisson B, et al. Genetic Diagnosis Using Whole Exome Sequencing in Common Variable Immunodeficiency. *Front Immunol*. 2016;7. doi:10.3389/fimmu.2016.00220

220. Cunningham-Rundles C, Casanova JL, Boisson B. Genetics and clinical phenotypes in common variable immunodeficiency. *Front Genet*. 2024;14. doi:10.3389/fgene.2023.1272912

221. Khan S, Hinks J, Shorto J, Schwarz MJ, Sewell WAC. Some cases of common variable immunodeficiency may be due to a mutation in the SBDS gene of Shwachman–Diamond syndrome. *Clin Exp Immunol*. 2008;151(3):448-454. doi:10.1111/j.1365-2249.2007.03556.x

222. Le Voyer T, Parent A V., Liu X, et al. Autoantibodies against type I IFNs in humans with alternative NF-κB pathway deficiency. *Nature*. 2023;623(7988):803-813. doi:10.1038/s41586-023-06717-x

223. Zhang Q, Pizzorno A, Miorin L, et al. Autoantibodies against type I IFNs in patients with critical influenza pneumonia. *J Exp Med*. 2022;219(11). doi:10.1084/jem.20220514

224. Pozzetto B, Mogensen KE, Tovey MG, Gresser I. Characteristics of Autoantibodies to Human Interferon in a Patient with Varicella-Zoster Disease. *J Infect Dis*. 1984;150(5):707-713. doi:10.1093/infdis/150.5.707

225. Meisel C, Akbil B, Meyer T, et al. Mild COVID-19 despite autoantibodies against type I IFNs in autoimmune polyendocrine syndrome type 1. *J Clin Invest*. 2021;131(14). doi:10.1172/JCI150867

226. Mathian A, Breillat P, Dorgham K, et al. Lower disease activity but higher risk of severe COVID-19 and herpes zoster in patients with systemic lupus erythematosus with pre-existing autoantibodies neutralising IFN-α. *Ann Rheum Dis*. 2022;81(12):1695-1703. doi:10.1136/ard-2022-222549

227. Manry J, Bastard P, Gervais A, et al. The risk of COVID-19 death is much greater and age dependent with type I IFN autoantibodies. *Proc Natl Acad Sci*. 2022;119(21). doi:10.1073/pnas.2200413119

228. Hetemäki I, Laakso S, Välimaa H, et al. Patients with autoimmune polyendocrine syndrome type 1 have an increased susceptibility to severe herpesvirus infections.

Clin Immunol. 2021;231:108851. doi:10.1016/j.clim.2021.108851

229. Gervais A, Rovida F, Avanzini MA, et al. Autoantibodies neutralizing type I IFNs underlie West Nile virus encephalitis in ~40% of patients. *J Exp Med*. 2023;220(9). doi:10.1084/jem.20230661

230. Bastard P, Rosen LB, Zhang Q, et al. Autoantibodies against type I IFNs in patients with life-threatening COVID-19. *Science (80-).* 2020;370(6515). doi:10.1126/science.abd4585

231. Bastard P, Michailidis E, Hoffmann HH, et al. Auto-antibodies to type I IFNs can underlie adverse reactions to yellow fever live attenuated vaccine. *J Exp Med*. 2021;218(4). doi:10.1084/jem.20202486

232. Alotaibi F, Alharbi NK, Rosen LB, et al. Type I interferon autoantibodies in hospitalized patients with Middle East respiratory syndrome and association with outcomes and treatment effect of interferon beta-1b in MIRACLE clinical trial. *Influenza Other Respi Viruses*. 2023;17(3). doi:10.1111/irv.13116

233. Bastard P, Gervais A, Le Voyer T, et al. Autoantibodies neutralizing type I IFNs are present in ~4% of uninfected individuals over 70 years old and account for ~20% of COVID-19 deaths. *Sci Immunol*. 2021;6(62). doi:10.1126/sciimmunol.abl4340

APPENDIX

A. Clinical features of the patients

Patients:	**P1**	**P2**	**P3**
Onset of infections	2 months	Childhood	Childhood
Infection profile	- Recurrent upper and lower RTI - Recurrent otitis media - Recurrent urinary tract infections - One episode of COVID-19 (mild, before vaccination) - Cutaneous candidiasis - Diarrhea in childhood	- Recurrent upper and lower RTI - Recurrent herpes labialis - Two episodes of COVID-19 (severe and mild, without vaccination)	- Recurrent upper and lower RTI - Recurrent urinary tract infections - *M. tuberculosis* infection in childhood
Other manifestations	- Adrenocorticotropic hormone deficiency - Autoimmune peripheral hypothyroidism	- Eczema in childhood - Recurrent oral ulcers and diarrhea in childhood	- Recurrent diarrhea - Asthma - Arterial hypertension - Nephrolithiasis - Adrenal Adenomas
Autoantibodies*	ANA: negative Anti-TPO: positive Anti-TG: positive	ANA: negative Anti-TPO: negative Anti-TG: negative	ANA: negative Anti-TPO: negative Anti-TG: negative
COVID-19 vaccination	Yes	No	Yes
Treatment	- Levothyroxine, hydrocortisone, and IgRT since the diagnosis	- IgRT since the age of 22	- IgRT and antibiotic prophylaxis since the diagnosis

RTI: respiratory tract infections, IgRT: Immunoglobulin replacement therapy, ANA: Antinuclear antibody, Anti-TPO: Thyroid peroxidase antibody, Anti-TG: Thyroglobulin antibody

*During IgRT

B. Gene List

The following list includes genes that are associated with CVID[197,219,220]

ACP5, ACTB, ADA, ADA2, ADAM17, ADAR, ADGRE2, AICDA, AIRE, AK2, ALG6, ALPK1, ANGPT1, ANKZF1, AP3B1, AP3D1, APOL1, ARHGEF1, ARID3A, ARPC1B, ASAH1, ATM, ATP6AP1, B2M, BACH2, BANK1, BCL10, BCL11B, BCL2L11, BLK, BLM, BLNK, BLOC1S3, BLOC1S6, BTK, C1QA, C1QB, C1QC, C1R, C1S, C2, C3, C4A, C4B, C5, C6, C7, C8A, C8B, C8G, C9, CAMLG, CARD11, CARD14, CARD8, CARD9, CARMIL2, CASP10, CASP8, CBL, CCBE1, CD19, CD247, CD27, CD3D, CD3E, CD3G, CD40, CD40LG, CD46, CD55, CD59, CD70, CD79A, CD79B, CD81, CD8A, CDC42, CDCA7, CEBPE, CFB, CFD, CFH, CFHR1, CFHR5, CFI, CFP,

CHD7, CIB1, CIITA, CLCN7, CLPB, COL7A1, COLEC11, COPA, CORO1A, CR2 (CD21), CSF2RA, CSF2RB, CSF3R, CTC1, CTLA4, CTNNBL1, CTPS1, CTSC, CXCR2, CXCR4, CYBA, CYBB, CYP27A1, DBR1, DCK1, DCLRE1B, DCLRE1C, DDX41, DEF6, DGAT1, DIAPH1, DKC1, DNAJC21, DNASE1L3, DNASE2, DNMT3B, DOCK2, DOCK8, DSG1, DTNBP1, DUOX2, EBF1, EFL1, EIF2AK3, ELANE, EPG5, ERBB2IP, ERBIN, ERCC2, ERCC3, ERCC6L2, EXTL3, F5, FADD, FANCA, FANCB, FANCE, FANCF, FANCI, FANCL, FAS, FASLG, FASN, FAT4, FBN1, FCGR3B, FCHO1, FCN3, FERMT1, FERMT3, FNIP1, FOXI3, FOXN1, FOXP3, FPR1, G6PC3, G6PD, GAB2, GATA1, GATA2, GFI1, GINS1, GTF2E2, GTF2H5, GUCY2C, HAX1, HELLS, HMOX1, HPS1, HPS3, HPS4, HPS5, HPS6, HTRA2, HYOU1, ICOS, ICOSLG, IFIH1, IFNAR1, IFNAR2, IFNGR1, IFNGR2, IGHM, IGKC, IGLL1, IKBKB, IKBKB, IKBKG, IKZF1, IL10, IL10RA, IL10RB, IL12B, IL12RB1, IL12RB2, IL17F, IL17RA, IL17RC, IL18, IL18BP, IL1A, IL1RN, IL21, IL21R, IL23R, IL2RA, IL2RB, IL2RG, IL2RG, IL36RN, IL6R, IL6ST, IL7R, INO80, INPP5D, IRAK4, IRF2BP2, IRF3, IRF4, IRF7, IRF8, IRF9, ISG15, ITCH, ITGAM, ITGAX, ITGB2, ITGB2, ITK, JAGN1, JAK1, JAK3, KAT6A, KDM6A, KMT2A, KMT2D, KRAS, LAMTOR2, LAT, LAX1, LCK, LCT, LIG1, LIG4, LIPA, LPIN2, LRBA, LRRC8A, LYN, LYST, MAD2L2, MAGT1, MALT1, MAP3K14, MASP1, MASP2, MBL2, MCM4, MEFV, MKL1, MOGS, MPLKIP, MPO, MRE11A, MS4A1, MSH5, MSN, MTHFD1, MVK, MX1, MYD88, MYH9, MYO5B, MYSM1, NBAS, NBN, NBPF15, NCF1, NCF2, NCF4, NCKAP1L, NCSTN, NEUROG3, NFKB2, NFAT5, NFE2L2, NFKB1, NFKB2, NFKBIA, NHEJ1, NHP2, NLRC3, NLRC4, NLRP1, NLRP12, NLRP2, NLRP3, NLRP3, NOD2, NOP10, NOTCH2NLC, NRAS, NSMCE3, OAS1, ORAI1, OSTM1, OTULIN, P2RX7, PARN, PAX1, PCNA, PEPD, PGM3, PIK3C2A, PIK3CD, PIK3CG, PIK3R1, PLCG2, PLVAP, PMS2, PNLIP, PNP,

POLA1, POLD1, POLD2, POLE, POLE2, POLR3A, POLR3F, POMP, PRF1, PRKCD, PRKD1, PRKDC, PSENEN, PSMA3, PSMB4, PSMB8, PSMB9, PSMG2, PSTPIP1, PTEN, PTPN2, PTPN6, PTPRC, RAB27A, RAC1, RAC2, RAG1, RAG2, RANBP2, RASGRP1, RBCK1, REL, RELA, RELB, RFWD3, RFX5, RFXANK, RFXAP, RHOH, RIGI, RIPK1, RMRP, RNASEH2A, RNASEH2B, RNASEH2C, RNASEL, RNF113A, RNF168, RNF31, RNU4ATAC, RORC, RPSA, RTEL1, SAM9, SAMD9, SAMD9L, SAMHD1, SAR1B, SASH3, SBDS, SCO2, SEC61A1, SEMA3E, SERPING1, SF3B1, SGPL1, SH2D1A, SH3BP2, SH3KBP1, SI, SIAE, SKIC2, SKIC3, SLC10A2, SLC11A1, SLC26A3, SLC29A3, SLC35C1, SLC37A4, SLC39A7, SLC46A1, SLC51B, SLC5A1, SLC7A7, SLC9A3, SLX4, SMARCAL1, SMARCD2, SNX10, SOCS1, SP110, SPINK5, SPINT2, SPPL2A, SRP54, SRP72, STAT1, STAT2, STAT3, STAT4, STAT5B, STIM1, STK4, STN1, STX11, STX3, STXBP2, SYK, TADA2A, TAOK2, TAP1, TAP2, TAPBP, TBK1, TBX1, TCF3, TCIRG1, TCN2, TECR, TERC, TERT, TFRC, TGFB1, TGFBR1, TGFBR2, THBD, TICAM1, TIMM50, TINF2, TLR1, TLR3, TLR7, TMC6, TMC8, TMC8, TMEM173, TMPRSS15, TNFAIP3, TNFRSF11A, TNFRSF13B (TACI), TNFRSF13C (BAFFR), TNFRSF1A, TNFRSF1A, TNFRSF4, TNFRSF6B, TNFRSF9, TNFSF11, TNFSF12 (TWEAK), TNFSF13 (APRIL), TNIP1, TONSL, TOP2B, TP63, TPP2, TRAC, TRAF3, TRAF3IP2, TREX1, TRNT1, TTC37, TTC7A, TUBB1, TYK2

C. Plasmid Maps

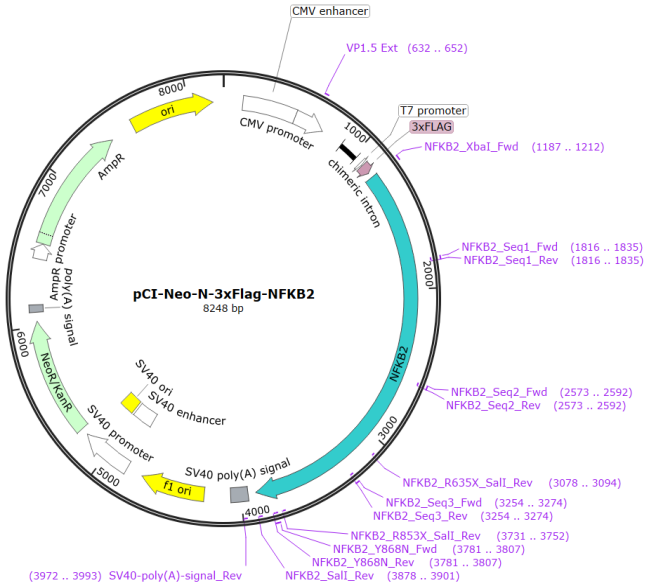

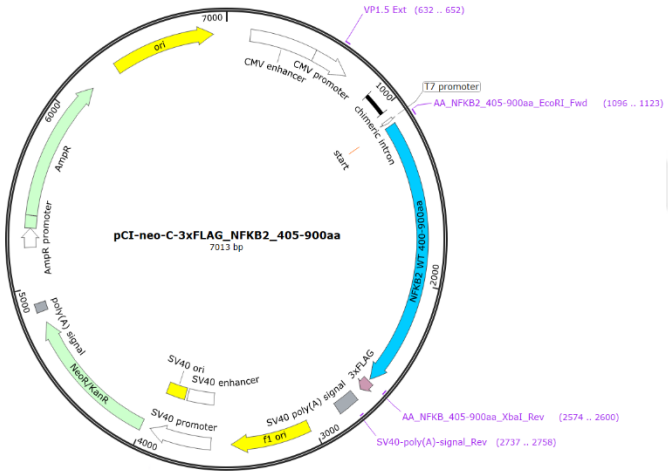

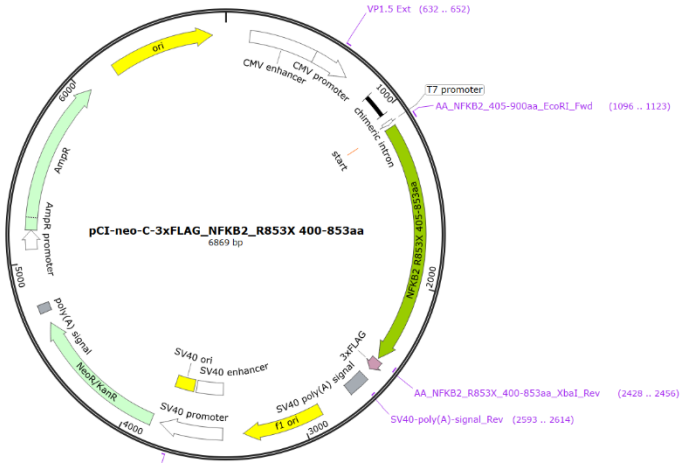

Appendix Figure 1 Constructed NFKB2 plasmid maps using pCI-neo-N-3xFLAG mammalian expression vector

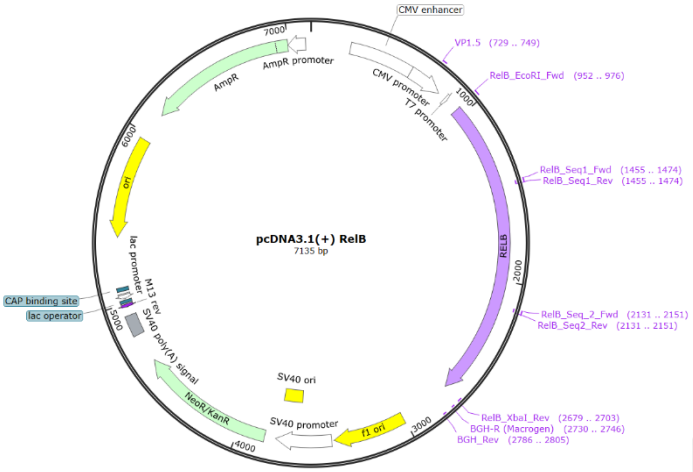

Appendix Figure 2 Constructed RELB plasmid map using pcDNA3.1(+) mammalian expression vector

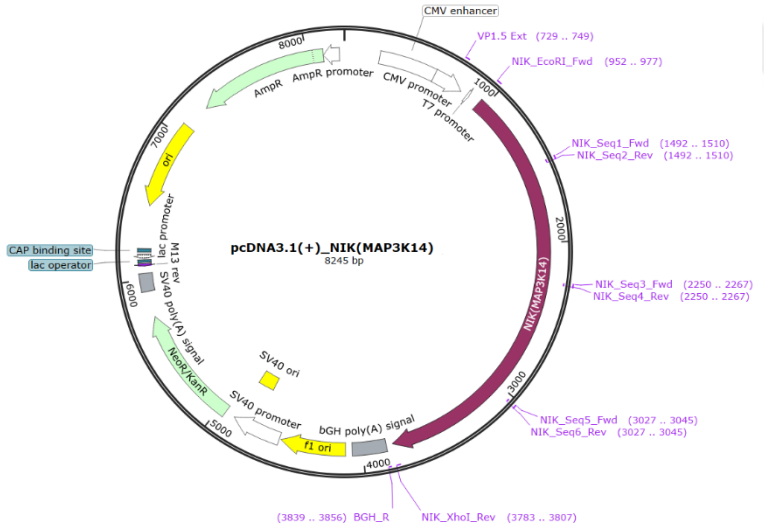

Appendix Figure 3. Constructed NIK plasmid map using pcDNA3.1(+) mammalian expression vector